

**CONTRIBUTION OF ELASTIN
TO CARDIOVASCULAR DEVELOPMENT
IN ZEBRAFISH**

by

Michelle Zorrilla

BS, Biology, Florida Atlantic University, 2010

MPH, Public Health Genetics, University of Pittsburgh, 2012

Submitted to the Graduate Faculty of
the Department of Human Genetics
the Graduate School of Public Health in partial fulfillment
of the requirements for the degree of
Doctor of Philosophy

University of Pittsburgh

2018

UNIVERSITY OF PITTSBURGH
GRADUATE SCHOOL OF PUBLIC HEALTH

This dissertation was presented

by

Michelle Zorrilla

It was defended on

June 1, 2018

and approved by

Dissertation Advisor:

Zsolt Urban, PhD

Associate Professor, Department of Human Genetics
Graduate School of Public Health, University of Pittsburgh

Committee Members:

Michael Tsang, PhD

Associate Professor, Department of Developmental Biology
School of Medicine, University of Pittsburgh

Beth Roman, PhD

Associate Professor, Department of Human Genetics
Graduate School of Public Health, University of Pittsburgh

Julie Phillippi, PhD

Assistant Professor, Department of Cardiothoracic Surgery
School of Medicine, University of Pittsburgh

Copyright © by Michelle Zorrilla

2018

CONTRIBUTION OF ELASTIN TO CARDIOVASCULAR DEVELOPMENT IN ZEBRAFISH

Michelle Zorrilla, MPH

University of Pittsburgh, 2018

ABSTRACT

Elastin is the main structural protein of elastic fibers that allows tissues in vertebrates to extend and recoil. Heterozygous loss of function mutations in the elastin gene (*ELN*) can cause supravalvular aortic stenosis (SVAS), a rare obstructive cardiovascular disease typically characterized by a narrowing of the ascending aorta. The association of SVAS with hypertension, valvular defects and other congenital heart defects (CHDs) is of broader public health significance. The main goal of this research is to generate and characterize a set of SVAS-like mutant zebrafish lines. Zebrafish have two elastin genes, *elna* and *elnb*. First, I investigated the genetic and transcript diversity of zebrafish elastins by sequencing 46 and 44 overlapping cDNA clones from *elna* and *elnb*, respectively. I uncovered substantial variation in from both genes with a total of 79 single nucleotide variants (SNVs) in *elna* and 89 in *elnb*. In addition, there were numerous in-del variants and alternative splicing events. To assess the role of *elna* in zebrafish development, a line of *elna* homozygous mutants was established. The mutation (*elna*^{sa12235} c.264T>A, p.Tyr88*) induces nonsense-mediated decay in a developmentally regulated fashion with close to complete elimination of the mutant transcript starting at 3 days post-fertilization. Phenotypic examination of mutant embryos displayed reduced blood flow, regurgitation, valve and heart looping abnormalities. Regurgitation and valve irregularities was also observed in a mutant adult male. Histological examination of the hearts in adult *elna* mutant fish showed

thinning and loss of the elastic cartilage-like morphology in bulboventricular valves. Further work with larger numbers of fish needs to be done, to obtain reliable estimates of the frequency and possible sex specificity, and clutch-to-clutch variability of valve and other cardiovascular defects in *elna* mutants. In conclusion, my studies show extensive sequence variation in *elna* and *elnb*. Mutants of *elna* have displayed promise to help explain cardiovascular development and detrimental effects of elastin mutations in humans with SVAS especially with respect to cardiac valve abnormalities.

TABLE OF CONTENTS

PREFACE	xiv
ABBREVIATIONS	xvii
1.0. INTRODUCTION	1
1.1. EXTRACELLULAR MATRIX	1
1.1.1. Major Components	1
1.2. ELASTIC FIBERS.....	2
1.2.1. Structure and Function of Elastic Fibers	2
1.2.2. Elastic Tissues.....	3
1.2.3. Elastin	5
1.2.3.1. Tropoelastin structure	6
1.2.3.2. Biophysical properties of tropoelastin.....	8
1.2.3.3. Elastin crosslinking, longevity and degradation	9
1.2.3.4. Expression and regulation of elastin.....	10
1.2.3.5. Alternative splicing of elastin.....	11
1.2.3.6. Evolution of elastin	12
1.2.4. Elastic Fiber Assembly	14
1.3. DISEASES CAUSED BY ELASTIN GENE MUTATIONS.....	15

1.3.1.	Autosomal Dominant Cutis Laxa (ADCL)	16
1.3.1.1.	Clinical manifestations, natural history and management.....	16
1.3.1.2.	<i>ELN</i> Mutations in ADCL	16
1.3.1.3.	Molecular mechanisms of ADCL	17
1.3.2.	Supravalvular Aortic Stenosis (SVAS)	17
1.3.2.1.	Clinical manifestations, natural history and management.....	18
1.3.2.2.	<i>ELN</i> Mutations in SVAS.....	21
1.3.2.3.	Molecular mechanisms of SVAS.....	22
1.4.	CARDIOVASCULAR DEVELOPMENT IN ZEBRAFISH.....	24
1.5.	ZEBRAFISH AS A MODEL IN ELASTIN STUDIES	29
1.6.	PUBLIC HEALTH SIGNIFICANCE	31
1.7.	DISSERTATION AIMS	33
2.0.	METHODS.....	35
2.1.	ZEBRAFISH MAINTENANCE AND CARE	35
2.2.	ZEBRAFISH LINES.....	35
2.3.	EXISTING TRANSCRIPT INFORMATION	36
2.4.	RNA EXTRACTION FOR TRANSCRIPT CLONING AND QUALITY CONTROL.....	37
2.5.	REVERSE TRANSCRIPTION AND POLYMERASE CHAIN REACTION (RT-PCR).....	37
2.6.	MOLECULAR CLONING, SEQUENCING, AND SNP CONFIRMATION	38
2.7.	SNP CONFIRMATION IN gDNA	39
2.8.	GENOTYPING OF ZEBRAFISH BY dCAPS	42
2.9.	RNA ISOLATION TO STUDY THE EXPRESSION OF MUTATIONS.....	43

2.10.	EMBRYO HEART RATE MEASUREMENT	44
2.11.	ADULT ORGAN EXTRACTION, WHOLE-MOUNT HART'S ELASTIN STAINING.....	44
2.12.	WHOLE-MOUNT IMMUNOSTAINING	45
2.13.	CONFOCAL IMAGING AND VIDEO MICROSCOPY	46
2.14.	ECHOCARDIOGRAPHY	47
3.0.	RESULTS.....	48
3.1.	TRANSCRIPT DIVERSITY IN ZEBRAFISH ELASTIN GENES.....	48
3.2.	VALIDATION OF <i>elna</i> MUTANT (<i>elna</i> ^{sa12235} , c.264T>A, p.Tyr88*).....	65
3.3.	STAGE-SPECIFIC DEGRADATION OF MUTANT RNA BY NONSENSE-MEDIATED DECAY	67
3.4.	REDUCED <i>ELNA</i> PROTEIN EXPRESSION IN <i>elna</i> ^{sa} MUTANTS.....	68
3.5.	CIRCULATION DEFECTS IN <i>elna</i> ^{sa} MUTANTS.....	70
3.6.	ELASTIN STAINING IN THE ZEBRAFISH ADULT CARDIOVASCULAR SYSTEM	79
3.7.	ECHOCARDIOGRAPHY IN ADULT FISH	80
3.8.	SURVIVAL OF <i>elna</i> MUTANTS TO ADULTHOOD	82
3.9.	VALIDATION OF <i>elnb</i> MUTANT	85
3.10.	EXPRESSION OF THE <i>elnb</i> ^{sa24024} MUTANT ALLELE.....	87
4.0.	DISCUSSION.....	89
4.1.	ELASTIN ISOFORM VARIATION AND ITS ROLE IN EVOLUTION	89
4.2.	ZEBRAFISH <i>elna</i> 's FUNCTION AND ROLE IN CARDIOVASCULAR DEVELOPMENT	91
5.0.	CONCLUSIONS.....	94
6.0.	FUTURE WORK	95
6.1.	Additional phenotype confirmation	95

6.1.1. Additional Look at Valve Structures in Adult Zebrafish	95
6.1.2. Whole-mount In Situ Time Series of Zebrafish Embryos	96
6.1.3. Generation of an <i>elnb</i> Mutant Line.....	96
6.2. Mechanistic pathways associated with <i>eln</i> loss	97
6.2.1. Integrin Beta 3 Signaling and Vessel Development	97
6.2.2. Hippo Signaling as a Mechanism of Disease	98
APPENDIX: TABLES	100
BIBLIOGRAPHY	106

LIST OF TABLES

Table 1. Examples of Genes Related to Zebrafish Cardiovascular Development.....	28
Table 2. Human and Zebrafish Elastin Genes	30
Table 3. Primers to Confirm SNPs in <i>elna</i> gDNA	40
Table 4. Primers to Confirm SNPs in <i>elnb</i> gDNA	41
Table 5. dCAPS Primers for Genotyping <i>elna</i> and <i>elnb</i>	43
Table 6. RT- PCR primers to investigate the expression of mutations	44
Table 7. Summary of Variations in <i>elna</i> and <i>elnb</i>	49
Table 8. Silent SNVs Identified in Exons 2-39 of <i>elna</i> cDNA	50
Table 9. Silent SNVs Identified in Exons 41-55 of <i>elna</i> cDNA	51
Table 10. Silent SNVs Identified in Exons 8-39 of <i>elnb</i> cDNA	52
Table 11. Silent SNVs Identified in Exons 46-56 of <i>elnb</i> cDNA	53
Table 12. Missense SNVs Identified in <i>elna</i> cDNA	53
Table 13. Missense SNVs Identified in Exons 2-28 of <i>elnb</i> cDNA	54
Table 14. Missense SNVs Identified in Exons 30-55 of <i>elnb</i> cDNA	55
Table 15. Nonsense SNVs Variants Identified in <i>elnb</i> cDNA.....	55
Table 16. Indel Variants Identified in <i>elna</i> cDNA	56
Table 17. Indel Variants Identified in <i>elnb</i> cDNA	56

Table 18. Clustering and Haplotypes in <i>elna</i> and <i>elnb</i>	59
Table 19. Annotated SNV Splice Sites and Splice Variants Identified in <i>elna</i> cDNA.....	60
Table 20. Annotated SNV Splice Sites and Splice Variants Identified in <i>elnb</i> cDNA.....	61
Table 21. gDNA Confirmation of SNVs in <i>elna</i> & <i>elnb</i>	63
Table 22. Whole Exons with Same Sequence	64
Table 23. Wildtype and <i>elnasa/sa</i> Cardiovascular Developmental Observations.....	71
Table 24. Ventricle and Bulbus Measurements in WT and <i>elna^{sa/sa}</i> transgenic larvae	77
Table 25. Survival of Genotyped Zebrafish at 3.5 months	83
Table 26. Survival of Genotyped Zebrafish at 18 months	83
Table 27. Survival Analysis of Zebrafish at 18 months	83
Table 28. Genotyping Distribution Results of <i>elnb</i> Heterozygous In-cross	86
Table 29. Primers used in amplifying <i>elna</i> cDNA fragments	100
Table 30. Primers used in amplifying <i>elnb</i> cDNA fragments	101
Table 31. Primers used to sequence <i>elna</i> cDNA fragments	102
Table 32. Primers used to sequence <i>elnb</i> cDNA fragments	103
Table 33. GenBank accession numbers of cDNA clones.....	104

LIST OF FIGURES

Figure 1. Schematic Representation of Elastic Fiber Formation.....	4
Figure 2. Elastin Conformation	7
Figure 3. Types of Alternative Splicing Observed in Elastin.....	11
Figure 4. The Structure of an Artery Wall.....	19
Figure 5. Anatomy of the Human Heart	19
Figure 6. Structures of the Human Aorta.....	20
Figure 7. Stages of Cardiac Development.....	26
Figure 8. Graphical Representation of Transcript and Genetic Variants in <i>elna</i>	57
Figure 9. Graphical Representation of Transcript and Genetic Variants in <i>elnb</i>	58
Figure 10. A cluster of 13 SNVs in exon 41 of <i>elna</i>	59
Figure 11. A Schematic Representation of the Domain Context and Sequence Features of a New Exon in <i>elna</i>	61
Figure 12. Sequencing of the <i>elna</i> wildtype and mutant alleles in gDNA from adult tail biopsy.	66
Figure 13. Genotyping of <i>elna</i> using dCAPS.....	66
Figure 14. Reduced Expression of the <i>elna^{sa}</i> allele.....	68
Figure 15. Whole-mount Immunostaining for <i>elna</i> in 7 dpf Embryos.....	69
Figure 16. Circulation Defects in <i>elna^{sa/sa}</i> mutants.....	72

Figure 17. Heart rates at 7 dpf by Genotype	73
Figure 18. Heart Rates at 5 dpf by Genotype	73
Figure 19. WT DIC Video Still of the Ventricular-Bulbar Valve at the End of Systole at 7dpf	75
Figure 20. <i>elna</i> ^{sa/sa} DIC Video Still of the Ventricular-Bulbar Valve at the End of Systole at 7 dpf	75
Figure 21. Abnormalities of the circulatory system in the developing embryo	78
Figure 22. Hart's Elastin Stain of Adult Zebrafish Hearts.....	79
Figure 23. Hart's Elastin Stain of Adult Zebrafish Hearts – high-magnification view of the VB Valve	80
Figure 24. <i>elna</i> ^{sa/sa} Echocardiography of a 18mo Male Heart	81
Figure 25. Echocardiography of a WT 18mo Female Heart.....	81
Figure 26. Survival of Zebrafish to 18 months	84
Figure 27. gDNA Sequencing of the Mutant Allele in <i>elnb</i> From Embryos at 12dpf	87
Figure 28. cDNA Sequencing of Heterozygous <i>elnb</i> Embryos at 12 dpf	88

PREFACE

First and foremost, I would like to thank Dr. Zsolt Urban for his willingness to work with me when I was looking for a laboratory in which to pursue my doctorate. Thank you also for your guidance, encouraging me to think independently and your patience. We may not have always seen eye to eye, but I have learned a lot and appreciate the time spent under your wing.

To my fellow lab members and colleagues, you always made the days seem shorter and brighter. Thank you for making me laugh, lending an ear, offering advice, pizza dates and countless potlucks. I will never forget our time together.

I would also like to thank my committee members, Dr. Beth Roman, Dr. Michael Tsang and Dr. Julie Phillippi. Your guidance throughout the years has brought a new perspective to my science career and for that I am grateful.

Dr. Candance Kammerer, thank you for always being there. It was a comfort to know your door was always open. I am grateful to have had such an encouraging point of view, especially when the times were tough and there didn't seem to be a light at the end of the tunnel.

To my best friend Lori, we have been through a lot over the past 18 years. We have laughed and cried, and sometimes laughed so hard we cried. Thank you for always being there through thick and thin.

My brother Michael. We were not the closest of siblings growing up, but I knew we could always count on each other. Your service in the military and dedication as an officer in the community has been an inspiration. I am so proud of what you have accomplished. Because of you I always try to do better and be all that I can be. Hooah. P.S. I have water and you don't.

Thank you to my husband Gregg. You have been so understanding through the long days, trials and tribulations of this journey. We met as I was entering this new phase of my life and I couldn't have asked for a better partner, friend and companion to walk with me now and always. Thank you for all the tasty meals you prepared and brought to lab when I was working late, and for never letting me quit.

Also, to our dog Roubaix, you bring so much joy to our lives. It wouldn't be the same without you greeting us every time with a toy or blanket in your mouth and a wiggly butt. You never let me forget when I need to take a break and just go for a walk.

To my parents, Rafael and Blazina, to whom I dedicate this dissertation. There are no words to describe how proud I am to be your daughter. I would not be who I am today without you. I wasn't always sure this day would come, but you never let me lose sight of who I am and what I

could be. So much of what I have learned is because of you and I couldn't have done it without your love and support. Gracias por todo mami y papi. Los quiero mucho.

And to all my other amazing family members and friends, life would not be such a joy without you in it. Thank you and mucho amor.

ABBREVIATIONS

ADAMTS: A Disintegrin and Metalloprotease with Thrombospondin motifs

ADCL: Autosomal Dominant Cutis Laxa

AV: atrioventricular

BA: Bulbus Arteriosus

BCP: Bromochloropropane

bre: *breakdance* mutation

BSA: Bovine Serum Albumin

CBI: Center for Biologic Imaging

cDNA: Complementary Deoxyribonucleic Acid

cfk: *cardiofunk* mutation

CHD: Congenital Heart Defects

df: Degrees of Freedom

DIC: Differential Interference Contrast

DMSO: Dimethyl Sulfoxide

dpf: Days Post Fertilization

ELN, *eln*: elastin

elnb: elastin b

elna: elastin a

EBP: Elastin Binding Protein

ECM: Extracellular Matrix

GAGs: Glycosaminoglycans

grl: *gridlock* mutation

gDNA: Genomic Deoxyribonucleic Acid

Het: Heterozygous

Homo: Homozygous

hpf: Hours Post Fertilization

IACUC: Institutional Animal Care and Use Committee

IGF-I: Insulin-like Growth Factor-I

IL- β : Interleukin-1 β

LTBPs: Latent Transforming Growth Factor Beta Binding Proteins

LOX: Lysyl Oxidase

MRA: Magnetic Resonance Angiography

MMPs: Matrix Metalloproteinases

MAGPs: Microfibril-associated Glycoproteins

OMIM: Online Mendelian Inheritance in Man

PBS: Phosphate-Buffered Saline

PCR: Polymerase Chain Reaction

PFA: paraformaldehyde

PTU: Phenylthiourea

RNA: Ribonucleic Acid

rs #: rs number (SNV accession number)

sih: *silent heart* mutation

SMCs: Smooth Muscle Cells

SMG: Suppressor with Morphological Effect on Genitalia Proteins

SNPs: Single Nucleotide Polymorphisms

SNVs: Single Nucleotide Variants

SVAS: Supravalvular Aortic Stenosis

TE: Tropoelastin

Tg: Transgenic

TGF β : Transforming Growth Factor β

TNF- α : Tumor Necrosis Factor- α

TX-100: Triton X-100

UPF: Up-Frameshift Suppressor

V: Ventricle

VB: Ventriculo-Bulbar

WBS: Williams-Beuren Syndrome

W:L: Width to Length Aspect Ratio

WT: Wildtype

zf: zebrafish

♀: Female

♂: Male

1.0 INTRODUCTION

1.1. EXTRACELLULAR MATRIX

The extracellular matrix (ECM) is a multifaceted, complex network consisting of polysaccharide chains, proteoglycans, and glycoproteins, some of which form fibers. It is these constituents that allow for a diverse number of structures that make up tissues and support them (Alberts et al., 2008).

1.1.1. MAJOR COMPONENTS

The ECM is produced by a wide variety of cells including fibroblasts, osteoblasts (in bone) chondroblasts (in cartilage). Fibrous proteins of the ECM lie within a “gel-like” substance made from polysaccharide glycosaminoglycans (GAGs), that when bound to proteins are called proteoglycans and form a scaffold-like structure of highly extended conformations (Alberts et al., 2008; Hynes & Naba, 2012). It is this complex nature that allows for cellular communication between blood and tissue, tissue repair and the passage of nutrients and hormones, while endowing tissues with mechanical properties requisite for their diverse functions. Over 300 ECM proteins make up the “core matrisome” in mammals, in conjunction with modifying enzymes, growth factors, and cytokines. The main components of ECM are proteoglycans, collagens,

fibronectins, tenascins, laminins and elastin (Alberts et al., 2008; Bosman & Stamenkovic, 2003; Hynes & Naba, 2012).

1.2. ELASTIC FIBERS

Elastic fibers are a type of fibrous component of the ECM, critical for tissue flexion, extension and resilience. They are found in large part in the cardiovascular system's large vessels such as the aorta and pulmonary artery, the skin, lungs, and elastic cartilage. These dynamic tissues all require the ability to extend and recoil repeatedly over a lifetime, with the elastic fibers contributing to their unique biomechanical roles (Baldwin, Simpson, Steer, Cain, & Kielty, 2013; Kielty, Sherratt, & Shuttleworth, 2002).

1.2.1. STRUCTURE AND FUNCTION OF ELASTIC FIBERS

The elastic fibers are insoluble and robust, making it a challenge to understand their biological and molecular components. Thanks in part to electron microscopy, genetics, immunohistochemistry and biochemical studies, the number of known components has grown substantially in recent years (Kielty et al., 2002). The main structural molecules tropoelastin and fibrillins work with microfibril and elastic fiber-associated molecules like the latent transforming growth factor beta binding proteins (LTBPs), a disintegrin and metalloprotease with thrombospondin motifs (ADAMTS) proteins, microfibril-associated glycoproteins (MAGPs), fibulins and the lysyl oxidase (LOX) family (Baldwin et al., 2013).

Mesenchymal cells and functional necessity dictate the organizational structure of the elastic fibers. Mature elastic fibers are composed of an outer microfibrillar network casing, with a core of elastin. Microfibrils are composed of fibrillin molecules that mature over time into beaded transglutaminase-crosslinked microfibrils of about 10 nm in diameter. The distance between the beads is approximately 56 nm and is dependent on calcium and physical tension. These beaded microfibrils will assemble into parallel bundles. Tropoelastin, the soluble precursor to polymeric elastin is cross-linked and deposited onto microfibril bundles to form elastic fibers (Figure 1). When elastic fibers are paired with collagen fibrils, tissues become strengthened and flexible, forming a scaffold. The elastin provides the extension and flexibility and the collagen limits the extent to which the tissue is stretched (Alberts et al., 2008; Kielty et al., 2002). In addition to providing structure, resilience and flexibility, elastic fibers also bind growth factors such as the transforming growth factor β (TGF β) family and influence when it becomes available for use. Cell surface receptors, such as integrins, bind components of the elastic fiber to modulate cell fate in embryogenesis, cell adhesion, wound healing and tumor growth (Alberts et al., 2008; Baldwin et al., 2013; Bosman & Stamenkovic, 2003; Kielty et al., 2002; Midwood & Schwarzbauer, 2002).

1.2.2. ELASTIC TISSUES

Blood vessels contain elastic fibers in the form of lamellae that lie between layers of smooth muscle cells (SMCs) allowing the vessels to adapt to blood flow. When the elastic properties are

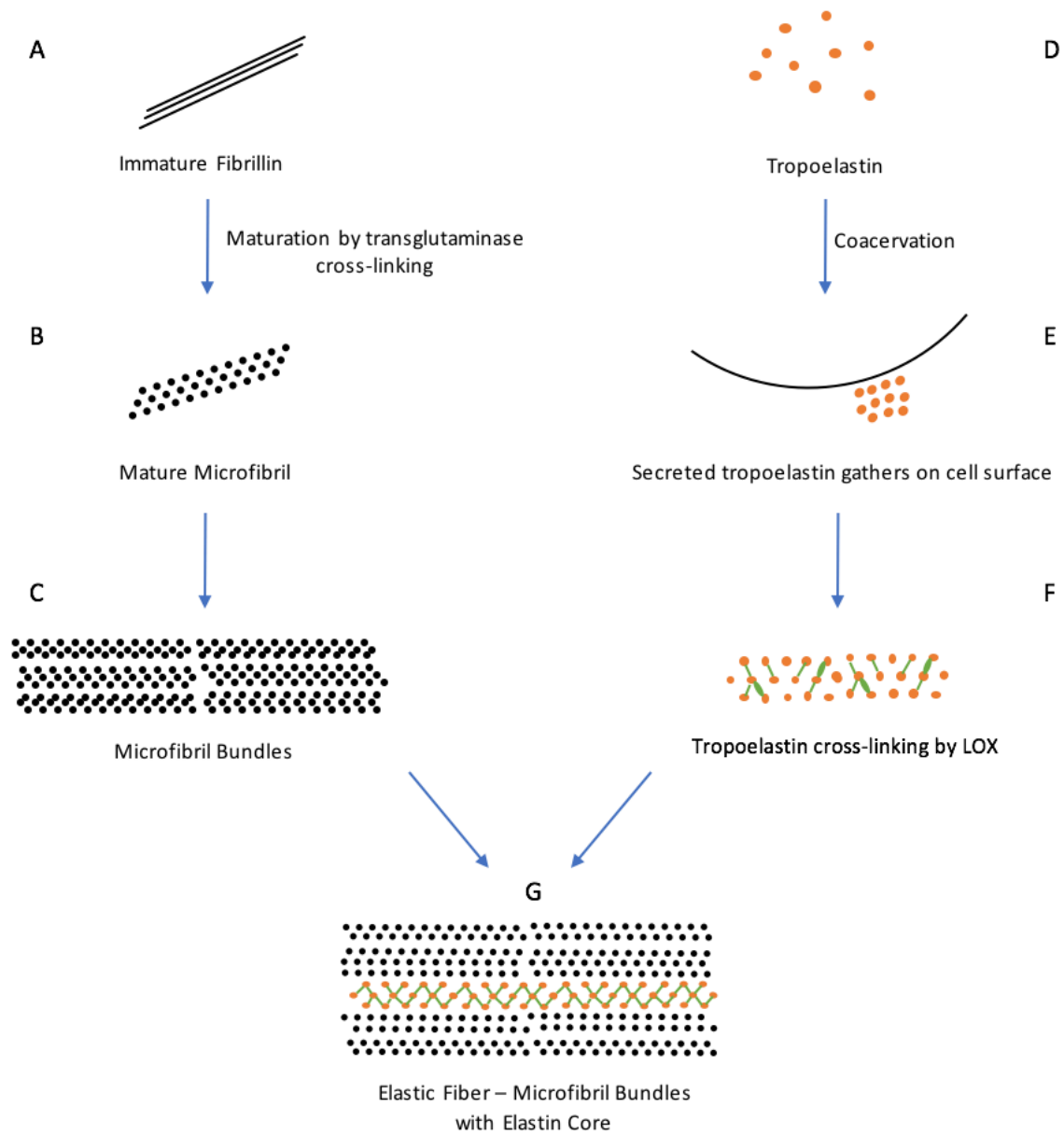


Figure 1. Schematic Representation of Elastic Fiber Formation

A) Fibrillin molecules (black solid lines) mature through cross-linking by transglutaminase into B) mature microfibrils (black dotted lines). The beaded fibrils form C) parallel bundles of microfibrils. D) The soluble precursor of elastin, tropoelastin (orange dots) is secreted from the cell. Through the endothermic process of coacervation, the E) tropoelastin aggregates on the cell surface. F) Lysyl oxidase (green oval) facilitates cross-linking (green lines) assembly of the tropoelastin molecules. G) The cross-linked tropoelastin is then deposited onto the microfibril bundles, where a mature elastic fiber is formed, containing an outer microfibrillar casing and a core of elastin. Diagram is not drawn to scale.

lost, hypertension and aneurysms can result (Kielty et al., 2002; Wagenseil & Mecham, 2012). In the skin, elastic fibers are found in the dermis and make up about 3% of the skin's dry weight, thickening as you proceed from the outer(papillary) to the inner (reticular) dermis. The fibers support the skin's integrity as they extend and recoil over time, maintaining its elasticity (Ackerman, Böer, Bennin, & Gottlieb, 2005; Pawlaczyk, Lelonkiewicz, & Wieczorowski, 2013; B. Starcher, Aycock, & Hill, 2005). In the lungs, elastic fibers play a role in the development of alveoli, lung function and the ability to expand and recoil during breathing. Elastic fibers are found throughout the lung interstitium, in the alveolar septa, the walls of the airways and blood vessels and in the pleura. Thin and highly branched, they provide support during breathing for normal functioning of the lungs (Kielty et al., 2002; Shifren & Mecham, 2006).

1.2.3. ELASTIN

Elastin, the main structural protein of elastic fibers is encoded by a single gene in amniotes. The human elastin gene contains 34 exons and is located at chromosome 7q11.23 (Fazio et al., 1991). The elastin gene encodes multiple soluble precursor proteins, tropoelastins, through the process of alternative splicing. Tropoelastins are crosslinked into the insoluble protein polymer of elastin in the extracellular matrix (ECM). Due to elastin's insolubility, it wasn't until tropoelastin was isolated from copper deficient animals with inhibited cross-linking, that its primary structure was determined (Gray, Sandberg, & Foster, 1973).

1.2.3.1. Tropoelastin structure

Tropoelastin (TE) is about 70 kDa in size composed of alternating hydrophobic and hydrophilic domains. Each domain has a characteristic amino acid composition. Hydrophobic domains, accounting for about 82% of tropoelastin's overall sequence, contain oligopeptide repeat sequences between three and six amino acid long and rich in the non-polar amino acids glycine, valine, proline and leucine, with VGVAPG (V - valine, G – glycine, A- alanine, P – proline) repeats being the most common. Crosslink domains on the other hand contain an abundance of lysines involved in crosslinking and alanines which ensure an alpha-helical conformation for the correct spacing of lysines (Vrhovski & Weiss, 1998; Wise et al., 2014). It is the flexible hydrophobic domains that account for recoil. They have a disordered structure in the relaxed state, with many possible conformations, and therefore high entropy. When elastin is stretched, the hydrophobic domains become more ordered with reduced entropy (Figure 2). Thus, the recoil of elastin is driven by the second law of thermodynamics, which states that entropy of a closed system increases with time (Wise & Weiss, 2009).

In addition to hydrophobic and crosslink domains, all vertebrate tropoelastins contain a C-terminal domain capable of cell adhesion and interaction with other ECM proteins essential for elastic fiber formation (Keeley, 2013). The C-terminal region is highly conserved throughout evolution, responsible for the assembly of elastic fibers and contains the only two cysteine amino acids in all of tropoelastin. The two cysteines create a disulfide bond, that when disrupted, hinders fiber assembly (Jensen, Vrhovski, & Weiss, 2000; Vrhovski & Weiss, 1998; Wise et al., 2014). Tropoelastin (TE) has a moderately conserved sequence, but less conserved especially in

the hydrophobic domains from one species to another, suggesting an overall domain character is more important (Chung et al., 2006).

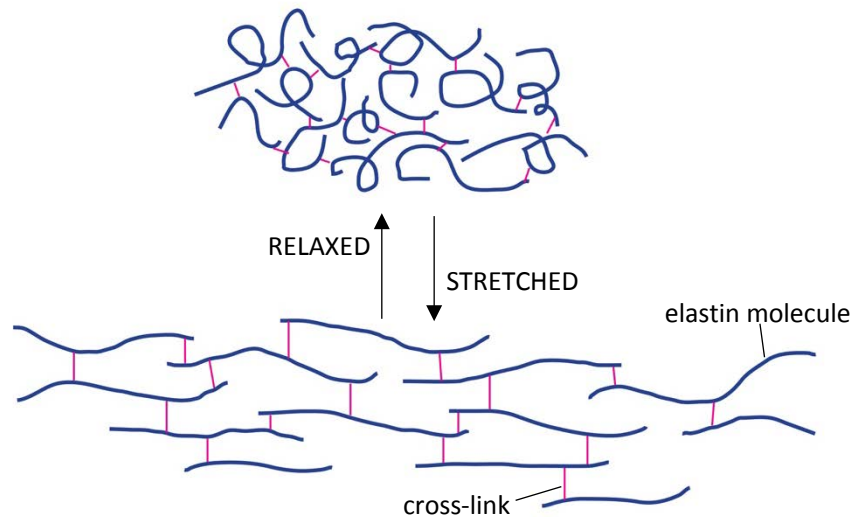


Figure 2. Molecular Basis of Elasticity

In mature elastin, tropoelastin monomers (blue) are crosslinked by desmosine or isodesmosine cross-links (pink). The monomers consist of flexible hydrophobic domains interspersed with cross-link domains. The protein chains in elastin remain disordered when in a relaxed state. Entropy is reduced upon stretching (below) and a more orderly conformation is obtained.

Tropoelastin's 3-dimensional structure was solved using small angle X-ray and neutron scattering experiments to reveal a structure composed of the N-terminus with a coil region, the C-terminus, bridge, foot, and hinge (Baldock et al., 2011). The N-terminal region likely plays a role in the protein's flexibility, structure, coacervation and integration into the ECM scaffold. It also contains a coiled region that may directly influence elasticity and the protein's overall structure. This role is also true of the hinge region, which consist of domains 21-23 and does not contain α -helices nor β -sheets, allowing it to change conformation. Whereas all other mammalian elastins retain

domain 22, in human elastin it is constitutively spliced out. Without domain 22, the structure becomes rigid (Yeo et al., 2016). The more recently discovered and still poorly understood bridge region encompasses domains 25 and 26, of which 26 is important for coacervation (Wise et al., 2014).

1.2.3.2. Biophysical properties of tropoelastin

Tropoelastin solutions can undergo a reversible phase separation process known as coacervation, the formation of droplets with high TE concentration suspended within a solution of low TE concentration (Cox, Starcher, & Urry, 1973; Kozel et al., 2006; Partridge, Davis, & Adair, 1955; B. C. Starcher & Urry, 1973). Increase in temperature, ionic strength and pH can induce coacervation (Ostuni, Bochicchio, Armentano, Bisaccia, & Tamburro, 2007; Vrhovski, Jensen, & Weiss, 1997) as can biomolecules such as GAGs, especially heparan sulfate (Y. Tu & Weiss, 2008, 2010), and integrins on the surface of cells. *In vitro* studies have shown that the process of coacervation occurs in two phases. The first phase is reversible, where the TE exists as a monomer and depends on a narrow window of temperature to begin assembling into a polymer as elastin. The second phase, maturation, is irreversible and has been shown through *in vitro* experiments to take place when temperatures reach levels close to normal body temperature of 37°C and a pH of 7 and kept for extended periods of time, allowing the coacervate to mature and tropoelastin molecules to more tightly bind each other (Bressan et al., 1986; Vrhovski et al., 1997; Vrhovski & Weiss, 1998).

1.2.3.3. Elastin crosslinking, longevity and degradation

Tropoelastin is secreted from smooth muscle cells, a variety of fibroblasts, and elastic chondrocytes and taken to the cell surface by elastin binding protein where it forms into globules, which are intermediate structures of elastic fiber formation (Czirok et al., 2006; Kozel et al., 2006). Next, the globules are deposited onto microfibrils and fused through active cell movements to make larger, branched structures stabilized by cross-linking. Lysyl oxidase (LOX) enzymes are needed to initialize the cross-linking through oxidizing of the lysine residues to produce α -amino adipic δ -semialdehyde (allysine). This is followed by spontaneous reactions forming cross-links, especially tetrafunctional desmosine and isodesmosine which are unique to elastin. Each is composed of three allysines and one lysine residue (Kagan & Li, 2003; Vrhovski & Weiss, 1998). It is the cross-linking that leads to a stable, mature elastin.

Elastin is produced early and has a long half-life. For example, human lung elastin has a mean carbon residence life of 74 years (Shapiro, Endicott, Province, Pierce, & Campbell, 1991). This longevity is partially explained by the resistance of elastin to degradation by most proteases. However, some proteases, called elastases, can degrade elastin and include the serine proteases neutrophil elastase, pancreatic elastase and cathepsin G as the most commonly seen in mammals (Vrhovski & Weiss, 1998). Matrix metalloproteinases (MMPs) -2, -9 and -12 also play a role in elastolysis (Van Doren, 2015). Controlled degradation of elastin is important for its other functions in wound healing, growth and tissue remodeling.

1.2.3.4. Expression and regulation of elastin

Studies of human skin fibroblasts, sheep ligaments, rat lungs and chick aorta have shown that mRNA expression and synthesis of elastin is highest during early development. Both the amount of mRNA and TE synthesis seem to impact how much elastin is made, possibly inhibiting its production if excess TE is accumulated in the ECM. In humans, the 5'-flanking region contains various transcription factor binding sites and activators, a CAAT promoter but no TATA box. Complementary RNA sequencing has shown that the elastin gene (*ELN*) has multiple transcription start sites. Comparison of transcript and gene sequences revealed substantial alternative splicing (Rosenbloom et al., 1991; Vrhovski & Weiss, 1998).

Elastin synthesis studies have shown a wide array of modulators that regulate elastin expression. In cell culture studies, soluble factors such as transforming growth factor- β (TGF β) (Kahari, Olsen, et al., 1992; Kuang et al., 2007), insulin-like growth factor-I (IGF-I) (Badesch, Lee, Parks, & Stenmark, 1989), and interleukin-1 β (IL- β) (Mauviel et al., 1993) upregulate expression of elastin (Milewicz, Urban, & Boyd, 2000). Tumor necrosis factor- α (TNF- α) (Kahari, Chen, Bashir, Rosenbloom, & Uitto, 1992), interferon- γ by inhibition of LOX (Song, Ford, Gordon, & Shanley, 2000), and vitamin D3 (Pierce, Kolodziej, & Parks, 1992) down-regulate elastin (Comper, 1996; Milewicz et al., 2000). Vitamin D3's effect on elastin was also demonstrated in a rabbit model. When an overdose of D3 was delivered transplacentally, the rabbits displayed SVAS-like pathology (Friedman & Roberts, 1966; Milewicz et al., 2000).

1.2.3.5. Alternative splicing of elastin

Elastin transcripts show significant variation (Indik et al., 1987). Alignments of human elastin have shown six exons to display some form of alternative splicing, with early alignments differing only in small segments of sequence (Uitto, Christiano, Kahari, Bashir, & Rosenbloom, 1991). Generally, there are two types of alternative splicing observed (Figure 3): 1. Complete excision of an exon, demonstrated by human exons 22, 23, and 32. 2. Only a portion of the exon is excised, through the use of either the 5' donor or 3' acceptor site, as seen with exon 26A. Extensive alternative splicing produces numerous isoforms of tropoelastin in humans. In some species such as the cow, the frequency of alternative splicing is up-regulated as the cow ages, seen more in adults than in the calf, demonstrating that developmental stage influence this process (Vrhovski & Weiss, 1998). Studies of various species have shown that alternative splicing is common, but species specific, and tissue-specificity has yet to be determined for the differing isoforms (Chung et al., 2006; Keeley, 2013).

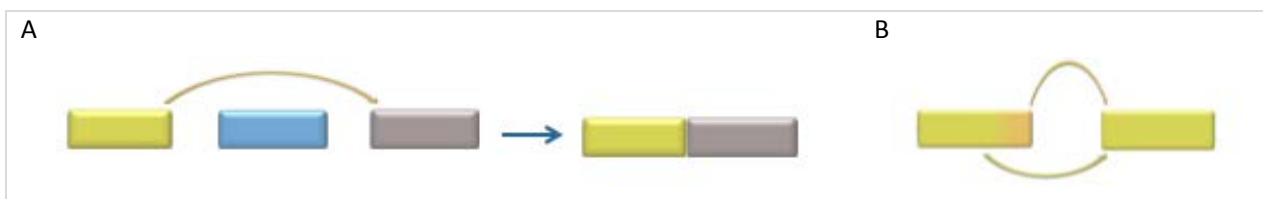


Figure 3. Types of Alternative Splicing Observed in Elastin

A) Complete excision of an exon. B) Portion of the exon is excised through an alternative 5' donor site.

1.2.3.6. Evolution of elastin

The evolution of elastin can be explained either through the conservation of the elastin sequence or the functional requirements of a species and its environment. The origin of tropoelastin is still unclear. Elastin is present in vertebrates, but absent in lower chordates and invertebrates, making it a rather new constituent of the ECM compared to collagens and fibrillins (Keeley, 2013). Elastin evolution has involved expansion of domains, making alignments of various species' entire elastin sequence futile. Variability in the sequence does not permit for alignment of mammalian, avian, amphibian and teleost tropoelastin, except for in the C-terminus where the amino acid sequence appears to be conserved throughout evolution (Chung et al., 2006; Keeley, 2013). Because of this, researchers have concentrated on sequence alignment scores instead. The result was clustering of exons from either the same species or between exons of similar structure; hydrophobic or cross-linking domains with minimal overlap between the two domain types. Extensive exon duplication can also be seen, for example, a 6-times multiplication of hydrophobic and crosslink exon pairs representing exons 20-31 in zebrafish (*Danio rerio*) *elna* (He et al., 2007). While there were certain motifs found throughout the various species, such as VPGVG for assembly coacervation and elasticity (Pepe et al., 2005), or PGVGA or PGVGV for self-assembly with fibrils, some motifs such as PGVGVA or GGVGVA resulted in abnormal tropoelastin aggregates in model peptides (He et al., 2007). However, it should be noted that short peptides may have different material behaviors when studied by themselves as opposed to in the context of the full-length TE molecule. Aside from the specific domain motifs found in elastin and TE, elastin may have adapted to a variety of species or taxons to fill a special functional role (Chung et al., 2006; Keeley, 2013). For example, in teleosts, elastin b (*elnb*) has evolved as a form of TE

specific to the bulbus arteriosus (BA) which helps regulate the pulsating pressure and protects the gills (Miao, Bruce, Bhanji, Davis, & Keeley, 2007).

Elastin's appearance coincides with the development of closed circulatory systems in higher organisms (R. P. Mecham, 2018). Amniotes and teleosts have vastly different blood pressures. The systolic blood pressure in humans and mice is 120 mmHg (Wang et al., 2013), whereas the rainbow trout has a systolic blood pressure of 35mmHg (Stevens & Randall, 1967; Wang et al., 2013). The elongation of hydrophobic domains in the teleosts may have allowed adaptation to altered physical demands. This is also demonstrated in zebrafish and other species with two *eln* genes (paralogues). The paralogue most similar to other organisms, *elna*, is expressed in the vascular tissue and functions similarly to other vertebrate elastins. In contrast, *elnb* has further diverged to have a specific function in the BA of teleosts (Keeley, 2013; Miao et al., 2007).

Elastin may have also adapted over time to function in varying environmental temperatures to allow for coacervation to take place at lower temperatures than the body temperatures of mammals. Frog and teleost elastin has a higher molecular weight and large numbers of repetitive exons, which are predicted to lower the coacervation temperature of tropoelastin. Elastin evolution is also seen in the extension and recoil cycles of heart and lungs, and varying heart rates of mammals. As with blood pressure, the rate at which a heart beats also varies widely, even among mammals alone; ~30 beats per minute in a whale to ~500 beats per minute in a mouse (Gosline, 1980). The TE sequence and rearrangements throughout evolution may be in part due to a response to the differing range of extension and recoil under which it must operate

(Keeley, 2013). These adaptations to tropoelastin throughout evolution may also be of significance in maintaining the integrity of elastic fibers, but more research is needed to show if such factors affect the matrix structure over time.

1.2.4. ELASTIC FIBER ASSEMBLY

Elastic fiber assembly is a complex, hierarchical process involving a number of proteins and their accessories early in development. They are made up of two ultra-structurally distinct components of the elastic fibers: an outer microfibrillar sheath composed of fibrillins and other accessory proteins that serve as a template which elastin can bind through its C-terminal domain, and an inner elastin core (Sato et al., 2007). To begin the process, fibrillin must form close to the cell surface into beaded microfibrils that mature to form parallel bundles of cross-linked microfibril regions. The elastin precursor, tropoelastin, then undergoes the process of coacervation which allows for proper alignment tropoelastin monomers for cross-linking by lysyl oxidase. Coupled to cell motion in a hierarchical, coordinated manner, the TE globules aggregate creating larger elastic fiber structures (Czirok et al., 2006; Kielty et al., 2002).

Elastin binding protein (EBP), integrins and GAGs, play integral parts in tropoelastin's ability to bind cells. It is through the C-terminal domain that tropoelastin interacts with GAGs and integrins to mediate fibroblast adhesion to tropoelastin. The EBP has a role in modulating cell behavior and assists with alignment of tropoelastin during self-assembly and preventing degradation of the protein (Almine et al., 2010). Although deposited mainly during late fetal stages and into

early neonatal periods, production of tropoelastin can be reactivated in the event of injury (Wise & Weiss, 2009). It also has the ability of influencing cell signaling and adhesion.

Further cross-linking of elastin creates a network of fibers facilitated by LOX, latent TGF β binding proteins (LTBPs) and fibulins, especially fibulin-4, to form the insoluble elastin core. This process of elastic fiber formation is referred to as “macro-assembly” (Baldwin et al., 2013). Elastic fiber formation can be tissue specific, depending on functional differences among tissues (Kielty et al., 2002). Elastic fibers that are not assembled correctly are the source of various diseases.

1.3. DISEASES CAUSED BY ELASTIN GENE MUTATIONS

Elastin is synthesized early during development and has remarkable longevity required for maintaining its function throughout life (Shapiro et al., 1991). Consequently, many common age-related diseases including hypertension (Arribas, Hinek, & Gonzalez, 2006), aneurysms (Halloran & Baxter, 1995) and emphysema (Shifren & Mecham, 2006) are associated with loss of compliance and gradual breakdown of elastin in tissues (Uitto, Ryhanen, Abraham, & Perejda, 1982). Human genetic studies provide evidence that elastic fiber abnormalities are not simply associated with age-related cardiovascular, pulmonary and connective tissue diseases, but can also cause them. Mutations in the elastin gene (ELN) can cause supravalvular aortic stenosis (SVAS) through a heterozygous loss of function mutation, and autosomal dominant cutis laxa (ADCL) by means of mutant elastin synthesis.

1.3.1 AUTOSOMAL DOMINANT CUTIS LAXA (ADCL)

Autosomal dominant cutis laxa (ADCL, OMIM #123700) is characterized by redundant, sagging and inelastic skin, aortic aneurysms, and emphysema and is caused by *ELN* mutations resulting in the synthesis of mutant elastin (Callewaert et al., 2011; Szabo et al., 2006; Urban, Gao, Pope, & Davis, 2005).

1.3.1.1. Clinical manifestations, natural history and management

Unlike the more severe autosomal recessive forms of cutis laxa, that sometimes leads to childhood death, ADCL manifests itself in a range of systems with mild to severe phenotypic results. In addition to the common loose, sagging skin that may worsen with age, typical facial features include a high forehead, enlarged earlobes and a beaked nose (Berk, Bentley, Bayliss, Lind, & Urban, 2012). Other systemic manifestations may encompass the gastrointestinal, pulmonary and cardiovascular systems with problems such as hernias, artery stenosis, dilation and tortuosity and emphysema (Tofolean et al., 2015; Weir, Joffe, Blaufuss, & Beighton, 1977). Management of systemic lesions and preventative checkups involving echocardiography and pulmonary function tests should be conducted to prevent complications. (Berk et al., 2012).

1.3.1.2. *ELN* Mutations in ADCL

Most ADCL-related mutations cause a frame-shift within the last 5 exons of *ELN* resulting in the production of a mutant tropoelastin where the C-terminus is replaced by an extended peptide sequence translated in the new reading frame past the wild type stop codon (Callewaert et al., 2011). This mutant protein has enhanced self-association properties but diminished binding

microfibrils, and thus interferes with elastic fiber formation in a dominant negative or a toxic gain of function manner (Callewaert et al., 2011; Q. Hu et al., 2010).

1.3.1.3. Molecular mechanisms of ADCL

Mouse models for ADCL have shown enlargement of airspace, emphysema, respiratory distress through a decrease in stiffness of the lung tissue, and premature death, but no skin abnormalities or cardiovascular pathologies (Q. Hu et al., 2010). Although increased endoplasmic reticulum (ER) stress and elevated TGF β signaling have been found in both human cells and a mouse model of ADCL, it remains unclear if these pathways contribute to the disease or if they could be targeted in treating ADCL.

1.3.2 SUPRAVALVULAR AORTIC STENOSIS (SVAS)

Supravalvular aortic stenosis (SVAS; OMIM 185500) is an obstructive cardiovascular disease affecting 1 in 20,000 live births causing a narrowing of the aorta and hypertension (Baldwin et al., 2013; Metcalfe et al., 2000). It is caused by a heterozygous loss of function mutation in the elastin gene (*ELN*) and is inherited autosomal dominantly. SVAS is a progressive disease with incomplete penetrance and variable expressivity (Merla, Brunetti-Pierri, Piccolo, Micale, & Loviglio, 2012; Metcalfe et al., 2000; Park, Seo, Yoo, & Kim, 2006; Pober, Johnson, & Urban, 2008; Wagenseil & Mecham, 2012).

1.3.2.1. Clinical manifestations, natural history and management

SVAS manifests at birth or in childhood as a narrowing of the ascending aorta and can be seen on its own as an isolated disease, or as part of Williams-Beuren syndrome (WBS; OMIM 194050). WBS is a complex developmental disorder associated with neurobehavioral, craniofacial, cardiovascular and metabolic abnormalities, caused by a microdeletion up to 1.8Mb in size at 7q11.23, a region that contains 27 genes including *ELN* (Merla et al., 2012; Micale et al., 2010; Pober et al., 2008).

The primarily affected artery in those with non-syndromic SVAS is the aorta, with thickening of the media (Figure 4) at the sinotubular junction (Figure 6) and can extend towards the ascending, transverse arch and descending aorta (McElhinney, Petrossian, Tworetzky, Silverman, & Hanley, 2000; Scott et al., 2009). Other branches such as those of the pulmonary (Figure 5, Figure 6) or coronary arteries have been observed with narrowing of the lumen as well, so determining the extent of vascular involvement is important in management of this disease. Patients typically present with a systolic murmur, although one is not always present, and become symptomatic by the age of twenty. Cases are divided into three categories with two of the lesions present as a physiological invagination: stenosis only present as a fibrous ring above the valve (10%), a diffuse narrowing of the ascending aorta with medial thickening (20%), and the most common type is an hourglass shaped stenosis that has medial layer thickening and sometimes accompanied by a thickened, fibrous intimal layer (70%). The stenosis of the artery causes blood pressure to become elevated in the left side of the heart, accompanied by enlargement and thickening of the cardiac muscle (Merla et al., 2012; Milewicz et al., 2000).

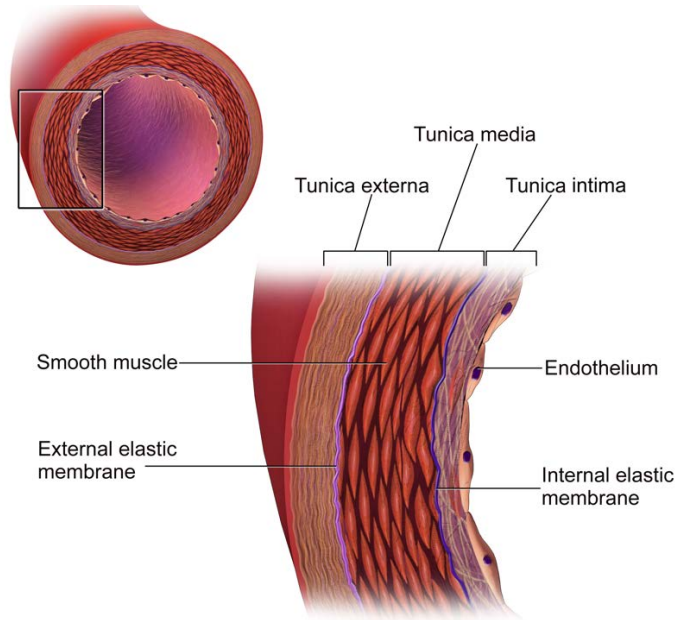


Figure 4. The Structure of an Artery Wall

Non-syndromic SVAS primarily affects the aorta and includes a thickening of the tunica media, made up of smooth muscle cells and elastin. Thickening of the media leads to a narrowing of the lumen. Blausen.com staff (2014). "Medical gallery of Blausen Medical 2014". *WikiJournal of Medicine* 1 (2). DOI: 10.15347/wjm/2014.010. ISSN 2002-4436.

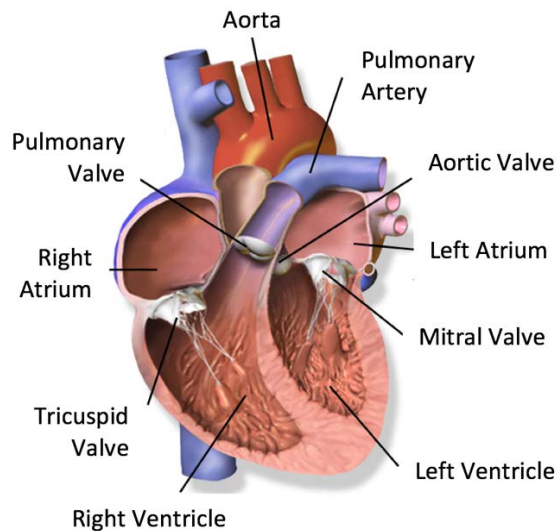


Figure 5 Anatomy of the Human Heart

The aorta is the primary affected vessel in SVAS, although other arteries including the pulmonary and coronary arteries may also contain a narrowing of the lumen. Blausen.com staff (2014). "Medical gallery of Blausen Medical 2014". *WikiJournal of Medicine* 1 (2). DOI:10.15347/wjm/2014.010. ISSN 2002-4436

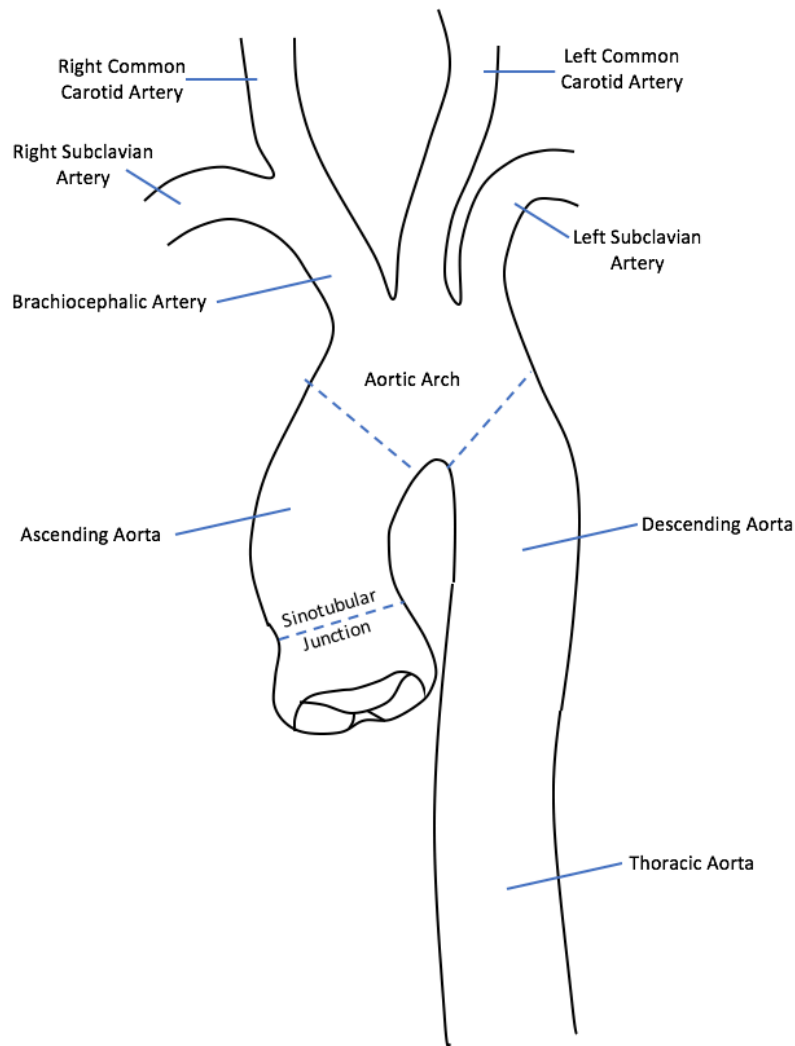


Figure 6 Segments of the Human Aorta

Diagnosis is best confirmed by echocardiography or a magnetic resonance angiography (MRA). Children diagnosed early benefit from timely surgical intervention to repair the diseased artery (Greutmann et al., 2012). However, surgical repair during infancy can be challenging and at higher risk of mortality if accompanied by concomitant lesions (Mitchell & Goldberg, 2011). In a group study of 113 adults, 55% of which had WBS, those without WBS had an increase in the severity of SVAS and associated more often with left ventricular outflow tract obstructions. Patients with

WBS displayed more often with mitral valve regurgitation. The study also found that adults remained at risk for cardiac complications and reoperation of the valve, but progression of the disease was rare (Greutmann et al., 2012).

The presenting aortic manifestations have been addressed as follows in some patients: removal of the affected area of the artery; balloon aortic catheter procedure to attempt to widen the stenosis; or incision of the artery to the root and augmentation with a tissue graft. No one type of surgical technique has shown to have an advantage over others in long term studies if the appropriate measures are taken to address the most prominent issue (McElhinney et al., 2000; Scott et al., 2009). Left untreated, SVAS has the potential to evolve into cardiac failure or death (Merla et al., 2012; Yeo, Keeley, & Weiss, 2011).

1.3.2.2. *ELN* Mutations in SVAS

Patients with SVAS have shown premature termination (nonsense or frameshift) mutations; some have splice site and very few have missense mutations or large deletions or translocations with breakpoints in the *ELN* gene (Metcalf et al., 2000; Micale et al., 2010; Milewicz et al., 2000; Yeo et al., 2011). *ELN* gene mutations in SVAS often lead to a truncated reading frame and nonsense-mediated decay of the mutant transcript resulting in an inactive, null allele (Dietz & Mecham, 2000; Urban et al., 2000; Yeo et al., 2011). The amount of tropoelastin secreted can be decreased in those with a splice site mutation (Urban et al., 1999). Alternatively, tropoelastin is secreted at normal levels but coacervation and assembly of the elastic fibers is hindered (Wachi et al., 2007; Wu & Weiss, 1999).

1.3.2.3. Molecular mechanisms of SVAS

The most widely supported molecular mechanism for SVAS is haploinsufficiency of the *ELN* gene (Baldwin et al., 2013; Micale et al., 2010). The haploinsufficiency can result from loss of an allele, unstable mRNA due to nonsense-mediated mRNA decay, or mutant protein production that hinders elastic fiber assembly (Dietz & Mecham, 2000). In a study conducted on patients with either isolated SVAS or syndromic WBS, patients exhibited a reduction in elastin mRNA levels resulting in low amounts of insoluble elastin deposition. In both cohorts, low levels of insoluble elastin in the artery walls led to an increase in proliferation of arterial SMCs and multilayer thickening of the tunica media, indicating that insoluble elastin is important for the regulation vascular cell division (Urban et al., 2002).

Mouse models have also been used extensively to study the molecular mechanisms of SVAS. Mice lacking elastin (*Eln*^{-/-}) due to a deletion of exon 1 and a portion of the promoter region, exhibited a perinatal lethal phenotype with an increase in vascular wall SMC proliferation that obstructed the artery lumen (Li, Brooke, et al., 1998). A model hemizygous for *ELN* (*Eln*^{+/-}), like that seen in SVAS human patients did not have an obvious phenotype and had similar appearance and longevity when compared to the wildtype (*Eln*^{+/+}) mice. Upon closer inspection of the vessels, the hemizygous mice had a 50% decrease in *Eln* mRNA at birth, with thinner lamellae. Although not all human SVAS characteristics were displayed, changes in the arterial wall was similar with characteristically increased number of lamellae, and increased blood pressure (Li, Faury, et al., 1998). A third study in an SVAS mouse model found an increase in integrin levels in the aorta of *Eln*^{-/-} mice. Integrin β 1 was increased in the endothelial cells and some SMCs of the outer smooth

muscle layers, and integrin $\beta 3$ was up-regulated in SMCs of the medial layer of the *Eln*^{-/-} aorta causing narrowing of the lumen. Inhibition of integrin $\beta 3$ reduced the hyper-muscularization and stenosis (Ashish Misra et al., 2016). Results seen in these murine models suggest that the absence of elastin has effect on cell proliferation, adhesion and fate determination through downregulation of integrin expression and signaling. Fibrillins are potent ligands of integrins (Bax et al., 2003), therefore, elastin may inhibit integrin signaling by masking integrin ligands on microfibrils as a part of elastic fiber formation.

Although other congenital heart defects (CHD) such as mitral valve prolapse, mitral valve insufficiency and bicuspid aortic valves are less common in WBS compared to SVAS (Lacro & Smooth, 2006) studies have nonetheless shown that elastin haploinsufficiency can affect valve development. *Eln*^{+/-} mice had normal ECM organization except for in the aorta at birth. As the mice aged, valves became thin and elongated with increased ECM disorganization, tensile stiffening, increased valve interstitial cell proliferation and elastin fragmentation. Valve disease which included regurgitation in the aortic valve became progressively worse in the *ELN*^{+/-} mice, with 70% of older adults displaying the valve abnormalities, establishing elastin's role in valve pathogenesis. These same mice also exhibited a decrease in TGF- β signaling in cardiac valves (Hinton et al., 2010).

1.4. CARDIOVASCULAR DEVELOPMENT IN ZEBRAFISH

As a disease model, zebrafish have come to be widely used for developmental biology studies due to their external fertilization, large numbers of offspring, and access to all stages of rapid development. Zebrafish embryos are transparent, and the heart is located in a prominent ventral position that allows for noninvasive *in vivo* observation of the cardiovascular system from the time of fertilization throughout the heart and vasculature's development in the embryo (Bakkers, 2011; Bournele & Beis, 2016; Lieschke & Currie, 2007; Nguyen, Lu, Wang, & Chen, 2008; S. Tu & Chi, 2012). Another advantage is the ease with which the developing embryo is able to be imaged. Fluorescent transgenic lines allow for easy visualization of cardiac and smooth muscle cells to determine cell differentiation (Bakkers, 2011; Lieschke & Currie, 2007). Zebrafish are also not dependent on the cardiovascular system within the first 7 days of life. Oxygen is acquired in sufficient amounts through passive diffusion (Pelster & Burggren, 1996), facilitating analysis of cardiac valve formation and the effects of mutations that would otherwise be lethal in mammals (Bournele & Beis, 2016). When compared to human cardiac disease-related genes, the Online Mendelian Inheritance in Man (OMIM) database shows that at least 82% of those genes contain at least one zebrafish ortholog. These genes are easily manipulated in the zebrafish and provide opportunities to study their function, especially in diseases of the cardiovascular system's development (Asnani & Peterson, 2014).

In vertebrates, the heart is the first functional organ formed (Moorman, Webb, Brown, Lamers, & Anderson, 2003; Schroeder, Jackson, Lee, & Camenisch, 2003). The zebrafish heart is made up

of four compartments that pump deoxygenated blood to the gills for oxygenation. The four parts are the sinus venosus, the atrium, the ventricle and the bulbus arteriosus (N. Hu, Sedmera, Yost, & Clark, 2000). The bulbus arteriosus is an elastic reservoir seen in the teleost outflow tract (OFT), comprised of smooth muscle cells and abundant elastic fibers, that absorbs high volumes of blood and prevents gill damage due to high blood pressure. (Grimes, Stadt, Shepherd, & Kirby, 2006; José M. Icardo, 2017; S. Tu & Chi, 2012).

Despite the human heart containing four chambers (two atria and two ventricles), and the absence of a separate pulmonary circulatory system in the zebrafish (S. Tu & Chi, 2012), there are similarities between the two chambers in zebrafish to those of the human that may lead to a better understanding of cardiovascular pathologies (Asnani & Peterson, 2014). Both humans and zebrafish undergo similar cardiovascular morphogenetic development (Figure 7). The cardiac cells of zebrafish start off laterally and migrate to the midline during segmentation to form a primitive heart tube. The heart tube develops through formation of a cardiac disc structure fused at the midline. This is followed by cardiac looping at 36 hours post fertilization (hpf) where it differentiates into the chambers. Development is rapid and by 24 hpf, the embryo's primitive heart tube begins peristaltic contractions which transition to coordinated chamber contractions by 48 hpf (Bakkers, 2011; Nguyen et al., 2008; Yelon, 2001). The valves of the zebrafish heart appear at 5 dpf (N. Hu et al., 2000) but they are not mature, developing further in two phases. During the initial phase through 16 dpf the valves elongate, followed by maturation in which the ECM collagen and elastin deposits thicken the valve structures (Martin & Bartman, 2009).

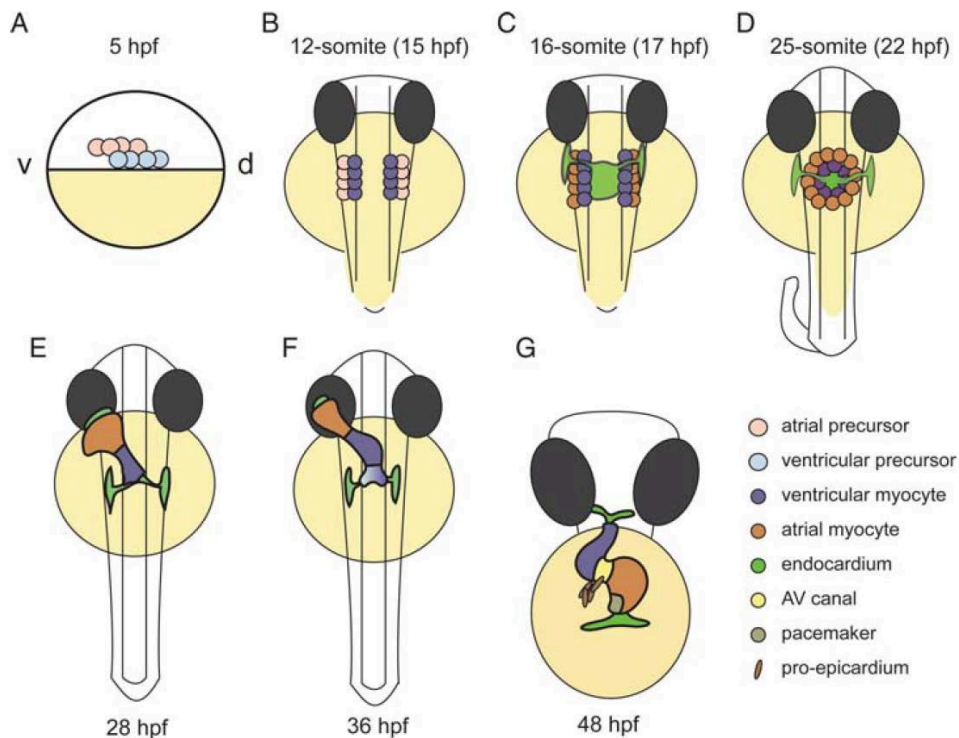


Figure 7. Stages of Cardiac Development

A) The cardiac progenitor cells (pink and blue) of zebrafish start off laterally and migrate to the midline during segmentation to form a primitive heart tube (D). The heart tube develops through formation of a cardiac disc structure fused at the midline and the endocardium (green) forms the inner lining. This is followed by cardiac looping (F) at 36 hours post fertilization (hpf) where the ventricle moves towards the midline and the structure differentiates into the chambers. Looping continues and forms an S-shaped loop (G). Development is rapid and by 24 hpf, the embryo's primitive heart tube begins peristaltic contractions which transition to coordinated chamber contractions by 48 hpf. Bakkers, J. (2011). Zebrafish as a model to study cardiac development and human cardiac disease. *Cardiovasc Res*, 91(2), 279-288. doi:10.1093/cvr/cvr098. Obtained for use with permission from publisher.

Some examples of how zebrafish express mutations analogous to human cardiovascular disease are as follows: the gridlock mutation (*grl*) in the *hey2* gene causes circulation development to fail by blocking aortic blood flow through occlusion of the proximal aorta, as seen in human aortic coarctation (Weinstein, Stemple, Driever, & Fishman, 1995; Zhong, Rosenberg, Mohideen,

Weinstein, & Fishman, 2000). Symptoms similar to human arrhythmias of type 2 long QT, where the atrium contracts twice and the ventricle once, are seen in fish of the *breakdance (bre)* mutation (Chen et al., 1996; Langheinrich, Vacun, & Wagner, 2003).

Zebrafish have also shown to be important in understanding advanced heart failure and end-stage cardiomyopathy in humans and could provide future insight into small molecule drug treatments. Adult zebrafish have the ability to regenerate their ventricular tissue through dedifferentiation of cardiomyocytes, where cells revert to earlier developmental stages, and express a molecular marker important in cardiac development, *gata4* (Asnani & Peterson, 2014; Jopling et al., 2010; Kikuchi, 2014; Kikuchi et al., 2010).

Mutations in zebrafish also have the potential to increase the understanding of certain cardiovascular developmental regulations in the human and may help explain how embryonic myocardial function mutations lead to congenital heart disease in humans and impact valve development (Asnani & Peterson, 2014; Bartman et al., 2004). Embryos with the *silent heart (sih^{-/-}; or tnnt2a)* and *cardiofunk (cfk^{-/-})* mutations, have irregularities in valve development and lack contraction as well as early blood flow (Bartman et al., 2004). A separate study has shown that endocardial cells differentiate in response to Notch signaling before the mesenchyme in valve formation (Beis et al., 2005). With the ability to easily observe cardiovascular development in the zebrafish, various groups have identified numerous genes that regulate cardiac patterning, cell fate determination and morphogenesis at various stages (Chen et al., 1996; Singh et al., 2016; Stainier et al., 1996; Yelon, 2001) (Table 1).

Table 1. Examples of Genes Related to Zebrafish Cardiovascular Development

Zebrafish Gene Name	Phenotype	Zebrafish Mutant	Human Gene Name	Related Human Cardiovascular Disease	Reference
<i>hey2</i> alias: <i>grl</i>	circulation fails to develop, blockage of aortic bloodflow	Gridlock (<i>grl^{-/-}</i>)	<i>HEY2</i>	aortic coarctation	(Weinstein et al., 1995; Zhong et al., 2000)
<i>bre</i>	type 2 arrhythmia (long QT)	Breakdance (<i>bre^{-/-}</i>)		type 2 arrhythmia	(Chen et al., 1996; Langheinrich et al., 2003)
<i>tnnt2a</i>	lack of contractility/heart beat	Silent heart (<i>sih^{-/-}</i>)	<i>TNNT2</i>	Familial hypertrophic cardiomyopathy	(Bartman et al., 2004)
<i>acta1b</i>	cardiac dilation and no early bloodflow	Cardiofunk (<i>cfk^{-/-}</i>)	<i>ACTA1</i>	structural congenital heart disease	(Bartman et al., 2004)
<i>tbx2b</i>	impaired heart valve formation	Ping pong (<i>png^{+/-}</i>)	<i>TBX2</i>	--	(Just, Hirth, Berger, Fishman, & Rottbauer, 2016)
<i>ugdh</i>	heart valve formation initiation impaired	Jekyll (<i>jek^{-/-}</i>)	<i>UGDH</i>	--	(Walsh & Stainier, 2001)

1.5. ZEBRAFISH AS A MODEL IN ELASTIN STUDIES

Zebrafish offer further advantages for elastin studies. Peak elastin expression occurs during the late fetal and early perinatal period in mammals (Kelleher, McLean, & Mecham, 2004) when the animals are less accessible to experimental manipulations. In contrast, zebrafish embryos and larvae have developmental stages with peak elastin expression (Miao et al., 2007) that are continually accessible and amenable to *in vivo* imaging. While the zebrafish elastin genes have been sequenced in their entirety, for comparison to each other and other species (Chung et al., 2006; He et al., 2007), little has been published regarding the diversity of these gene transcripts in zebrafish.

A limitation of zebrafish in genetic studies is that many of the human genes have two paralogs in zebrafish. Zebrafish have two tropoelastin genes, *elna* and *elnb*, due to whole-genome duplication in teleosts (Chung et al., 2006). The orthologous relationships are sometimes challenging to establish, but not so for elastin, where sequence similarity, the size of the encoded protein and expression pattern supports *elna* (Table 2) as the ortholog of human elastin (Keeley, 2013; Miao et al., 2007). Nevertheless, work on both elastin genes is of importance, as localized expression of *elnb* to the bulbus arteriosus (outflow tract of the heart), presents an opportunity to obtain mutants with phenotypes limited to this organ.

Table 2. Human and Zebrafish Elastin Genes

	Human	Zebrafish (2 genes)	
Gene(s)	<i>ELN</i>	<i>elna</i>	<i>elnb</i>
Exons	34 exons	56 exons	58 exons
Location	7q11.23	chromosome 15	chromosome 21
Coding sequence size	2.3kb	3.5kb	6.2kb
Protein weight	69kDa	~100 kDa	~170 kDa

There is some overlap of elastin expression in the zebrafish larvae. Previous research has shown that *elna* first appears in the brain at 1-day post fertilization (dpf). At 2 dpf it is in the cerebral ventricles, at 3 dpf it is present in the bulbus arteriosus (BA) and outflow tract and by 4 dpf *elna* is in the swim bladder. On the other hand, *elnb* does not appear until 3 dpf in the BA. At 4 dpf it is in the cranium, BA and in the swimbladder at 5 dpf. Both *elna* and *elnb* peak at 6-7 dpf, but *elna* is only expressed 24 times stronger at this time point than at 1 dpf, while *elnb* is 300 times more expressed. Transcript abundance begins to decrease at 8 dpf and reaches a basal expression at 23 dpf in both genes (Miao et al., 2007). Recently, zebrafish *elnb* morphants and mutants were found to have cardiac outflow tracts populated by cardiomyocytes instead of smooth muscle cells observed in control fish, indicating that *elnb* is essential for correct cell fate decisions in the developing teleost heart (Moriyama et al., 2016).

While research has been done on the development of the cardiovascular system in zebrafish, not much is known about elastin's role in its development, especially the valve leaflets. In humans, the valve cusps contain about 50% collagen and 13% elastin (Bashey, Torii, & Angrist, 1967). In

porcine aortic valve leaflets, elastin is required to maintain tissue integrity and to assist in returning the valves to their original shape through recoil once pressure from blood flow has ceased (Vesely, 1998). Research conducted in the teleost family, which includes zebrafish, has shown that the atrioventricular (AV) region of the heart gives rise to the valves through signaling pathways, conserved from zebrafish to mammals (J. M. Icardo & Colvee, 2011). The Notch pathway regulates bone morphogenetic protein (Bmp) signaling and defines the atrioventricular canal and inner curvature areas of the heart (Rutenberg et al., 2006). Notch (Timmerman et al., 2004), Wnt/ β -catenin (Hurlstone et al., 2003), *Itbp3*-TGF β (Zhou et al., 2011) and Cox2 (Scherz, Huisken, Sahai-Hernandez, & Stainier, 2008) are needed for proper formation of the heart's endocardial cushions and valves. Due to this conservation of elastin from zebrafish to humans, further research of elastin's role in zebrafish cardiovascular development can lend some insight into human cardiovascular diseases.

1.6. PUBLIC HEALTH SIGNIFICANCE

Rare diseases are defined as having a prevalence of less than 4-5/10,000 (Richter et al., 2015) or less than 200,000 affected individuals in the United States, as specified in a 1984 amendment to the Orphan Drug Act (P.L. 97-414) of 1983. Although individually uncommon, rare diseases collectively affect approximately 25 million people in the US or about 10 % of the population. Many of 5,000-8,000 rare diseases are genetic in origin, which provides a clear path to understanding their cause and developing treatments for them. However, the large number of

different diseases and the scarcity of individuals affected by each pose a substantial challenge to progress and represent a major unmet medical need (Medicine, 2010).

Animal models are essential for understanding the developmental and physiological basis of disease and as tools to develop and test therapeutic approaches (Simmons, 2008). The main goal of my study was to establish and characterize zebrafish with mutations in the elastin genes as possible models for SVAS, an obstructive cardiovascular disease affecting 1 in 20,000 live births that causes a narrowing of the aorta and hypertension (Baldwin et al., 2013; Metcalfe et al., 2000) that occurs as isolated, familial condition (OMIM 185500), or as a part of a multisystem developmental disorder, Williams-Beuren syndrome (OMIM 194050).

The mechanistic and therapeutic insights from rare diseases are often applicable to common disorders because of a shared underlying biological pathway (Bauer-Mehren et al., 2011) or similarities in clinical presentation. The association of SVAS with hypertension (Wagenseil & Mecham, 2012), valvular defects (Greutmann et al., 2012) and other congenital heart defects (CHDs) is of broader public health relevance. The Centers for Disease Control and Prevention report that 1 in 3 adults suffers from hypertension and costs the United States \$46 billion each year ("High Blood Pressure Facts," 2018; Nwankwo, Yoon, Burt, & Gu, 2013). Cardiovascular disease accounts for about 17 million deaths per year worldwide ("Cardiovascular diseases (CVDs)," 2017) and in 2014 at least 1,100 deaths each day were due to hypertension in the United States alone ("High Blood Pressure Facts," 2018). About 40,000 infants in the United States are born each year with CHDs, the leading cause of birth defect related death, and over 2 million

people from infants to adults had some form of a CHD in 2010. Overall hospital costs for patients with CHD totaled about \$1.4 billion in 2004, with the average cost per patient increasing based on the severity of their CHD ("Data & Statistics," 2018).

1.7. DISSERTATION AIMS

Zebrafish have two tropoelastin genes, *elna* and *elnb*. While research has been done to sequence the genes in their entirety, for comparison to each other and other species (Chung et al., 2006; He et al., 2007), little has been published about the genetic diversity of these gene transcripts in zebrafish. Characterizing the genetic and transcript diversity is important since genetic diversity helps to explain how adapting genomes contribute to the survival of a species. In addition, the sequence variation in the zebrafish elastin genes critically affects the design and interpretation of experiments that genetically manipulate them.

While extensive research has been done on the development of the cardiovascular system in zebrafish, elastin's role has received less attention. Only recently, zebrafish *elnb* morphants and mutants were found to have cardiac outflow tracts populated by cardiomyocytes instead of smooth muscle cells observed in control fish, indicating that *elnb* is essential for correct cell fate decisions in the developing heart (Moriyama et al., 2016).

The main goal of this research is to generate and characterize a set of SVAS-like mutant zebrafish lines. The animals will be valuable tools for the understanding and development of molecular

mechanisms of elastin-related disorders and targeted treatments, as the zebrafish is an excellent animal model for small molecule screening and chemical genetics (Murphey & Zon, 2006).

Based on published knowledge, I hypothesize that elastins are essential for the development of specific components of the cardiovascular system, including the cardiac valves and outflow tract. To address this hypothesis, the developmental and physiological consequences of elastin mutations in an *in vivo* zebrafish model must be investigated. Therefore, two specific aims were pursued:

Aim 1: Characterize the genetic and transcript diversity of *elna* and *elnb* in zebrafish by sequencing cDNA clones.

Aim 2: Characterize *elna* and *elnb* mutants by genetic and gene expression studies, investigate the cardiovascular and connective tissue phenotypes of mutants using transgenic reporter fish, confocal and video microscopy and echocardiography.

2.0 METHODS

2.1. ZEBRAFISH MAINTENANCE AND CARE

Adult zebrafish (*Danio rerio*) were housed in the Zebrafish Facility of the University of Pittsburgh. Animal maintenance and husbandry was conducted according to the facility's standard operating procedures, NIH guidelines and The Zebrafish Book (Westerfield, 2007), and a research protocol approved by the University of Pittsburgh Institutional Animal Care and Use Committee (IACUC). To limit pain and discomfort, the FDA-approved anesthetic tricaine (ethyl 3-aminobenzoate methylsulfonate) is prepared as a 4mg/mL solution and used as a 0.16mg/mL solution in tank water to minimize stress in handling fish when immobilizing for injection or photographic procedures. Embryos were staged using published guidelines (Kimmel, Ballard, Kimmel, Ullmann, & Schilling, 1995) and grown at 28.5°C in 30% Danieau solution [17mM NaCl, 2mM KCl, 0.12mM MgSO₄, 1.8 mM Ca(NO₃)₂, 1.5mM HEPES]. In cases where melanin development had to be prevented, the embryo medium also included 0.0003% phenylthiourea (PTU).

2.2. ZEBRAFISH LINES

The wildtype (WT) Tü/AB* line of fish is a cross between the wildtype Tübingen and AB lines (Staff, 2016). These fish are from established lines maintained in the lab. For *elna* and *elnb*,

mutant lines were obtained from the Sanger Institute Zebrafish Mutation Project, *elna*^{sa12235}, c.264T>A, p.Tyr88* and *elnb*^{sa24024}, c.1771C>T, p.Gly591Asp. Several rounds of breeding were done to establish a homozygous mutant *elna*^{sa/sa} and *elnb*^{sa/sa} lines. (For brevity, I will use *elna*^{sa} and *elnb*^{sa} for these mutants throughout the dissertation.) Homozygous mutants (*elna*^{sa/sa}) were outcrossed with a Tg(*acta2:mCherry*)^{ca8};Tg(*myl7:eGFP*)^{twu34} transgenic line to develop a double transgenic mutant line of *elna* fish (Raya et al., 2003; Whitesell et al., 2014).

2.3. EXISTING TRANSCRIPT INFORMATION

Transcript sequences of *elna* and *elnb* were downloaded from the GenBank database of *elna* & *elnb* and imported into CLC Main Workbench 6 to be used as reference sequences. *elna* reference sequences are NM_001080063, and XM_009291325.1 – XM_009291348.1, and *elnb* reference sequences are NM_001048064.1, NM_001048064.2, and XM_005161444.1. The XM prefix associated with these sequences indicate model RefSeqs that contain differences, errors, or gaps in the sequence either predicted or from submissions and vary from the NM curated sequences available. The pipelines used to create these prediction sequences are automated and periodically the data are refreshed, and the sequences eliminated from the database ("The NCBI Eukaryotic Genome Annotation Pipeline," 2018). At the time of the download, June 15, 2015, these were the available reference sequences.

2.4. RNA EXTRACTION FOR TRANSCRIPT CLONING AND QUALITY CONTROL

Total RNA was extracted from thirty 72 hours post fertilization (hpf) WT Tü/AB* larvae from a single clutch obtained by group breeding of 13 adults. I used 500µL Trizol and immediate homogenization with a pestle homogenizer. For phase separation, 50µL of BCP was added, shaken manually for 15 seconds to form an emulsion, incubated on ice for 5 minutes, then subjected to centrifugation at 12,000xg for 10 minutes at 4°C. The aqueous phase on top was transferred to a Qiagen RNeasy spin column from the RNeasy Mini Kit. The rest of RNA extraction was conducted by following the RNeasy protocol. Final concentrations of RNA were measured using UV spectrophotometry. RNA integrity was verified by agarose gel electrophoresis.

2.5. REVERSE TRANSCRIPTION AND POLYMERASE CHAIN REACTION (RT-PCR)

Reverse transcription was conducted using the Superscript IV Reverse Transcriptase Kit (Invitrogen) following the manufacturer's instructions using 1µg of RNA and random hexamers. PCR amplification of *elna* and *elnb* cDNA fragments was done using the Qiagen Multiplex Kit with HotStarTaq DNA Polymerase using primer sets (Table 29, Table 30), with a 30 second annealing time, 1-minute extension for amplicons up to 1 kb, 3-minute extension for amplicons over 1 kb, and 35 total cycles. The sizes and quality of RT-PCR products were verified by agarose gel electrophoresis.

2.6. MOLECULAR CLONING, SEQUENCING, AND SNP CONFIRMATION

Amplicons were cloned using the pCR™II-TOPO® TA vector with the TOPO Cloning Kit (Invitrogen) into One Shot® TOP10 chemically competent *E. coli* cells and plated onto LB agarose with ampicillin overnight at 37°C. Following incubation, colonies were picked and incubated overnight in 2mL LB Broth with 100 µg/mL ampicillin. Plasmid DNA was isolated using the Monarch Plasmid Miniprep Kit (New England Biolabs) according to the manufacturer's instructions. For the final step, the plasmids were eluted from the column using 20µL of Elution Buffer to achieve high concentration, which was measured by UV spectrophotometry. Plasmid clones were digested with EcoRI to liberate the cDNA fragments and confirm their size by agarose gel electrophoresis. Plasmid clones were subjected to fluorescent dideoxy cycle sequencing using primers complementary to the plasmid backbone and additional, regularly spaced internal primers, (Table 31, Table 32) against the cDNA. Operon was used as a sequencing service provider. Sequence traces were imported into Sequencher v5.4, were trimmed to remove low quality regions and aligned. Vector sequences were removed. The alignments contained complete bidirectional coverage of each cDNA clone with the depth of coverage ranging 2-6. Complete cDNA clone sequences were imported into CLC Main Workbench v6 and annotated for exon and variant content using sequence searching and multiple alignment functions.

Exon-exon boundaries were confirmed by comparisons against cDNA and genomic reference sequences. Amplification primer sequences were trimmed, and sequences were exported in FASTA format for submission to GenBank using the BankIt web interface. The splice site scores

were determined using a website algorithm (Reese, 2018). Variants with existing rs numbers were identified through data mining on the Ensembl website. Filters were applied to narrow down existing variants that were similar to those found in the sequences.

2.7. SNP CONFIRMATION IN gDNA

Confirmation of single nucleotide polymorphisms (SNPs) found in the cDNA from embryos was executed using gDNA from tail-clips of the adult zebrafish parents of the clutch. gDNA was amplified using the Qiagen Multiplex Kit with HotStarTaq DNA Polymerase and sets of primers (Table 3, Table 4), with a 30 second annealing time, 30 second extension and a total of 32 total cycles. PCR products underwent quality control by agarose gel electrophoresis, were treated with exonuclease I and shrimp alkaline phosphatase using 1 μ L of ExoSAP-IT (Thermo Fisher Scientific) in a reaction with 5 μ L of PCR sample and 9 μ L of water. The reaction was incubated for 40 minutes at 37°C followed by 20 minutes at 80°C to inactivate the enzymes. Samples were then sent to sequence using the Operon service and analyzed with the Sequencher v5.4 software.

Table 3. Primers to Confirm SNPs in *elna* gDNA

Primer Name	Sequence	Intron (I) or Exon (E) #
zf <i>elna</i> I10.1s*	TCAAACCTCGTGATCATCAT	10 (I)
zf <i>elna</i> I10.2s*	TAGCTGCCCTCCATTACACAG	10 (I)
zf <i>elna</i> I14.1s*	ACCATGAGTATTGTCTGCT	14 (I)
zf <i>elna</i> I17.1a*	AGACCAACCTATCCCAGCAA	17 (I)
zf <i>elna</i> I33.1s*	TTCAGCAGGGATAGCATATTC	33 (I)
zf <i>elna</i> I35.1a*	AGACAGCTGAAACAGAAAAG	35 (I)
zf <i>elna</i> I36.1s*	TCTGAGGTTTTGAGGATTGT	36 (I)
zf <i>elna</i> I39.1a*	ATAAAGGGACTAAGCCGAAA	39 (I)
zf <i>elna</i> I40.1s*	ATGTGGCAATGTTGTGTATG	40 (I)
zf <i>elna</i> I45E46.1a*	GAAGCTTGGCTGTGGATAGA	45 (I), 46 (E)
zf <i>elna</i> I50.1s*	TGAACAGCAGACAGACAGTA	50 (I)
zf <i>elna</i> I51.1a*	ACAACACCACCTTCATCTCCA	51 (I)
zf <i>elna</i> I13.1a*	TTATTGGGTGCTAAAGCTGG	13 (I)
zf <i>elna</i> I35.2a*	AATACTCGATTCACACTCAG	35 (I)
zf <i>elna</i> I39.2a*	ATAAGTTGGCGGTTTCATTCC	39 (I)
zf <i>elna</i> I43.1s*	ACCAACGAACAGGTCACAAT	43 (I)
zf <i>elna</i> I41.1a*	GAAACGCACTGTTATGACAA	41 (I)
zf <i>elna</i> I50.2s*	AAACAGCCCAACGGGTCAAA	50 (I)

Table 4. Primers to Confirm SNPs in *elnb* gDNA

Primer Name	Sequence	Intron (I) or Exon (E) #
<i>zf elnb</i> I6E7.1s	TGCTTAAAGGTGTGGGTGGA	6 (I), 7 (E)
<i>zf elnb</i> I9E10.1a	ACCATAGCCACCTAAAAACA	9 (I), 10 (E)
<i>zf elnb</i> I9E10.2a	ATAAATACCTCCTGGCCCAC	9 (I), 10 (E)
<i>zf elnb</i> E31I31.1s	ATGGTACGGGGAAATGAAAC	13 (I)
<i>zf elnb</i> E33.1a	TTTAAGGCTTTTGTCCAC	33 (I)
<i>zf elnb</i> I33.1a	AAAGCTGCAGAACAAAACAC	33 (I)
<i>zf elnb</i> E40.1s	TGATTGGCAGCCCTGATGG	40 (I)
<i>zf elnb</i> I40.1s	ACCCAATACCTAACCACAAC	40 (I)
<i>zf elnb</i> I43.1a	AAAATGCTAAGAGTCACGAG	43 (I)
<i>zf elnb</i> E47.2a	AATCCTGTGCCTGCAGCTC	47 (E)
<i>zf elnb</i> E47.3a	CAACACCTCCAACCTCAAGA	47 (E)
<i>zf elnb</i> I33.2s	GACATTGTGTTTTGTTCTGC	33 (I)
<i>zf elnb</i> I34.1a	AGTTGATCAGACTACAGCAT	34 (I)
<i>zf elnb</i> I50.1a	ACCCATGTTAACCCAAAACCT	50 (I)
<i>zf elnb</i> I50.2a	GAAAATCCAAAAAGAGCCAC	50 (I)

2.8. GENOTYPING OF ZEBRAFISH BY dCAPS

Confirmation of the mutations (*elna*^{sa12235}, c.264T>A, p.Tyr88*) and (*elnb*^{sa24024}, c.1771C>T, p.Gly591Asp) in mutants obtained from the Sanger Institute Zebrafish Mutation Project was done by genotyping using the derived cleaved amplified polymorphic sequences (dCAPS) method (Neff, Neff, Chory, & Pepper, 1998). The technique requires the creation of primers that introduce a polymorphism based on the target mutation and induce a restriction endonuclease recognition site in either the mutant or WT DNA sequence through base mismatch. Primers (Table 5) were designed using a web-based primer design software to detect the mutations (Neff, Turk, & Kalishman, 2002). Genotyping was performed on whole embryos and adult tail-clip biopsies. Genomic DNA (gDNA) was isolated using the DNeasy Blood and Tissue Kit (QIAGEN). 10ng of gDNA was used for each PCR amplification reaction. The amplifications for *elna* and *elnb* were digested at 37°C for 90 minutes, using DdeI and Hpy188I respectively, and run on 3% Metaphor agarose gel. DNA sequencing was done with the service provider Operon.

Table 5. dCAPS Primers for Genotyping *elna* and *elnb*

Gene Amp	Amp Size (bp)	Primer Name	Exon	Sequence	Enzyme	Enzyme Recognition Sequence
<i>elna</i>	276	zf <i>elna</i> l4E5s*DdeI	intron 4 – exon 5	TATCTCTCTGGCTGTAGGTGG <u>C</u> TA	DdeI	5'...C [^] TNAG...3'
		zf <i>elna</i> E6.1a*	6	ACCTCCAGGCAGAACTCCTC		
<i>elnb</i>	285	zf <i>elnb</i> E17.1s Hpy188I	17	TCTCAGGCTAAAGCTGCCAAGT <u>C</u> TG	Hpy188I	5'...TCN [^] GA...3'
		zf <i>elnb</i> E18.3a	18	AATGCCTCCAACACCTGGTA		

For both *elna* and *elnb*, the C mismatch (green and underlined) changed an A base in the original sequence. The enzyme cutting site (indicated by ^ in the recognition sequence) targeted the mutant alleles (*elna*: T>A, *elnb*: C>T). If the mutant allele was present, the enzyme would cut.

2.9. RNA ISOLATION TO STUDY THE EXPRESSION OF MUTATIONS

Total RNA was extracted from adult zebrafish hearts, swim bladders, tail-clips and 10-30 embryos using the same method as described in Section 2.4. The number of embryos was dependent on their age. Reverse transcription was performed as described in Section 2.5. PCR was done using the Qiagen Multiplex Kit with HotStarTaq DNA Polymerase, primers (Table 6) with a 30 second annealing time, 30 second extension and a total of 35 total cycles. The sizes and quality of RT-PCR products were verified by agarose gel electrophoresis. PCR product cleanup and sequencing were performed as described in Section 2.7.

Table 6. RT- PCR primers to investigate the expression of mutations

Gene Amp	Amp Size (bp)	Primer Name	Exon	Sequence
<i>elna</i>	787	zf <i>elna</i> KE1.1s	1	TTGCTCCTTCTCGGATTCTT
		zf <i>elna</i> E9.1a	13	TGGGAGATTTGAGGGGGT
<i>elnb</i>	285	zf <i>elnb</i> E17.1s Hpy188I	17	TCTCAGGCTAAAGCTGCCAAGTCTG
		zf <i>elnb</i> E18.3a	18	AATGCCTCCAACACCTGGTA

2.10. EMBRYO HEART RATE MEASUREMENT

Embryos were kept in individual wells of 24-well plates, removed from the incubator and brought to room temperature to equalize environmental conditions of all embryos. Embryos at 5 days post fertilization (dpf) and 7 dpf were placed into a drop of water to eliminate the need for tricaine and keep them in place for observation using a stereomicroscope. Heart rates were measured by counting heart beats for 1 minute through direct observation.

2.11. ADULT ORGAN EXTRACTION, WHOLE-MOUNT HART'S ELASTIN STAINING

Adult zebrafish were euthanized using 0.64mg/mL tricaine. Dissection and extraction of the adult heart was done using published guidelines (Gupta & Mullins, 2010). The hearts were fixed in 10% buffered formalin (Protocol, Fisher Scientific) and stored at 4°C until ready for sectioning. The heart tissue was embedded in paraffin wax and sectioned by the Tissue and Research Pathology Services of the University of Pittsburgh Cancer Institute and mounted onto glass slides. A

modified version of the Hart's Elastin Staining Protocol was used to stain the hearts for elastin (R. Mecham, 2018). Slides were first deparaffinized by soaking in Histo-clear (National Diagnostics) for 15 minutes, followed by rehydration in an ethanol series (100%, 95%, 80%, 70%, 50%, 30%, tap water) with 10 dips per solution. The slides then were immersed in 0.25% potassium permanganate solution for 5 minutes, rinsed by dipping 10 times in tap water, incubated in 5% oxalic acid solution for 5 minutes, and rinsed again by dipping 10 times in tap water. Slides were stained in resorcin-fuchsin working solution (PolyScientific) for 2 hours and rinsed in tap water by dipping 30 times, with a change of water every 10 dips, followed by a soak for 5 minutes. Slides were counterstained in tartrazine working solution (2% tartrazine, 2% acetic acid) for 2 hours, dipped once in tap water, and dehydrated in the same ethanol series in reverse order with 1 dip per concentration. The slides were soaked in histoclear for 2 minutes and mounted under coverslips using Permount. Viewing and imaging of slides was done using a Leica DM5000 fluorescent microscope using transmitted light settings.

2.12. WHOLE-MOUNT IMMUNOSTAINING

Whole embryos were fixed in 4% paraformaldehyde (PFA) at 4°C overnight. After fixation, the embryos were washed 2 times for 5 min each with 0.1% Triton X-100 (TX-100) in 1X phosphate-buffered saline (PBS), followed by an incubation in PBS containing 0.5% TX-100 at room temperature for one hour. After the incubation, the embryos were blocked in blocking buffer containing 1% dimethyl sulfoxide (DMSO), 1% TX-100, 0.2% bovine serum albumin (BSA) and 5% goat serum prepared in PBS for 3 hours. Embryos were then incubated overnight at 4°C in a 1:250

dilution of *elna* primary antibody prepared in blocking buffer. The following day, the embryos were washed in 1 mL of blocking buffer for 5 minutes, then washed 4 times with 500 μ L of 0.1% TX-100 in PBS for 30 minutes each wash. Embryos were then blocked in 500 μ L of blocking buffer for 1 hour, then stained with secondary antibody Alexa Fluor 568 anti-rabbit IgG (Thermo Fisher Scientific, A-11011) in a 1:250 dilution for 3 hours. Staining was followed by 4 washes of 5 minutes each in 0.1% TX-100 in PBS, then left overnight at 4°C in 1X PBS. Imaging of embryos was done using an Olympus BX51 microscope and DP71 camera.

2.13. CONFOCAL IMAGING AND VIDEO MICROSCOPY

Homozygous mutants (*elna*^{sa/sa}) were outcrossed with a *Tg(acta2:mCherry)^{ca8};Tg(myf7:eGFP)^{twu34}* transgenic line to obtain *elna*^{sa/+}; *Tg(acta2:mCherry)^{ca8};Tg(myf7:eGFP)^{twu34}* adults, which were in-crossed to obtain homozygous mutant double transgenic fish. Both wildtype *Tg(acta2:mCherry;myf7:eGFP)* and *elna*^{sa/sa} *Tg(acta2:mCherry;myf7:eGFP)* embryos were grown in 30% Danieau solution [17mM NaCl, 2mM KCl, 0.12mM MgSO₄, 1.8 mM Ca(NO₃)₂, 1.5mM HEPES] containing 0.0003% phenylthiourea (PTU) up to 7 dpf. Larvae were mounted ventral side down on 35mm glass bottom plates (MatTek, P35G-0.170-14-C) using 2% low-melt agarose with 0.16mg/mL tricaine. Imaging was done using a Nikon A1 Confocal microscope at the Center for Biologic Imaging (CBI) at the University of Pittsburgh. Maximum projection images were then analyzed, and measurements taken using the Nikon NIS-Elements software. Wildtype Tü/AB* and *elna*^{sa/sa} fish were also grown to 7 dpf in the same manner and mounted using the same technique for taking videos of the hearts using a differential interference contrast (DIC) microscope, the

Nikon Ti Live Cell microscope and Photometrics PRIME 95B camera, and the Nikon NIS-Elements software for analysis.

2.14. ECHOCARDIOGRAPHY

Working with one zebrafish at a time, an adult zebrafish was first placed into Tricaine at a concentration of 0.12mg/mL made in system water to induce anesthesia for a length of 2 minutes. Fish were monitored to assure respiration did not cease. The fish was then transferred into a separate container containing Tricaine at a concentration of 0.096mg/mL used to maintain anesthesia for the length of the echocardiography scanning. Fish were held in the ventral position using a sponge immersed in a container with 0.096mg/mL maintenance Tricaine. Concentration of Tricaine for anesthesia induction and maintenance may need to be adjusted for each line.

Echocardiography imaging was done using a Fujifilm Visualsonics Vevo 2100 Micro-ultrasound animal imaging system. The probe was placed on the ventral side of the immersed fish to obtain blood flow images using the system's color Doppler modes. Once images were obtained, the zebrafish was placed into system water without Tricaine.

3.0 RESULTS

3.1 TRANSCRIPT DIVERSITY IN ZEBRAFISH ELASTIN GENES

To assess transcript diversity in *elna* and *elnb*, cDNA clones were generated from thirty 72 hours post fertilization (hpf) wildtype Tü/AB* larvae. The RNA was subjected to reverse transcription using random hexamers and to PCR amplification using sets of primers (Table 29, Table 30) designed to cover *elna* and *elnb* transcripts in 6 and 8 overlapping fragments, respectively. For each cDNA fragment, at least 5 clones were sequenced completely on both strands using primers complementary to the plasmid backbone and additional, regularly spaced internal primers (Table 31, Table 32) against the cDNA. A total of 46 *elna* and 44 *elnb* clones were sequenced.

I uncovered substantial variation in cDNA sequences from both genes (Table 7). The possible sources of these sequence variants include genetic variation, alternative splicing, and reverse transcriptase or PCR errors. Assignment of the observed sequence variation to these causes is not straightforward and required making the following assumptions. Single nucleotide variants and insertion deletion variation with breakpoints within exons were assumed to be genetic, whereas insertion-deletion variants with breakpoints at exon-exon junctions or at cryptic splice sites were assumed to be alternative splicing variants. I considered variants observed in more than one clone to less likely be the result of PCR errors.

Table 7. Summary of Variations in *elna* and *elnb*

Alternative Splicing: <i>elna</i> – 5 (2), <i>elnb</i> – 3 (2)
SNV (splice): <i>elna</i> – 1 (0)
SNV (silent): <i>elna</i> – 52 (29), <i>elnb</i> – 36 (10)
SNV (missense): <i>elna</i> – 19 (6), <i>elnb</i> – 41 (13)
SNV (nonsense): <i>elnb</i> – 2 (0)
In-del variants: <i>elna</i> – 9 (3), <i>elnb</i> – 10 (4)

Note: the number of variants found in more than one clone is shown in brackets

The majority of variants were single nucleotide variants (SNVs) with a total of 79 SNVs in *elna* and 89 in *elnb*. In addition, there were numerous length variants, transcript and genetic diversity represented by alternative splicing events and in-del variants. All SNPs observed were cross-checked with the transcript sequences obtained from ensemble.org and the available variant table. 11 out of 79 variants in *elna* (9 silent and 2 missense), and 2 out of 89 variants in *elnb* (both silent) were found to already have a corresponding accession number (rs #). The majority of SNVs for these genes with rs #s in the current dbSNP database are intronic. I found more silent SNVs in *elna* than *elnb* (51 and 36 respectively), but *elnb* had a larger number of missense mutations than *elna* (41 and 19 respectively). The full list of variations (Table 8 to Table 17, Table 19, Table 20) in *elna* and *elnb* that were found in the cDNA sequences are visualized in Figure 8 and Figure 9.

Table 8. Silent SNVs Identified in Exons 2-39 of *elna* cDNA

Variant Name	Type	Type Detail	Exon #	rs #	# of Clones
c.90A>G	SNV	Silent	2		2
c.105A>G	SNV	Silent	2		3
c.201A>G	SNV	Silent	4		1
c.267G>A	SNV	Silent	5		1
c.645A>G	SNV	Silent	10		1
c.657A>G	SNV	Silent	11		1
c.660A>G	SNV	Silent	11	rs503122350	1
c.684G>A	SNV	Silent	11	rs508262317	4
c.717G>A	SNV	Silent	12		3
c.753G>A	SNV	Silent	13		1
c.798C>T	SNV	Silent	13	rs505315146	1
c.819T>C	SNV	Silent	14		1
c.936G>A	SNV	Silent	15		5
c.999T>C	SNV	Silent	17	rs509607459	3
c.1008A>G	SNV	Silent	17		3
c.1041T>C	SNV	Silent	17		3
c.1287G>C	SNV	Silent	21		1
c.1314C>T	SNV	Silent	31		1
c.1647T>C	SNV	Silent	25		1
c.1800T>G	SNV	Silent	27		1
c.2010A>G	SNV	Silent	29		1
c.2043A>G	SNV	Silent	30		1
c.2058T>C	SNV	Silent	31		1
c.2094T>C	SNV	Silent	31		1
c.2262T>C	SNV	Silent	33		2
c.2430T>C	SNV	Silent	36		1
c.2481T>C	SNV	Silent	37		1
c.2505G>T	SNV	Silent	38	rs40920497	11
c.2571T>C	SNV	Silent	39		10

Table 9. Silent SNVs Identified in Exons 41-55 of *elna* cDNA

Variant Name	Type	Type Detail	Exon #	rs #	# of Clones
c.2640A>T	SNV	Silent	41		10
c.2643A>G	SNV	Silent	41		10
c.2646T>C	SNV	Silent	41		1
c.2655A>G	SNV	Silent	41		10
c.2661A>T	SNV	Silent	41		3
c.2667G>A	SNV	Silent	41		10
c.2673A>T	SNV	Silent	41		3
c.2676A>T	SNV	Silent	41		3
c.2679A>G	SNV	Silent	41		3
c.2682T>A	SNV	Silent	41		10
c.2685T>A	SNV	Silent	41		16
c.2688T>A	SNV	Silent	41		6
c.2814T>C	SNV	Silent	43		2
c.2847T>C	SNV	Silent	44		1
c.2862G>T	SNV	Silent	45	rs41232150	17
c.2892T>G	SNV	Silent	45	rs41056348	5
c.2898C>T	SNV	Silent	45	rs41239681	5
c.3219G>C	SNV	Silent	50	rs40973069	6
c.3252T>G	SNV	Silent	51		6
c.3255C>T	SNV	Silent	51		2
c.3290A>G	SNV	Silent	52		1
c.3363A>T	SNV	Silent	54		1
c.3435A>G	SNV	Silent	55		1

Table 10. Silent SNVs Identified in Exons 8-39 of *elnb* cDNA

Variant Name	Type	Type Detail	Exon #	rs #	# of Clones
c.678T>C	SNV	Silent	8		1
c.726C>T	SNV	Silent	8		3
c.747C>A	SNV	Silent	8		3
c.891T>C	SNV	Silent	8		3
c.1074G>A	SNV	Silent	9		3
c.1392T>C	SNV	Silent	12		2
c.2394A>G	SNV	Silent	22		1
c.2514T>A	SNV	Silent	22		1
c.2538G>A	SNV	Silent	23		1
c.2583T>A	SNV	Silent	24		1
c.2589T>C	SNV	Silent	24		1
c.2595A>T	SNV	Silent	24		1
c.2598T>C	SNV	Silent	24		1
c.2692C>T	SNV	Silent	24		1
c.3133T>C	SNV	Silent	26		1
c.3168G>T	SNV	Silent	26		1
c.3222A>G	SNV	Silent	27		1
c.3304T>C	SNV	Silent	28	rs501804407	1
c.3306A>G	SNV	Silent	28		2
c.3423A>G	SNV	Silent	28		1
c.3471T>C	SNV	Silent	30		1
c.3531T>G	SNV	Silent	30		1
c.3570A>G	SNV	Silent	30		1
c.3717A>G	SNV	Silent	31		1
c.3738T>C	SNV	Silent	32		1
c.3909G>T	SNV	Silent	32	rs511964010	2
c.3924A>T	SNV	Silent	32		2
c.3933G>A	SNV	Silent	32		2
c.4422A>G	SNV	Silent	39		2
c.4425T>C	SNV	Silent	39		1

Table 11. Silent SNVs Identified in Exons 46-56 of *elnb* cDNA

Variant Name	Type	Type Detail	Exon #	rs #	# of Clones
c.4743A>G	SNV	Silent	46		1
c.4872A>G	SNV	Silent	46		1
c.4965T>C	SNV	Silent	46		1
c.5139T>C	SNV	Silent	46		1
c.5391C>A	SNV	Silent	49		1
c.6003A>G	SNV	Silent	56		1

Table 12. Missense SNVs Identified in *elna* cDNA

Variant Name	Type	Type Detail	Exon #	rs #	# of Clones
c.10A>G p.Arg3Gly	SNV	Missense	1		1
c.627A>C p.Gln209His	SNV	Missense	10		1
c.664G>A p.Val222Ile	SNV	Missense	11		1
c.1037T>C p.Val346Asp	SNV	Missense	17		3
c.1693A>G p.Ile565Val	SNV	Missense	25		1
c.1876A>G p.Thr626Ala	SNV	Missense	27		3
c.1973T>C p.Ile658Thr	SNV	Missense	29		1
c.2168G>A p.Gly723Glu	SNV	Missense	31		1
c.2341C>T p.Leu781Phe	SNV	Missense	34		4
c.2587A>G p.Thr863Ala	SNV	Missense	39		1
c.2683G>A p.Gly895Ser	SNV	Missense	41		1
c.2735T>C p.Val912Ala	SNV	Missense	41		1
c.2810G>A p.Gly937Ala	SNV	Missense	41		1
c.2833G>A p.Gly945Ser	SNV	Missense	41		10
c.2876C>T p.Thr959Ile	SNV	Missense	41	rs40859418	5
c.3007C>T p.Leu1003Phe	SNV	Missense	41		1
c.3214G>A p.Gly1072Arg	SNV	Missense	41		1
c.3527A>G p.Glu1086Gly	SNV	Missense	41		1
c.2876C>T p.Thr959Ile	SNV	Missense	45	rs40859418	5

Table 13. Missense SNVs Identified in Exons 2-28 of *elnb* cDNA

Variant Name	Type	Type Detail	Exon #	rs #	Clone #
c.235A>G p.Thr79Ala	SNV	Missense	2		1
c.376G>A p.Gly126Ser	SNV	Missense	3		1
c.580G>A p.Thr194Ala	SNV	Missense	5		1
c.686T>C p.Thr229Ile	SNV	Missense	8		3
c.709G>A p.Val237Ile	SNV	Missense	8		3
c.1232C>T p.Ala411Val	SNV	Missense	11		2
c.1294A>G p.Thr432Ala	SNV	Missense	11		1
c.1375C>T p.Pro459Ser	SNV	Missense	12		2
c.1498C>T p.Pro500Ser	SNV	Missense	13		1
c.1553A>G p.Gln518Arg	SNV	Missense	14		1
c.1571A>G p.Gln524Arg	SNV	Missense	15		1
c.1624G>A p.Val542Met	SNV	Missense	16		1
c.2077G>A p.Gly693Arg	SNV	Missense	20		2
c.2179T>C p.Ser727Pro	SNV	Missense	20		2
c.2230G>T p.Val744Leu	SNV	Missense	20		3
c.2333G>A p.Gly778Asp	SNV	Missense	22		2
c.2507G>A p.Gly836Glu	SNV	Missense	22		1
c.2510T>C p.Ile837Thr	SNV	Missense	22		1
c.2534C>T p.Thr845Ile	SNV	Missense	22		2
c.2547C>G p.Asp849Glu	SNV	Missense	23		1
c.2617A>G p.Thr873Ala	SNV	Missense	24		1
c.2642G>T p.Gly881Val	SNV	Missense	24		1
c.2830A>G p.Gly944Ala	SNV	Missense	24		1
c.3181C>A p.Leu1061Ile	SNV	Missense	26		1
c.3274G>A p.Gly1092Ser	SNV	Missense	28		1
c.3427G>A p.Gly1143Arg	SNV	Missense	28		1

Table 14. Missense SNVs Identified in Exons 30-55 of *elnb* cDNA

Variant Name	Type	Type Detail	Exon #	rs #	# of Clones
c.3551T>C, p.Ile1184Thr	SNV	Missense	30		1
c.3604A>G, p.Ile1202Val	SNV	Missense	30		1
c.3625C>T, p.Pro1209Ser	SNV	Missense	30		1
c.3635T>C, p.Val1212Ala	SNV	Missense	30		1
c.3653G>A, p.G1218E	SNV	Missense	30		1
c.3725T>C, p.Ile1242Thr	SNV	Missense	32		2
c.4175C>T, p.Pro1392Leu	SNV	Missense	34		1
c.4354G>A, p.Gly1452Ser	SNV	Missense	38		10
c.4943T>C, p.Val1648Ala	SNV	Missense	46		1
c.5324A>G, p.Gln1775Arg	SNV	Missense	47		1
c.5326A>G, p.Lys1776Glu	SNV	Missense	47		1
c.5342A>G, p.Tyr1781Cys	SNV	Missense	48		2
c.5533G>A, p.Gly1845Ser	SNV	Missense	50		4
c.5762G>A, p.Gly1921Asp	SNV	Missense	52		1
c.6007T>C, p.Phe2003Leu	SNV	Missense	55		1

Table 15. Nonsense SNVs Variants Identified in *elnb* cDNA

Variant Name	Type	Type Detail	Exon #	rs #	Clone #
c.3463A>T, p.K1155*	SNV	Nonsense	29		1
c.4153C>T, p.Gln1385*	SNV	Nonsense	34		1

Table 16. Indel Variants Identified in *elna* cDNA

Variant Name	Type	Type Detail	Exon #	rs #	# of Clones
c.107_109del	Deletion	In-frame	2		1
c.330_345del	Deletion	+2 frameshift	Part 5 to part 6		1
c.1115_2188del	Deletion	In-frame	Part 18 to 31		1
c.1418_1636del	Deletion	In-frame	Part 23 to part 25		1
c.1453_2085del	Deletion	In-frame	Part 23 to part 31		1
c.1595_1636del	Deletion	In-frame	25		2
c.1808_1828del	Deletion	In-frame	27		3
c.434...468dup	Duplication	+2 frameshift	Part 6 to 7		1
c.1037_1078dup	Duplication	In-frame	17		4

Table 17. Indel Variants Identified in *elnb* cDNA

Variant Name	Type	Type Detail	Exon #	rs #	# of Clones
c.2071_2250del	Deletion	In-frame	20		1
c.2198_2821del	Deletion	In frame	Part 20 to part 24		1
c.2629_3291del	Deletion	In-frame	Part 24 to part 28		1
c.2635_3042del	Deletion	In-frame	Part 24 to part 26		1
c.2704_3318del	Deletion	In-frame	Part 24 to part 28		1
c.2861_3556del	Deletion	In-frame	Part 24 to part 30		1
c.3902_3931del	Deletion	In-frame	32		5
c.4872_5018del	Deletion	In-frame	46		3
c.5095_5136del	Deletion	In-frame	46		2
c.5538_5561del	Deletion	In frame	50		4

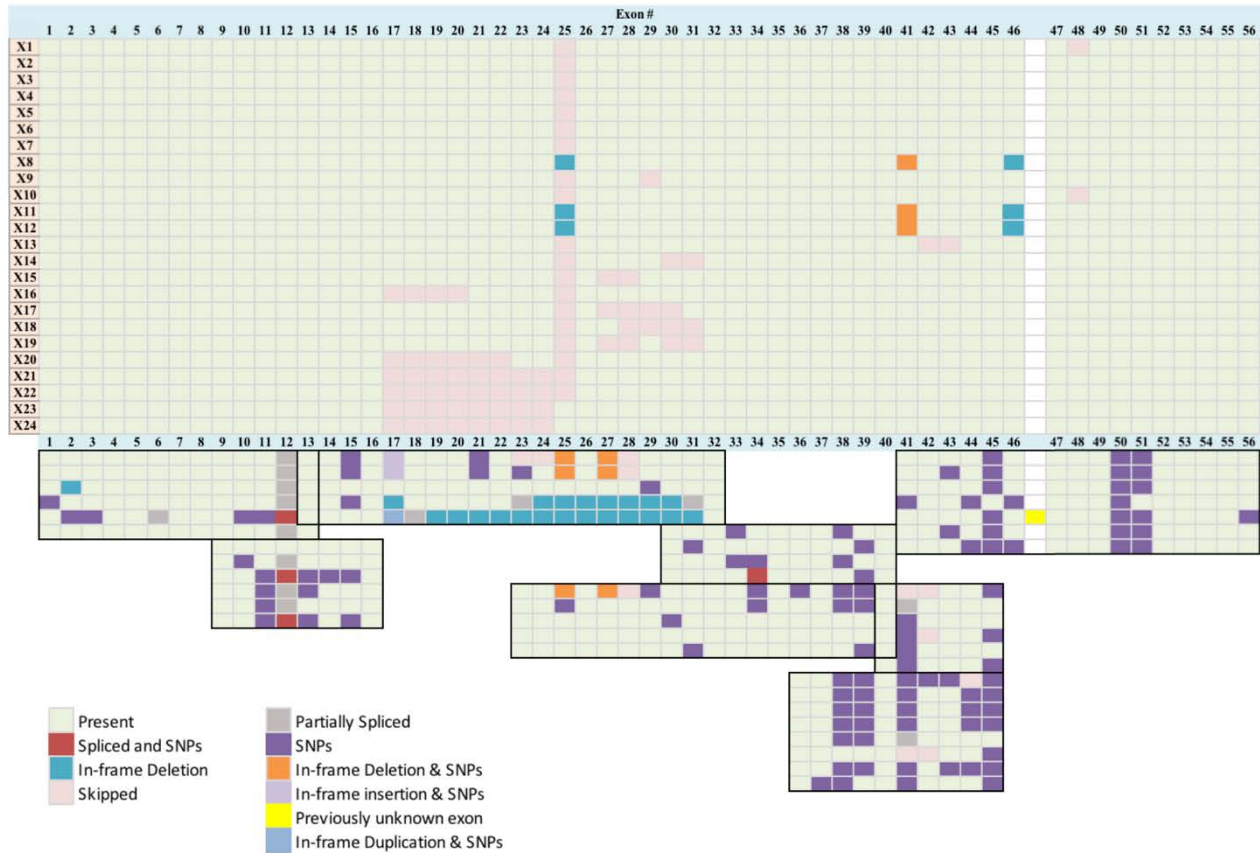


Figure 8. Graphical Representation of Transcript and Genetic Variants in *elna*

Each exon of *elna* is displayed as a column of cells. The rows show transcripts annotated in Ensembl (X1-X24, top), or individual cDNA clones sequenced in this study (bottom). Each group of clones is surrounded by a black outline. A large number of SNVs are observed from exons 38-51. Pale green – the exon’s full sequence is present and matches the reference sequence.

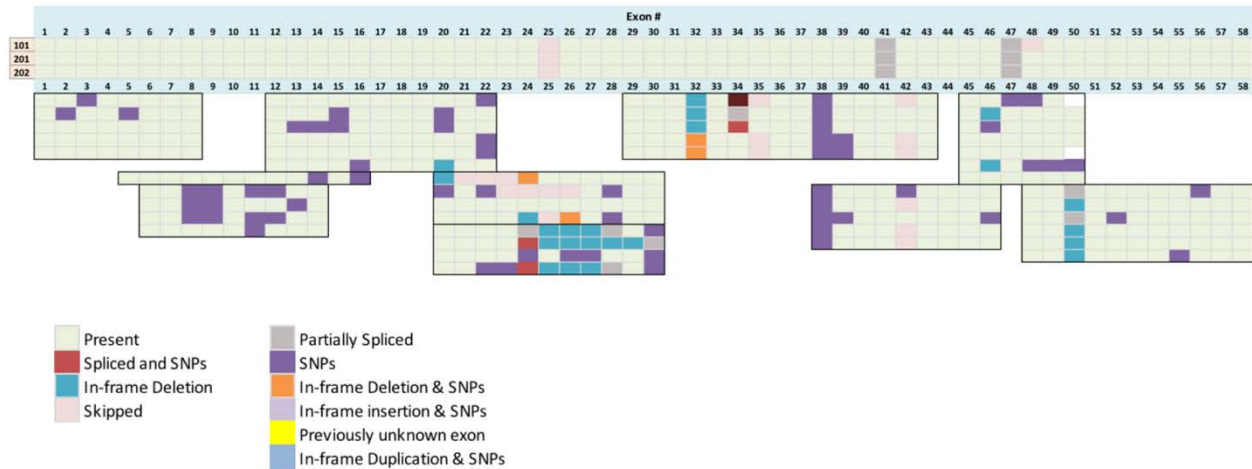


Figure 9. Graphical Representation of Transcript and Genetic Variants in *elnb*

Each exon of *elna* is displayed as a column of cells. The rows show transcripts annotated in Ensembl (101, 201, 202, top), or individual cDNA clones sequenced in this study (bottom). Each group of clones is surrounded by a black outline. Pale green – the exon’s full sequence is present and matches the reference sequence.

Upon annotating the sequences in CLC Main, I noticed a non-random distribution (clustering) of SNVs throughout the *eln* genes (Figure 8, Figure 9). In *elna*, 3 exons had 4 or more SNVs (exon 11 - 4, exon 41 - 13, and exon 45 - 4), and *elnb* had 2 exons with 5 SNVs each (exon 28 – 5, exon 46 – 5). Exon 41 had the largest cluster (Figure 10) consisting of 13 SNVs (1 missense and 12 silent). Because I sequenced cDNA clones, it was possible to assign SNVs to haplotypes. Assuming 2 parents for the clutch I would expect to find a minimum of 2 and a maximum of 4 haplotypes. For each cluster, there were more than 2 haplotypes, with the number of haplotypes ranging from 3 to 6 (Table 18). The finding of more than 4 haplotypes suggests that there were more than 2 parents of the clutch used to isolate RNA. Indeed, I used a group breeding of 13 adults to obtain the embryos for this experiment. An alternative explanation, supported by the observation of 16 haplotypes marked by a single SNV, is that some of the SNVs represent PCR errors.

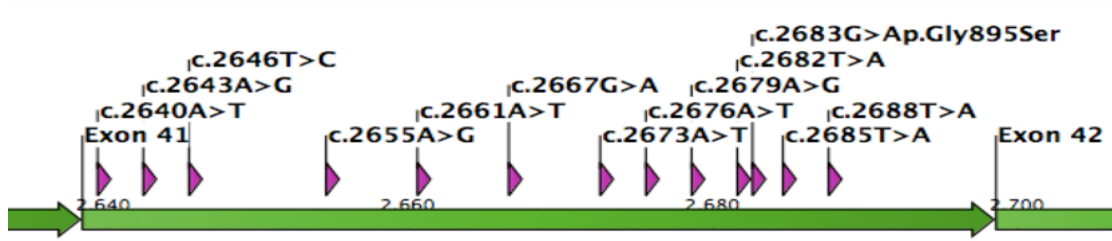


Figure 10. A cluster of 13 SNVs in exon 41 of *elna*

This is an example of how SNVs have shown a tendency to cluster in portions of the cDNA.

Table 18. Clustering and Haplotypes in *elna* and *elnb*

Gene	Exon	# of SNVs	# and Type of SNV	Haplotype #
<i>elna</i>	11	4	Silent – 3 Missense - 1	4
	41	13	Silent – 12 Missense – 1	3
	45	4	Silent – 3 Missense – 1	3
<i>elnb</i>	28	5	Silent – 3 Missense – 2	5
	46	7	Silent – 4 Missense – 1 Deletions - 2	6

Splice site scores for SNVs located close to exon-exon boundaries and for sites of possible alternative 5' or 3' splice site use were determined using a website algorithm. The correlation coefficient cut off identifies real splice sites with 5-9% false negative, and 5% false positive rates. The closer the score is to 1, the more likely it is to be a real splice site. For example, the splice site variant, changing the last nucleotide of exon 3 in *elna* c.196G>Tp.A66S, returned a Wildtype Score

of 0.98 and a Mutant Score of 0.18., indicating that this variant is likely to inactivate the splice site. Predicted exon skipping events could not be interrogated this way, as they involve the use of existing splice consensus sequences. I found 2 SNVs with substantial effect on the corresponding splice site scores, a new exon between exons 46 and 47, one instance of an alternative 3' and another of an alternative 5' splice site use and 3 exon skipping events in *elna* (Table 19). The newly discovered exon also has a high splice site score and encodes an overall hydrophobic sequence (Figure 11) with only a single lysine and glutamic acid. The amino acid sequence of this domain is similar to other hybrid hydrophobic/crosslink domains encoded by exons 45, 49 and 51, but one of the usual 2 lysines is replaced by a glutamic acid, which is very rare in elastin sequences. In *elnb*, only one alternative 5' splice site and 2 exon skip events were noted (Table 20).

Table 19. Annotated SNV Splice Sites and Splice Variants Identified in *elna* cDNA

Variant Name	Type	Type Detail	Exon #	Splice Score	# of Clones
c.196G>Tp.A66S	SNV	Splice site	3	WT: Score 0.98 GCAGgtga Var: Score 0.18 GCATgtga	1
c.431_445del	Splice	Alt splice 5'	6	WT: Score 0.01 GGAGgtgg Var: Score 0.08 GGAGgtgc	1
c.709_710insCTGCAG	Splice	Alt splice 3'	12	WT: Score 0.25 TCAGgtgg Var: Score 0.88 ctgcagGTGG	10
c.1883_1927del	Splice	Exon skip	28		3
c.2639_2731del	Splice	Exon skip	41 & 42		1
c.2825_2857del	Splice	Exon skip	44		1
g.46522_46563		New Exon	Between 46 & 47	Score 0.95 gcagGACC Score 0.84 CCCAgtaa	1

Exons and introns in the splice junction sequences are shown in capital and lower case type, respectively. Clone # indicates the number of clones that displayed variant upon sequencing.

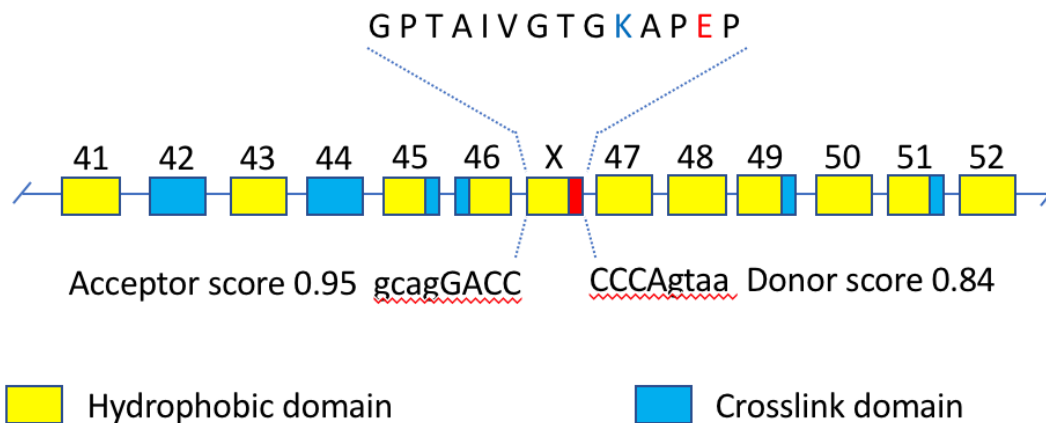


Figure 11. A Schematic Representation of the Domain Context and Sequence Features of a New Exon in *elna*

Exons 41 through 52 are shown. Note that some exons (45, 46, 49 and 51) have both hydrophobic and crosslink sequences. The newly discovered exon (X) has high-scoring splice sites and encodes an overall hydrophobic sequence with a single lysine (K, blue) and glutamic acid (E, red).

Table 20. Annotated SNV Splice Sites and Splice Variants Identified in *elnb* cDNA

Variant Name	Type	Type Detail	Exon #	rs#	# of Clones
c.5519_5599del	Splice	Alt splice 5'	50	WT: Score 0.25 GGTGgtaa Var: Score: 0.25 CCAGgtgg	2
c.2537_3199del	Splice	Exon skip	23 to 26		1
c.4541_4567del	Splice	Exon skip	42		3

Capital letters in the Splice Score sequence indicate EXON/intron boundary. Clone # indicates the number of clones that displayed variant upon sequencing.

Once all sequences were analyzed and annotated, the amplification primer sequences were trimmed, and sequences were exported in FASTA format and submitted to GenBank using the BankIt web interface (Table 33).

For further confirmation, 30 SNVs were examined in gDNA isolated from tail clips in 5 of the 13 possible parents that were bred to produce the embryos used to obtain the mRNA. I considered a variant confirmed if it was either found to be polymorphic in gDNA or monomorphic for the minor (non-reference) allele. Of the 30 mutations, 8 of them were not reproduced in gDNA. Three silent SNVs in the SNV cluster in *elna*'s exon 41 were not reproduced. The nonsense variant found in *elnb* cDNA was not reproduced in gDNA, and only 1 of 2 missense variants was reproduced (Table 21).

Table 21. Genomic DNA Confirmation of SNVs in *elna* & *elnb*

Exon	SNV Name	Type	Type Detail	cDNA # of clones	gDNA # of clones (AA, Aa, aa)*
<i>elna</i>					
34	c.2341C>Tp.Leu781Phe	SNV	missense	4 of 9	0, 4, 1
	c.2640A>T	SNV	silent	10 of 21	0, 0, 5
	c.2643A>G	SNV	silent	10 of 21	0, 0, 5
	c.2646T>C	SNV	silent	1 of 21	5, 0, 0
	c.2655A>G	SNV	silent	10 of 21	0, 0, 5
	c.2661A>T	SNV	silent	3 of 21	3, 2, 0
	c.2667G>A	SNV	silent	10 of 21	0, 0, 5
41	c.2673A>T	SNV	silent	3 of 21	2, 3, 0
	c.2676A>T	SNV	silent	3 of 21	2, 3, 0
	c.2679A>G	SNV	silent	3 of 21	2, 3, 0
	c.2682T>A	SNV	silent	10 of 21	5, 0, 0
	c.2685T>A	SNV	silent	16 of 21	5, 0, 0
	c.2688T>A	SNV	silent	6 of 21	0, 0, 5
	c.2683G>Ap.Gly895Ser	SNV	missense	1 of 21	0, 0, 5
44	c.2833G>Ap.Gly945Ser	SNV	missense	10 of 21	0, 5, 0
	c.2847T>C	SNV	silent	1 of 21	5, 0, 0
	c.2862G>T	SNV	silent	17 of 21	0, 1, 4
45	c.2876C>Tp.Thr959Ile	SNV	missense	5 of 21	0, 4, 1
	c.2892T>G	SNV	silent	5 of 21	0, 4, 1
	c.2898C>T	SNV	silent	5 of 21	0, 4, 1
51	c.3252T>G	SNV	silent	6 of 7	2, 2, 1
	c.3255C>T	SNV	silent	2 of 7	5, 0, 0
<i>elnb</i>					
29	c.3463A>Tp.K1155*	SNV	nonsense	2 of 13	5, 0, 0
	c.3725T>Cp.Ile1242Thr	SNV	missense	2 of 5	5, 0, 0
	c.3738T>C	SNV	silent	1 of 5	5, 0, 0
32	c.3909G>T	SNV	silent	2 of 5	1, 2, 2
	c.3924A>T	SNV	silent	2 of 5	1, 2, 2
	c.3933G>A	SNV	silent	2 of 5	1, 2, 2
	c.3902_3931del	Deletion		5 of 5	5, 0, 0
38	c.4354G>Ap.Gly1452Ser	SNV	missense	10 of 10	0, 0, 5

* A: major or reference allele, a: minor, derived or new allele. Variants not reproduced by genomic DNA sequencing are shaded grey.

This leads one to question the validity of the other SNVs found in cDNA. According to studies on PCR induced errors, base substitution errors and other false mutations can be induced via the PCR amplification process and make identifying rare genetic variations a challenge (Kebschull & Zador, 2015; Potapov & Ong, 2017). Otherwise one must consider PCR reaction conditions' influence on fidelity and the primers used. Precautions were taken to assure that primers were unique to a specific sequence, but both *elna* and *elnb* have highly repetitive sequences that could lead to primers annealing to partially homologous complementary strands. As is seen in *elna* (Table 22), where even exons 20 to 30 are the same or differ by only a single base.

Table 22. Whole Exons with Same Sequence

Exon 20	gtgctggtgcactctccccgctcaggcaaaagctgctaaatag
Exon 22	gtgctggtgcactctccccgctcaggcaaaagctgctaaatag
Exon 24	gtgctggtgcactctccccgctcaggcaaaagctgctaaatag
Exon 26	gtgctggtgcactctccccgctcaggcaaaagctgctaaatag
Exon 28	gtgctggtgcactctcccc t gctcaggcaaaagctgctaaatag
Exon 30	gtgctggtgcactctcccc t gctcaggcaaaagctgctaaatag

The elastin genes have repetitive sequence throughout the genome. These sequences are from *elna* and are an example of how entire exons share the same sequence. The t bases in red found in exons 28 and 30 are the only difference between those exons and the other three.

In addition to PCR errors, the discrepancy between the cDNA and gDNA sequences could also be a result of allele dropout in gDNA amplicons, in which one allele is preferentially amplified so that at heterozygous loci the other allele is underrepresented or missing (Hahn, Garvin, Di Naro, & Holzgreve, 1998). Furthermore, genotyping variants in a subset of the breeding parents could

also explain not being able to reproduce all mutations in gDNA. The unreproducible mutations may have come from un-sequenced parents. Sequencing the other parental gDNA for the mutations could eliminate this as a concern, but because of cost and time considerations we decided against further sequencing.

3.2 VALIDATION OF *elna* MUTANT (*elna*^{sa12235}, c.264T>A, p.Tyr88*)

To investigate the role of *elna* in zebrafish development, I obtained F0 *elna*^{sa/+} female (♀) mutants (*elna*^{sa12235}, c.264T>A, p.Tyr88*) from the Sanger Institute Zebrafish Mutation Project. This nonsense mutation, located in exon 5, was confirmed by DNA sequencing of gDNA isolated from tail biopsies of F0 and F1 fish (Figure 12). A genotyping assay was developed using the dCAPS method (Figure 13), which generates a restriction enzyme site. F0 females were first out-crossed to Tü/AB* WT males. The resulting F1 generation was in-crossed (*elna*^{sa/+} ♂ x *elna*^{sa/+} ♀) and 341 out of 1,001 embryos survived to adulthood (3 months). Genotyping of the 341 adults exhibited a distribution of Mendelian frequencies: *elna*^{sa/+} – 183 (54%), *elna*^{sa/sa} – 80 (23%), *elna*^{+/+} – 78 (23%) at 3 months of age., indicating that this mutation was compatible with survival to adulthood. A series of F1 in-crosses established an *elna*^{sa/sa} colony.

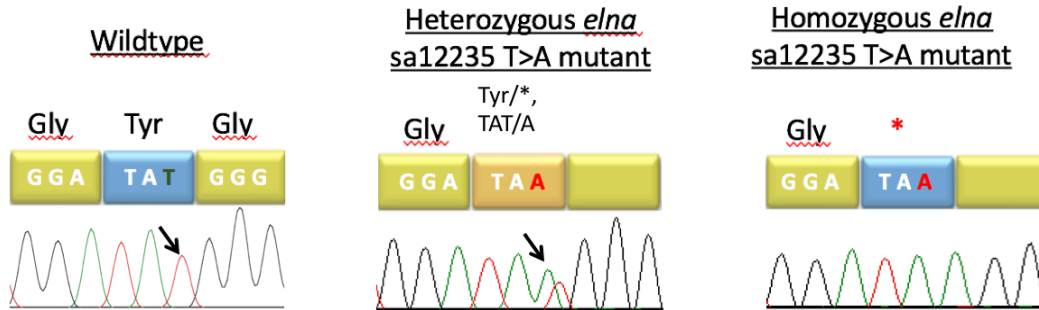


Figure 12. Sequencing of the *elna* wildtype and mutant alleles in gDNA from adult tail biopsy

Tail biopsies were taken at 3 months of age. The peaks of the mutant allele (A - green) and wildtype allele (T - red) are of close to equal height in the heterozygous fish.

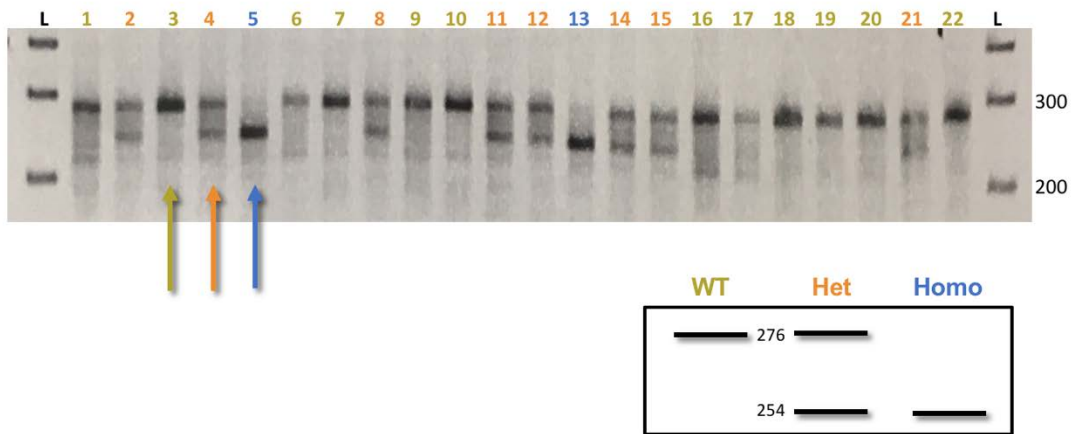


Figure 13. Genotyping of *elna* using dCAPS

The assay allows for easy identification of the genotype by single or double bands. A wildtype (WT - yellow) will have a single band at 276bp (top band, not cleaved by DdeI), a heterozygous (Het - orange) mutant have 2 bands at 276bp and 254bp, and homozygous (Homo - blue) mutants have a single band (bottom) at 254bp (cleaved by DdeI). There are 12 WT, 8 Het and 2 Homo. L- 1kb ladder

3.3 STAGE-SPECIFIC DEGRADATION OF MUTANT RNA BY NONSENSE-MEDIATED DECAY

To determine if the mutation (c.264T>A, p.Tyr88*) destabilizes the mRNA, I sequenced cDNA (Figure 14) from heterozygous (*elna^{sa/+}*) embryos of various stages, from 1 dpf through 5 dpf, and 7 dpf. The cDNA was obtained from a pooled clutch derived from a WT Tü/AB* to *elna^{sa/sa}* cross, to assure that all embryos were heterozygous (*elna^{sa/+}*) for the mutation. The wildtype allele (T) in heterozygous embryos gets higher as they age, while the mutant allele (A) is reduced and disappears by 3 dpf. Wildtype embryos and homozygous *elna* mutants only display their respective alleles. These findings support the conclusion this nonsense mutation activates nonsense-mediated decay in a developmentally regulated fashion with close to complete elimination of the mutant transcript at relevant developmental stages and therefore is a null mutation.

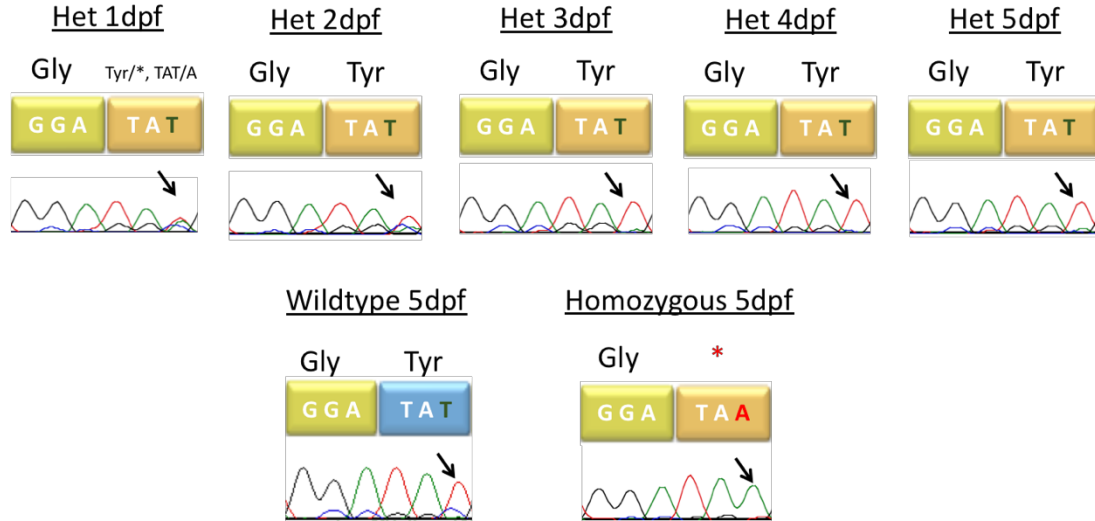


Figure 14. Reduced Expression of the *elna^{sa}* allele

Embryos heterozygous (Het) for *elna* show a gradual increase in wildtype allele's (T) peak (arrow) with development and the mutant allele (A) shown in red is gradually reduced. Wildtype embryos at 5 dpf (days post fertilization) show only the wildtype allele, and homozygous embryos only display the mutant allele

3.4 REDUCED *ELNA* PROTEIN EXPRESSION IN *elna^{sa}* MUTANTS

To study the *elna* protein expression, I performed whole-mount immunostaining in *elna^{+/+}*, *elna^{sa/+}* and *elna^{sa/sa}* larvae at 7 dpf (n = 3, 5, and 5 respectively). Wildtype had the most expression in the blood vessels and the skeleton of the head. Heterozygous *elna* larvae exhibited a decrease in expression, while homozygous mutants lacked *elna* expression in the head vessels and skeleton (Figure 15).

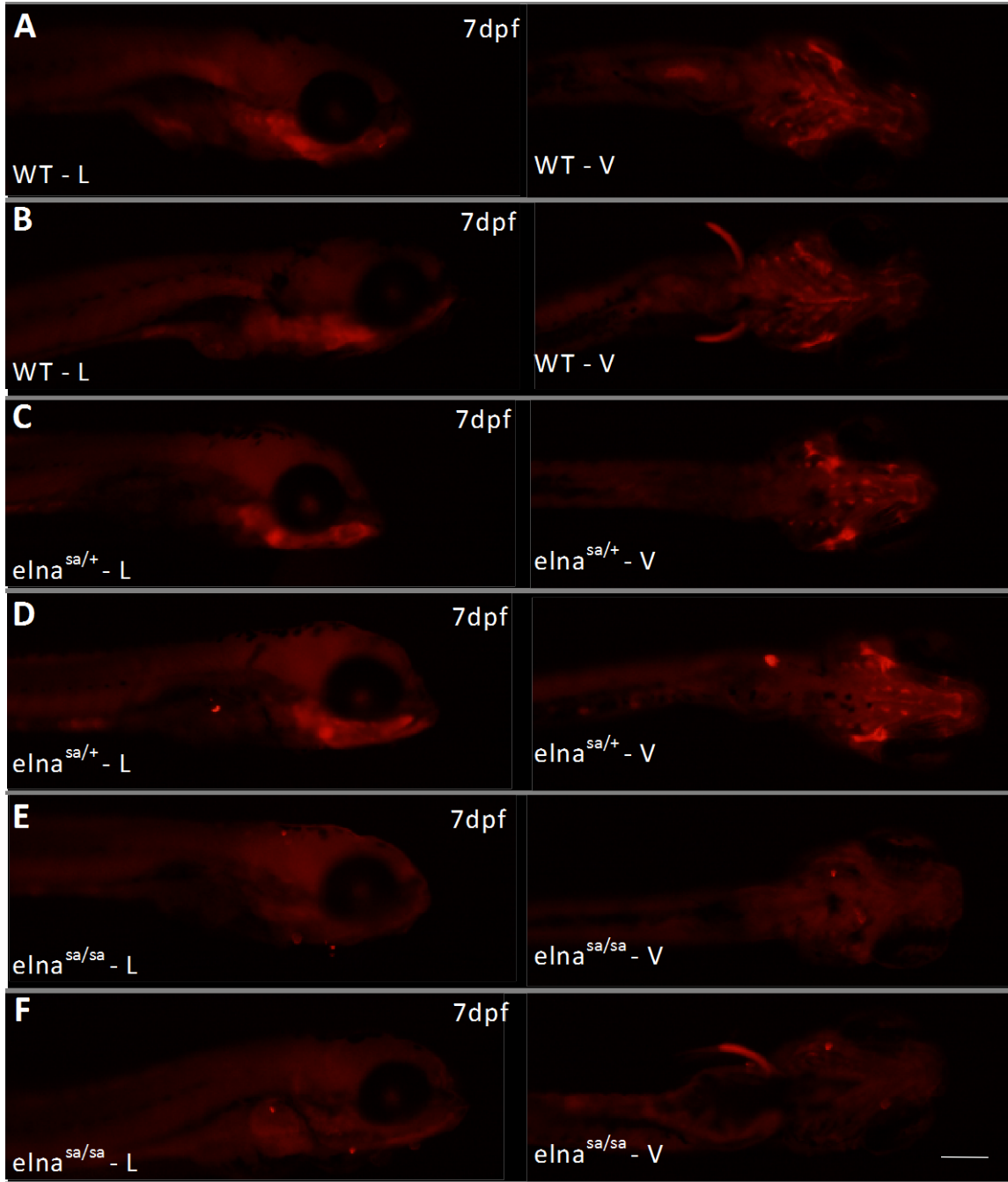


Figure 15. Whole-mount Immunostaining for *elna* in 7 dpf Embryos

Wildtype *elna*^{+/+}, (C,D) *elna*^{sa/+}, (E,F) *elna*^{sa/sa} 7dpf larvae in lateral (L) and ventral (V) views for immunostaining of *elna* expression. Expression of *elna* (fluorescence - bright red) is brightest in wildtype embryos (A,B), and decreased in heterozygotes (C,D). Homozygous mutants (E,F) do not display specific staining for *elna*. Scale bar: 200 μ m

3.5 CIRCULATION DEFECTS IN *elna^{sa}* MUTANTS

WT and *elna^{sa/sa}* embryos at 3 dpf, and larvae at 5 dpf, and 7 dpf were observed for heart abnormalities. Embryos were split into groups of fed and unfed at 5 dpf, as this is when the yolk has been fully absorbed and feeding is generally started under usual husbandry protocols. Mutant embryos fed starting at 5 dpf, displayed reduced blood flow through the heart in 32.5% and regurgitation between the atrium and ventricle (or ventricle and BA) in 32.5% of the clutch. Reduced blood flow was defined as the presence of fewer red blood cells, a reduction in the speed at which the cells flowed through the chambers of the heart or both. Regurgitation was not always observed to be associated with reduced blood flow. Mutants also exhibited heart looping abnormalities in 42.5%, where the atrium and ventricle were not in the proper orientation and position relative to the embryo's developmental stage (Table 23, Figure 16). This experiment was performed once on a set of 100 WT and 100 *elna^{sa/sa}* embryos. Each set of 100 was split into two groups of 50 (fed and unfed) at 6 dpf. Further quantification of blood flow will need to be conducted and the experiment repeated to determine if the phenotype is observed in other embryo clutches.

Table 23. Wildtype and *elna*^{sa/sa} Cardiovascular Developmental Observations

	WT Tü/AB*				<i>elna</i> ^{sa/sa}			
	3 dpf	5 dpf	7 dpf (fed)	7 dpf (unfed)	3 dpf	5 dpf	7 dpf (fed)	7 dpf (unfed)
Blood flow	6	4	9	9	26	30	13	17
Regurgitation	2	1	4	3	14	31	13	27
Edema	2	2	0	2	9	20	2	1
Looping Issue	6	2	3	7	12	11	17	7
Blood pooling	0	2	1	0	2	1	1	0
Total Survival (n)	100	100	50	48	100	100	40	50
%								
Blood flow	6.0%	4.0%	18.0%	18.8%	26.0%	30.0%	32.5%	34.0%
Regurgitation	2.0%	1.0%	8.0%	6.3%	14.0%	31.0%	32.5%	54.0%
Edema	2.0%	2.0%	0.0%	4.2%	9.0%	20.0%	5.0%	2.0%
Looping Issue	6.0%	2.0%	6.0%	14.6%	12.0%	11.0%	42.5%	14.0%
Blood pooling	0.0%	2.0%	2.0%	0.0%	2.0%	1.0%	2.5%	0.0%

This experiment was performed on n = 100 WT and n = 100 *elna*^{sa/sa} embryos. Each set of 100 was split into two groups of n = 50 (fed and unfed) at 6 dpf.

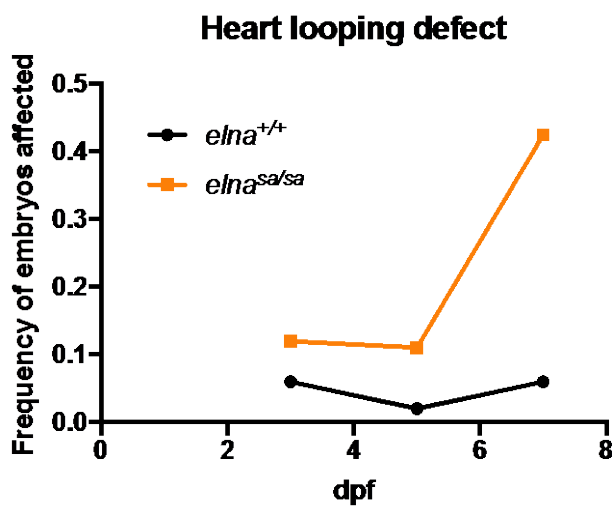
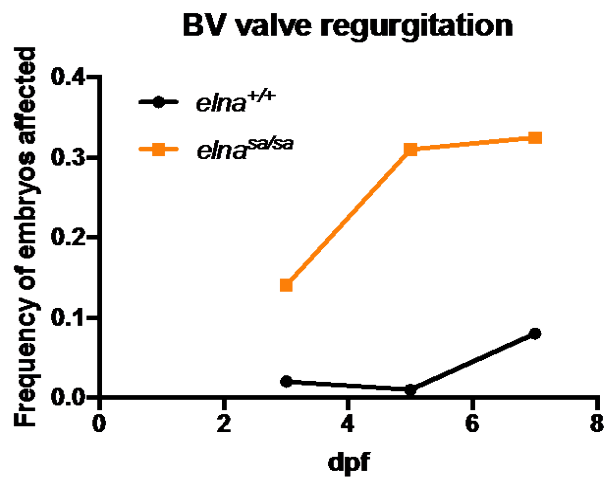
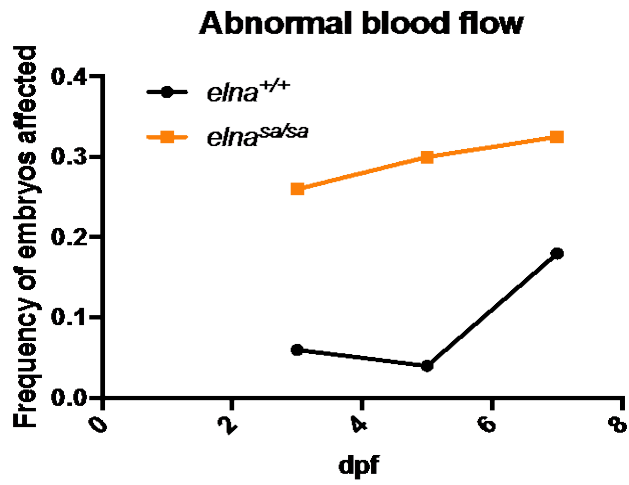


Figure 16. Circulation Defects in *elna*^{sa/sa} mutants. The 7 dpf values are of fed larvae.

Embryos of all three genotypes (wildtype Tü/AB*, *elna^{sa/+}*, *elna^{sa/sa}*) were also closely examined using a stereo microscope for phenotypic abnormalities including: heart rates, length, swim bladder inflation, head and heart structure and blood flow. Heterozygous mutant animals did not have any obvious abnormalities. Based on t-tests conducted, there was no significant difference between genotypes with respect to swim bladder inflation, length, or head structure. Heart rate varied significantly from one clutch to another, but overall there was no correlation with genotype at 5 dpf (Figure 18). However, at 7 dpf, there was a slightly but significantly reduced heart rate of in *elna^{sa/sa}* mutants compared to wildtype ($p = 0.01698$) (Figure 17). Heart rates in 5 dpf embryos were collected from 7 different clutches and in 7 dpf, WT and *elna^{sa/sa}* embryo heart rates were obtained from single clutches of 42 embryos each.

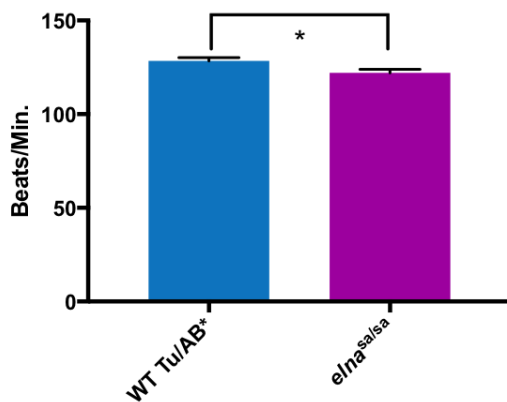


Figure 17. Heart rates at 7 dpf by Genotype

There was a significant difference between the wildtype Tü/AB* (blue) and *elna^{sa/sa}* (purple) heart rates at 7 dpf. Wildtype ($n = 42$) mean: 128.4 beats per minute, *elna^{sa/sa}* ($n = 42$) mean: 122.1 beats per minute. T-test $p = 0.01698$. dpf – days post fertilization.

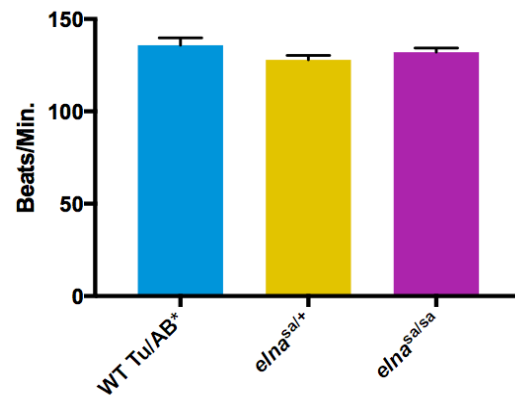


Figure 18. Heart Rates at 5 dpf by Genotype

There was no significant difference between the wildtype Tü/AB* (blue), *elna^{sa/+}* (yellow) and *elna^{sa/sa}* (purple) heart rates at 5 dpf. Wildtype ($n = 25$) mean: 135.8 beats per minute, *elna^{sa/+}* ($n = 45$) mean: 127.9 beats per minute, *elna^{sa/sa}* ($n = 76$) mean: 132.1 beats per minute. One-way ANOVA $p = 0.2246$. dpf – days post fertilization.

To follow up on the common observation of blood regurgitation in the hearts of mutant fish, I used DIC video microscopy and obtained a closer look at the heart valve structure and function in wildtype (WT) and *elna*^{sa/sa} mutants at 7dpf, at which stage I observed the highest frequency of regurgitation. Consistent with this observation *elna* expression peaks between 6 dpf and 7 dpf before decreasing to baseline (Miao et al., 2007). In the resulting videos, mutants display ventriculo-bulbar (VB) heart valve regurgitation and irregular formation and movement of the valves. Wildtype embryos (Figure 19) appear to have normal blood flow and valves that do not appear to have structural or functional defects. In addition to normal appearance of the valves in WT, the ventricular contraction appears to be stronger. The ventricle contracts (becomes rounder and shorter) and empties completely, while the *elna*^{sa/sa} mutant ventricle remains elongated and does not empty completely, giving the appearance of a weaker contraction (Figure 20). These results were consistent in two WT clutches (n = 4) but varied between the two mutant clutches (n = 8). This could be due to variable compensation by other genetic factors in this outbred line, health and natural variability of zebrafish clutches, or as will be discussed later, sex differences in adults as seen in human patients with SVAS; males have more severe phenotypes than females.

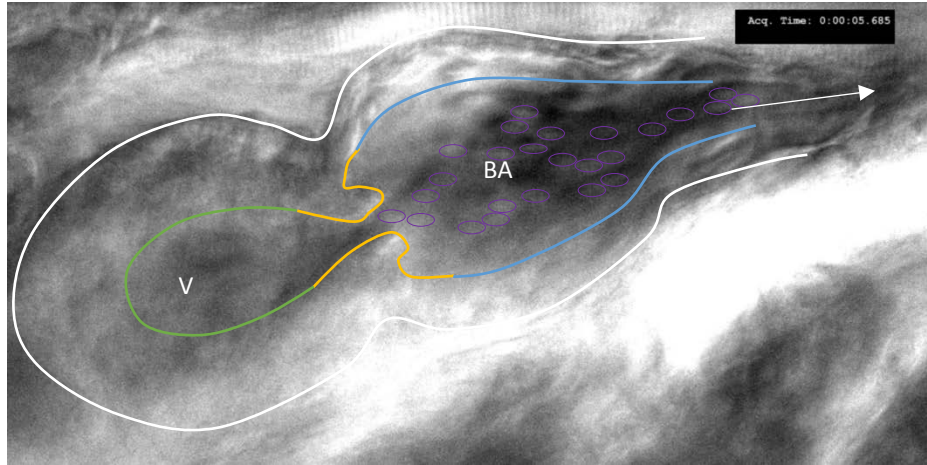


Figure 19. WT DIC Video Still of the Ventricular-Bulbar Valve at the End of Systole at 7dpf

Wildtype 7dpf embryo heart (white outline) displays normal blood flow from the ventricle (V) to the bulbus arteriosus (BA). Ventricular-bulbar valves (yellow outline) appear to have normal development. The V has normal contraction with the ventricular lumen narrowing (green) and the V becoming shorter. The BA widens (blue) to accept blood cells (purple). Blood flows from the BA to the ventral aorta (arrow). dpf – days post fertilization

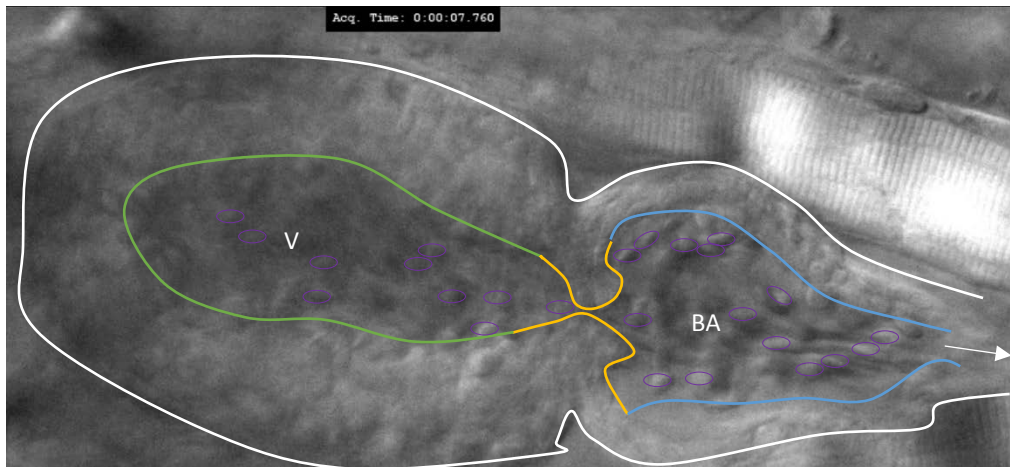


Figure 20. *elna*^{sa/sa} DIC Video Still of the Ventricular-Bulbar Valve at the End of Systole at 7 dpf

elna^{sa/sa} mutant 7dpf embryo heart (white outline) displays blood regurgitation from the bulbus arteriosus (BA) to the ventricle (V). The Ventricular-bulbar valve (yellow outline) appears to have abnormal shape and an incomplete, more narrowed opening. The V has reduced contraction with the ventricular lumen and V remaining elongated (green). The BA widens (blue) to accept blood cells (purple). Blood flows from the BA to the OFT (arrow), but the V and BA do not empty completely of blood cells. dpf – days post fertilization

To investigate if there were alterations in the size of the cardiac chambers, colonies of *Tg(myl7:eGFP);Tg(acta2:mCherry)* transgenic *elna^{sa/sa}* mutants and *elna^{+/+}* wildtype fish were developed. In these transgenic animals, mCherry marks smooth muscle cells in the bulbus arteriosus, ventricle, atrium and large arteries, and eGFP marks the myocardium. Confocal microscopy was used to take high-resolution images of the heart at 7 dpf from a clutch of WT (n = 6) and a clutch of *elna^{sa/sa}* mutants (n = 7). Wildtype embryos' pharyngeal arch arteries were consistently more visible than in the mutants, suggesting reduced transcriptional activity of the *acta2* promoter or incomplete covering of these vessels by smooth muscle cells. Mutant embryos displayed abnormalities of the ventricle and BA (Figure 21). Measurements were performed with the use of NIS-Elements software. Mutant fish had slightly larger ventricles, and smaller BA, but because of substantial variation in the size of these chambers in both groups of fish, these differences did not reach statistical significance (Table 24).

Table 24. Ventricle and Bulbus Measurements in WT and *elna^{sa/sa}* transgenic larvae

Genotype	#	Ventricle Length (μm)	Aspect Ratio Ventricle (W:L)	Bulbus Length (μm)	Aspect Ratio Bulbus (W:L)
<i>elna^{sa/sa}</i>	1	151.18	0.79	75.39	0.75
	2	164.23	0.57	61.68	1.01
	3	147.56	0.70	57.30	1.08
	4	178.89	0.65	76.51	0.81
	5	168.31	0.51	59.76	1.07
	6	156.73	0.69	75.09	0.79
	7	165.09	0.82	100.62	0.85
WT (Tü/AB*)	1	165.59	0.62	68.85	0.68
	2	165.16	0.72	81.86	0.57
	3	137.11	0.69	89.10	0.85
	4	133.25	0.65	81.52	0.98
	5	159.54	0.89	91.86	0.70
	6	142.94	0.64	77.59	0.77

Unpaired T-test (two-tailed)

P-value	0.1416	0.6677	0.1952	0.0831
t, df	t=1.584 df=11	t=0.441 df=11	t=1.379 df=11	t=1.906 df=11
Significant?	No	No	No	No
Mean <i>elna^{sa/sa}</i>	161.71	0.68	72.34	0.91
Mean WT Tu(AB*)	150.60	0.70	81.80	0.76
Diff. of means	11.11 \pm 7.019	-0.02595 \pm 0.059	-9.461 \pm 6.859	0.1502 \pm 0.079

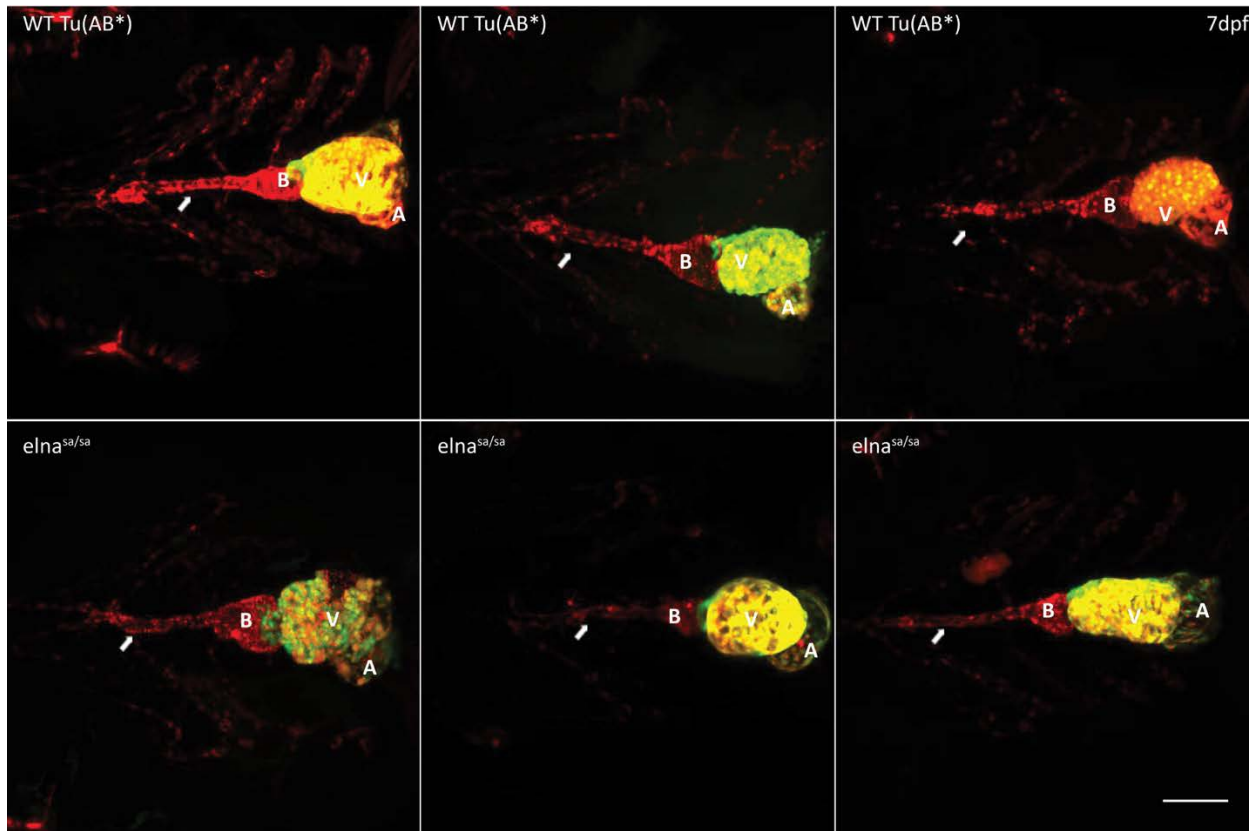


Figure 21. Abnormalities of the circulatory system in the developing embryo

Representative images of the ventral view of wildtype $Tü/AB^*$ $Tg(myl7:eGPF; ca8:mCherry)$ and $elna^{sa/sa}$ $Tg(myl7:eGPF; ca8:mCherry)$ homozygous mutants at 7 dpf. Mutant embryos displayed abnormalities of the ventricle (V - yellow), atrium (A - red/orange), bulbus arteriosus (B - red) and ventral aorta (solid arrow). Scale bar: 100 μ m. dpf – days post fertilization

3.6 ELASTIN STAINING IN THE ZEBRAFISH ADULT CARDIOVASCULAR SYSTEM

Adult hearts were dissected from wildtype Tü/AB*, *elna^{sa/+}* and *elna^{sa/sa}* male and female fish, fixed in formalin, embedded in paraffin, sectioned and stained using Hart's elastin stain to visualize elastin deposition and the morphology of the hearts (Figure 22). Histological sections show thinner valves in mutants, supporting the notion that the valve form and function observed in the DIC videos of mutant embryos remains in adults (Figure 23).

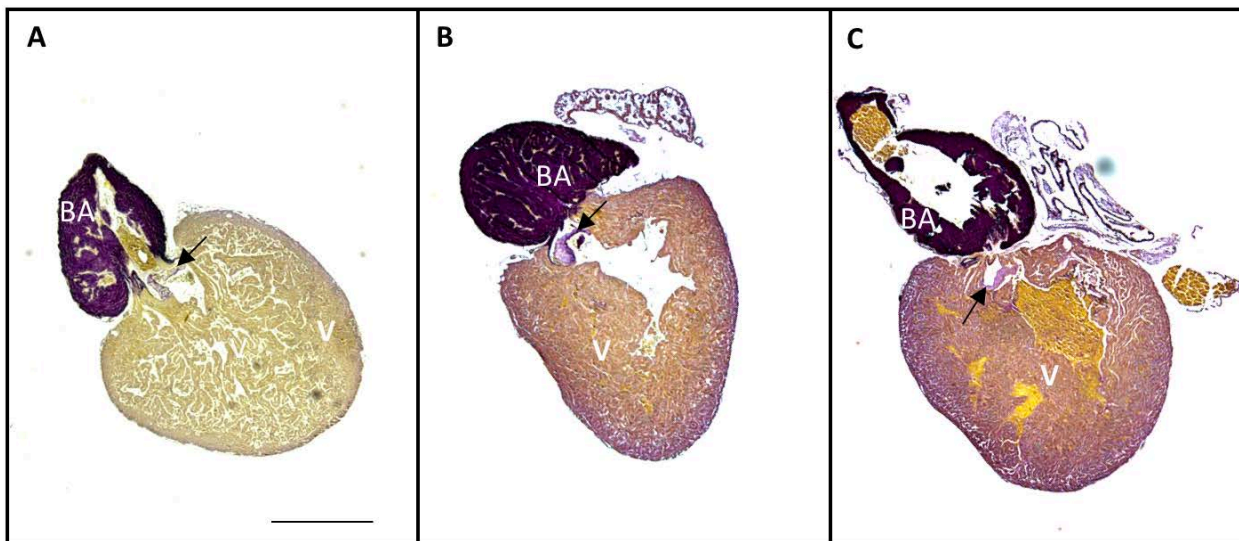


Figure 22. Hart's Elastin Stain of Adult Zebrafish Hearts

(A) WT Tü/AB* male adult heart, (B) *elna^{sa/+}* female adult heart, (C) *elna^{sa/sa}* female adult heart. Cardiac muscle (yellow) is observed throughout the ventricle (V) with elastin deposition (deep purple) in the bulbus arteriosus (BA). The ventricular-bulbar valves (arrow) appear thinner and more irregular in the mutant (C). Scale bar: 500 μ M.

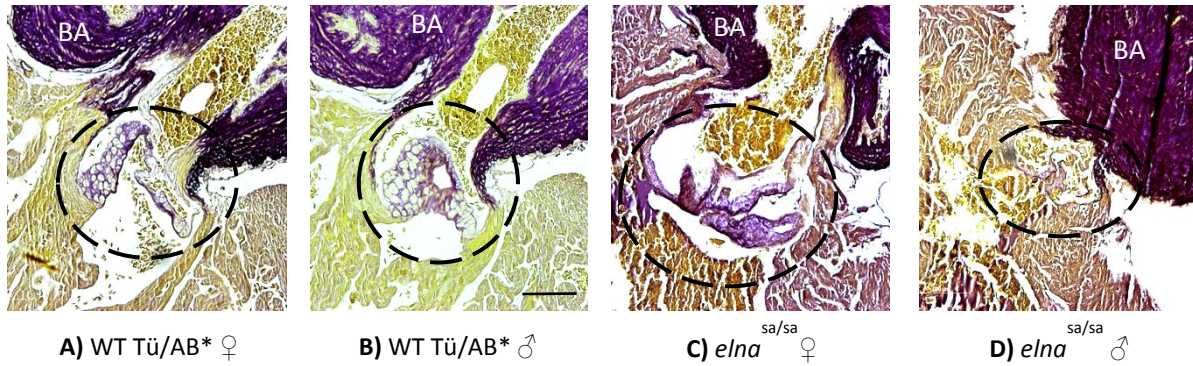


Figure 23. Hart's Elastin Stain of Adult Zebrafish Hearts – high-magnification view of the VB Valve

(A) WT Tü/AB* female adult heart, (B) WT Tü/AB* male adult heart, (C) *elna*^{sa/sa} female adult heart, (D) *elna*^{sa/sa} male adult heart. Histological sections show thinner valves (dotted circle) in mutants (C,D) than in wildtype (A,B) adult hearts extracted at 18 months of age. Valve composition also seems to appear more cartilaginous in wildtype (A,B) hearts, while mutants (C,D) appear to have a more fibrous and dense composition. (BA: bulbus arteriosus. Scale bar: 100 μM)

3.7 ECHOCARDIOGRAPHY IN ADULT FISH

Echocardiography was done on 18-month-old WT and *elna*^{sa/sa} adult zebrafish hearts. These adults were obtained from the same *elna*^{sa/+} in-cross clutch to eliminate husbandry and environmental bias that may occur from observing different clutches. Four WT (3♀ and 1♂) and four *elna*^{sa} (3♀ and 1♂) hearts were examined. The preliminary findings show blood regurgitation of the VB valve in the *elna*^{sa/sa} male (Figure 24). None of the *elna*^{sa/sa} females nor any of the WT hearts showed signs of VB valve regurgitation (Figure 25). Echocardiography of a larger number of fish will be necessary to determine if mutant males are more susceptible to developing valve disease than females, similar to increased cardiovascular disease in male WBS patients compared to females (Sadler et al., 2001).

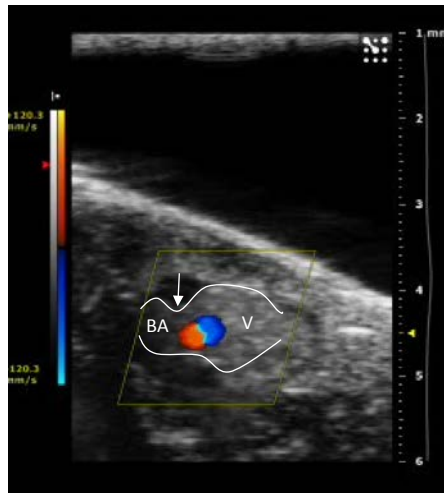


Figure 24. *elna^{sa/sa}* Echocardiography of a 18mo Male Heart

Echocardiography of the male *elna^{sa}* ventricular-bulbar valve (arrow) displays regurgitation. Forward flow of blood (dark blue) from ventricle (V) to bulbus arteriosus (BA) and backwards flow (red) from bulbus arteriosus towards ventricle. Red and blue colliding circles (light blue line) indicates blood flow regurgitation point.

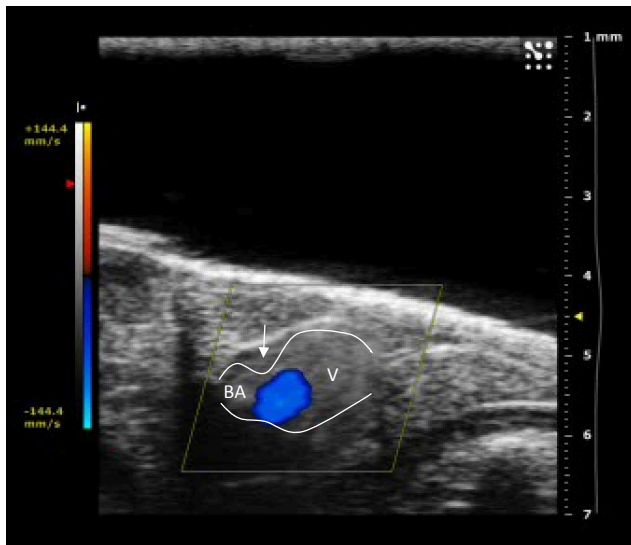


Figure 25. Echocardiography of a WT 18mo Female Heart

Echocardiography of the female WT ventricular-bulbar valve (arrow) displays only forward blood flow (blue) from the ventricle (V) to the bulbus arteriosus (BA).

3.8 SURVIVAL OF *elna* MUTANTS TO ADULTHOOD

The generation of embryos bred from an in-crossed *elna*^{sa/+} ♂ x *elna*^{sa/+} ♀ breeding resulted in 341 out of 1,001 embryos surviving to 3 months (Table 25). Genotyping of the 341 survivors exhibited a distribution of Mendelian frequencies: *elna*^{+/+} – 78 (23%), *elna*^{sa/+} – 183 (54%), and *elna*^{sa/sa} – 80 (23%). A portion of those fish were used for experiments and the new ratios at 3.5 months were as follows: *elna*^{+/+} – 66 (21.6%), *elna*^{sa/+} – 171 (56.1%), and *elna*^{sa/sa} – 68 (22.3%). These fish were followed for survival until 18 months of age.

At 18 months of age, homozygous *elna*^{sa/sa} had the lowest percentage of survival at 19%, but WT *elna*^{+/+} fish also had poor survival (30%, Table 26) presumably as a result of sub-optimal husbandry conditions. Further analysis was done to compare survival between the genotypes and also by sex. Despite the log-rank test for survival P value showing significance of 0.0025 by genotype comparison, suggesting that survival curves by genotype are different, the log-rank test for trend showed no significant trends by genotype or by sex (Table 27). The log-rank test for trend tests a null hypothesis that there is no linear trend between the groups and their median survival. With no significant P value for any of the groups, one can conclude that there is no significant trend of survival (Figure 26). The relatively low number of fish included in this preliminary experiment, as well as the high baseline mortality, reduced the power to detect significant genotype or sex effects.

Table 25. Survival of Genotyped Zebrafish at 3.5 months

Genotype	Genotyped at 3.5 months of age (% - Mendelian Ratios)			Fish Genotyped @3.5 months of age Minus # Removed for Experiments		
	# Females	# Males	Total # Survived	# Females	# Males	Total # Survived
<i>elna</i> ^{+/+}	54	24	78 (22.87%)	48	18	66
<i>elna</i> ^{sa/+}	130	53	183 (53.67%)	124	47	171
<i>elna</i> ^{sa/sa}	54	26	80 (23.46%)	48	20	68
			341			305

Table 26. Survival of Genotyped Zebrafish at 18 months

Genotype	Survival of Fish Genotyped @3.5 months Minus # Removed for Experiments Until 18 months of age (% survival of that genotype)		
	# Females	# Males	Total # Survived
<i>elna</i> ^{+/+}	14 (29%)	6 (33%)	20 (30%)
<i>elna</i> ^{sa/+}	55(44%)	18 (38%)	72 (43%)
<i>elna</i> ^{sa/sa}	11 (23%)	2 (10%)	13 (19%)
			106

Table 27. Survival Analysis of Zebrafish at 18 months

	By Genotype	Females	Males
Log-rank test			
Chi square	11.98	8.21	5.309
P value	0.0025	0.0165	0.0703
Are the survival curves significantly different?	Yes	Yes	No
Log-rank test for trend			
Chi square	1.948	0.4033	2.608
P value	0.1628	0.5254	0.1063
Significant trend?	No	No	No

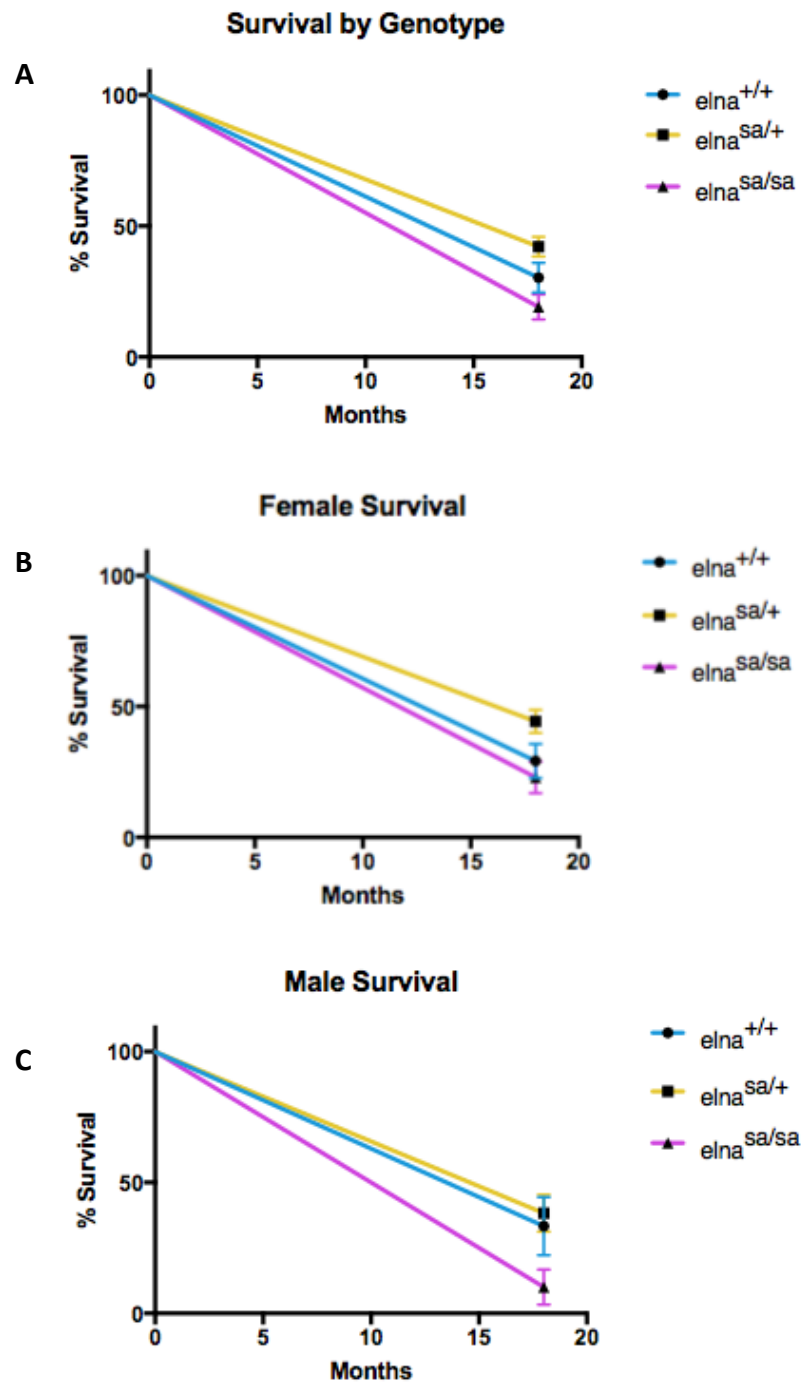


Figure 26. Survival of Zebrafish to 18 months

(A) Total surviving number of zebrafish by genotype at 18 months of age. (B) Survival of only female fish by genotype. (C) Survival of only male fish by genotype. Zebrafish were genotyped at 3.5 months of age, represented by 0 on the X-axis. All fish were siblings from an *elna*^{sa/+} in-cross.

3.9 VALIDATION OF *elnb* MUTANT

For future studies on the developmental function *elnb*, I obtained F1 embryos with a splice site mutation in intron 17 of *elnb* (*elnb*^{sa24024}, c.1771+1G>A) from the Sanger Institute Zebrafish Mutation Project. The embryos were allowed to reach adulthood and genotyped at 3 months, once again using the dCAPS method (Table 5). Sixty out of 101 embryos survived to adulthood, and of those, 47% were *elnb*^{sa/+} and 53% were *elnb*^{+/+}. An in-cross series of breeding of *elnb*^{sa/+} ♂ and ♀ was performed to establish a colony of *elnb*^{sa/+} and *elnb*^{sa/sa}. 24 out of 51 embryos survived to adulthood, with 71% *elnb*^{sa/+} and 29% were *elnb*^{+/+}. Due to a lack of any homozygous adults, a time series was conducted to determine at what stage the homozygotes were dying. Embryos collected and genotyped at 4 dpf, 12 dpf and 25 dpf were acquired from the same breeding clutch and showed survival of *elnb*^{sa/sa} up to 25 dpf (Table 28). The genotype of selected *elnb*^{+/+}, *elnb*^{sa/+} and *elnb*^{sa/sa} progeny was confirmed by DNA sequencing (Figure 27).

Table 28. Genotyping Distribution Results of *elnb* Heterozygous In-cross

Age	# of Embryos	Genotype	Count (%)
4 dpf	22	<i>elnb</i> ^{+/+}	4 (18)
		<i>elnb</i> ^{sa/+}	13 (59)
		<i>elnb</i> ^{sa/sa}	5 (23)
5 dpf	22	<i>elnb</i> ^{+/+}	6 (30)
		<i>elnb</i> ^{sa/+}	14 (70)
		<i>elnb</i> ^{sa/sa}	0 (0)
12 dpf	25	<i>elnb</i> ^{+/+}	2 (8)
		<i>elnb</i> ^{sa/+}	9 (36)
		<i>elnb</i> ^{sa/sa}	14 (56)
25 dpf	70	<i>elnb</i> ^{+/+}	11 (16)
		<i>elnb</i> ^{sa/+}	25 (36)
		<i>elnb</i> ^{sa/sa}	34 (48)
Time Series (12 hpf – 5dpf)	72 total for series	<i>elnb</i> ^{+/+}	24 (33)
		<i>elnb</i> ^{sa/+}	30 (42)
		<i>elnb</i> ^{sa/sa}	18 (25)
3 mph (adults)	24	<i>elnb</i> ^{+/+}	7 (29)
		<i>elnb</i> ^{sa/+}	17 (71)
		<i>elnb</i> ^{sa/sa}	0 (0)

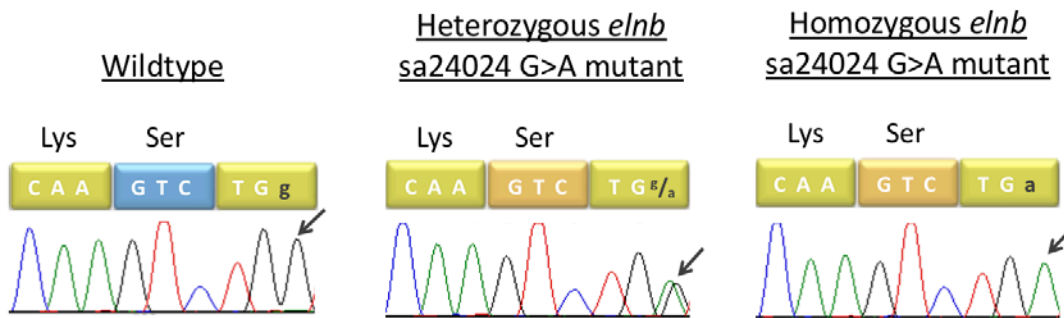


Figure 27. gDNA Sequencing of the Mutant Allele in *elnb* From Embryos at 12dpf

The peaks of the mutant allele (G - black) and wildtype allele (A - green) are of close to equal height in the heterozygous fish. Wildtype and homozygous mutants display their respective alleles.

3.10 EXPRESSION OF THE *elnb*^{sa24024} MUTANT ALLELE

Because the mutation c.1771+1G>A eliminates a critical G residue of the donor splice site in intron 17, I expected that this mutation would interfere with splicing. To uncover the exact splice outcome of the mutation, I sequenced cDNA from larvae at 12 dpf (Figure 28). Sequence of the heterozygous fish displayed overlapping sequence of exons 17 and 18 in 100% of the sequences, indicating an exon 17 skipping induced by the mutation.

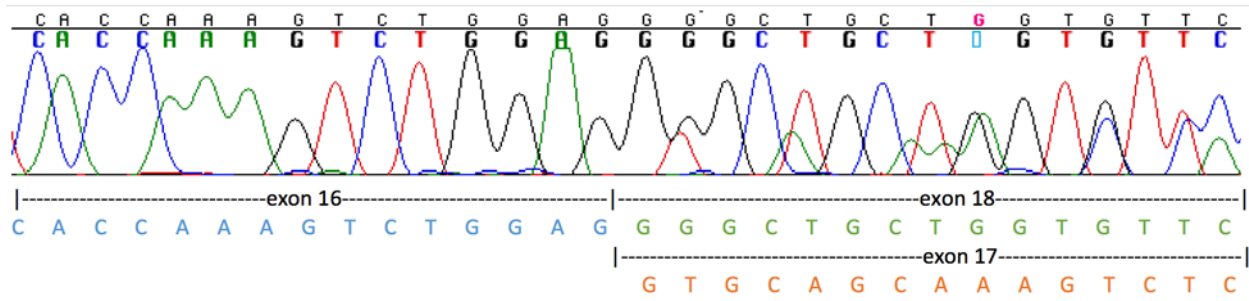


Figure 28. cDNA Sequencing of Heterozygous *elnb* Embryos at 12 dpf

4.0 DISCUSSION

In this study I have characterized the genetic and transcript diversity of *ELN* in both zebrafish genes, *elna* and *elnb*. Little information was available about the genetic diversity of these gene transcripts in zebrafish, despite research that has been done to sequence the genes in their entirety, for comparison to each other and among species (Chung et al., 2006; He et al., 2007). Diversity helps to explain how adapting genomes contribute to the survival of a species. Understanding genetic and transcript variation is also essential for interpreting the functional consequences of targeted mutations. Furthermore, this work will help to assess the structural similarities and differences between *elna* and *elnb* to clarify the function of each gene and whether there is any genetic compensation in mutants. Looking at zebrafish with a mutation in *elna* and characterizing the phenotype will help uncover the contribution of elastin to the development of the cardiovascular system and the congenital heart defects associated with supravalvular aortic stenosis (SVAS).

4.1 ELASTIN ISOFORM VARIATION AND ITS ROLE IN EVOLUTION

To characterize genetic and transcript diversity in *elna* and *elnb*, cDNA clones were generated from WT zebrafish larvae. There was large variation (Table 7) in the sequences compared to

already available transcripts in Ensembl, GenBank and in the literature (Chung et al., 2006), with the majority being SNVs, along with alternative splicing, numerous length variations and in-dels. High sequence variability has also been observed in the human *ELN* gene (Indik et al., 1987), therefore I propose that extensive sequence variation is an evolutionarily conserved feature of vertebrate elastin genes, producing a large ensemble of protein isoforms.

A closer look at the SNVs, and comparison to the available transcripts of *elna* and *elnb* (24 and 2 respectively), reveals that the majority of SNVs with accession numbers in the current dbSNP database for zebrafish elastin were intronic. The same observation was made from studies in avian populations (Backstrom, Fagerberg, & Ellegren, 2008; Strand et al., 2012; Zhan et al., 2015). Since introns are not translated, intronic SNVs are considered benign unless they influence the splicing of introns or the function of intronic transcriptional regulatory regions. However, SNVs found in exons and conserved regions of the elastin genes may prove more useful in studying adaptation and fitness among species (Barreiro, Laval, Quach, Patin, & Quintana-Murci, 2008; Norrgard & Schultz, 2008; Zhan et al., 2015)

The density of SNVs has been extensively studied in the human genome, which is useful for providing a context to my results. Overall, the ratio of non-synonymous (missense) to synonymous (silent) SNVs in the human genome is 1.18, which is less than half of what is expected under a neutral mutation theory (Zhao, Fu, Hewett-Emmett, & Boerwinkle, 2003). A reduced missense/silent SNV ratio is considered a measure of natural or purifying selection. By comparison, I found a missense/silent ratio of $18/51=0.35$ in *elna* and $41/36=1.14$ in *elnb*. Thus,

zebrafish *elna* is under a considerably stronger purifying selection than an average human gene, whereas the selection on *elnb* is similar to an average human gene. Strong purifying selection on *elna* is consistent with its widespread expression in multiple organs and its orthologous relationship to amniote elastin genes. In contrast, weaker purifying selection, and perhaps ongoing evolution of *elnb* may be related to its specialized function in the bulbus arteriosus and marked sequence divergence from a putative ancestral elastin gene.

4.2 ZEBRAFISH *ELNA*'S FUNCTION AND ROLE IN CARDIOVASCULAR DEVELOPMENT

Examination of the *elna*^{sa} point mutation in mRNA from zebrafish embryos reveals that nonsense-mediated decay (NMD) is activated through developmental regulation. In the *elna*^{sa/sa} mutant, there is elimination of the mutant transcript, creating a null allele. NMD is essential in the detection and elimination of premature termination codons (PTCs) for proper gene expression. Both mammals (Nagy & Maquat, 1998) and zebrafish (Wittkopp et al., 2009) require an exon-exon boundary at least 50 basepairs (bp) downstream of the PTC to efficiently activate NMD. While the PTC for *elna*^{sa} is far upstream of the last exon-exon junction, and is thus expected to activate NMD, other factors may also play a role in the effectiveness of NMD. Several genes are found to make up a group of NMD effectors or surveillance complex, responsible for the acceleration of degradation when interacting with other pathway complexes (Behm-Ansmant & Izaurralde, 2006), such as the up-frameshift suppressor (UPF) 1, or suppressor with morphological effect on genitalia (SMG) proteins SMG1 and SMG7. Studies in zebrafish have shown mixed results, in which downregulating of SMG7 did not produce a phenotype, but the

downregulation of UPF1 through the use of morpholinos did produce a phenotype and had high mortality rates leaves questions as to whether NMD is necessary for embryo viability (Hwang & Maquat, 2011; Wittkopp et al., 2009). It is possible that these factors are developmentally regulated and thus would explain the late activation of NMD in *elna*. An alternative explanation for the late activation of NMD for the *elna^{sa}* mutation is that NMD may require a certain threshold of mutant mRNA expression to be activated. Thus at developmental stages where *elna* expression is low, such as earlier than 3dpf, the mutant transcripts escape NMD. However, irrespective of whether the product of the *elna^{sa}* allele is degraded by NMD or results in a truncated protein lacking most of the coding region, it is expected to be a null allele, which was confirmed by my immunostaining results.

In light of evidence for *elna^{sa}* being a null allele, and signs of strong purifying selection in *elna*, it is surprising that homozygous mutants are viable to adulthood (3 mpf) at Mendelian ratios. A possible explanation for the survival of *elna* mutants is genetic compensation where the expression of key genes is altered through development to counteract the phenotypic effects of the mutation. This was observed in *egfl7* mutants, where genetic compensation was induced by deleterious mutations but not by gene knockdowns with the use of morpholinos and CRISPR (Rossi et al., 2015). Compensation may occur through the upregulation of a seemingly unrelated gene, such as *emilin2a*, *emilin3a* and *emilin3b* in the case of *egfl7* mutants, or through the upregulation of the paralog of the mutated gene such as *vegfab* in *vegfaa* mutants.

Possible functional overlap and compensation between *elna* and *elnb* will be tested in future work with my *elnb*^{sa} zebrafish line to create a double knockout for *elna* and *elnb*. A limitation that must be taken into consideration with the generation of a double mutant is lethality. Elastin is essential in a wide number of systems in the body and its elimination could prove fatal. Although, creation of a heterozygous loss of function elastin mutant, with complete elimination of *elnb* and only one functioning allele of *elna*, may prove more informative in relation to SVAS and cardiac development. In humans SVAS, especially when part of WBS, has variable manifestation of the phenotype and is often seen with valvular defects (Sadler et al., 2001) as observed in both the *elna*^{sa} embryos and adults.

In more detailed investigation of how elastin depletion affects cardiovascular development, DIC video microscopy of 7dpf embryos showed WT embryos with normal blood flow, ventricular contraction and valve development at the VB valve. Mutants displayed blood regurgitation, abnormal ventricular contraction and VB valve deformities but with varying degrees of abnormalities. When compared to adult hearts using echocardiography, a male *elna*^{sa/sa} mutant had regurgitation, and histological sections show thinner valves in mutants. This is promising since cardiovascular deformities are seen more often in human males than in females. A limitation of this study is the small number of fish used for imaging and the variability that is observed in clutches. This may explain the lack of significant difference between WT and mutant heart rates observed as well as in the confocal heart measurements. The preliminary results are encouraging considering the variability of penetrance and phenotypes observed in human SVAS, thus further work with larger numbers of fish is needed.

5.0 CONCLUSIONS

In summary, the work shows that elastin has been conserved through its ability to adapt to evolutionary stressors with extensive sequence variation, and in zebrafish in particular, the neofunctionalization of a second elastin gene *elnb* that may still be evolving. Mutants of *elna*^{sa} have displayed promise to help explain cardiovascular development and detrimental effects of elastin mutations in humans with SVAS with a display of valvular abnormalities and regurgitation of blood flow in the heart. However, further testing must be done to determine the molecular mechanisms of this phenotype and to rule out genetic compensation through the presence of two elastin genes, *elna* and *elnb*, in zebrafish.

6.0 FUTURE WORK

6.1 ADDITIONAL PHENOTYPE CONFIRMATION

6.1.1 Additional Look at Valve Structures in Adult Zebrafish

Based on the preliminary results obtained in the echocardiography and Hart's elastin staining studies, a larger number of adult hearts obtained from the same *elna^{sa/+}* in-cross will need to be examined to determine the frequency of BA valve defects and other possible cardiac anomalies.

Method: The same protocols established earlier in the dissertation will be used to assure consistency in the steps used to obtain results and to maintain the ability to compare preliminary data to those in the future.

Expected Results: I expect to see regurgitation and valve developmental abnormalities in at least some of the mutant hearts. Given the variability of SVAS in humans, I may find the same in zebrafish.

6.1.2 Whole-mount In Situ Time Series of Zebrafish Embryos

As another method to observe elastin expression in the embryos in addition to the whole-mount immunostaining, and to compare results to work done in previous research, a time series in embryos using whole-mount in situ hybridization will be conducted.

Method: WT Tü/AB* and *elna*^{sa/sa} embryos will be collected at 3dpf, 5dpf and 7dpf and treated with riboprobes for *elna* and *elnb*. Embryos from all 3 time points will be processed and imaged simultaneously.

Expected Results: Some overlap of expression of *elna* and *elnb* is to be expected at earlier time points in WT embryos, but by 7dpf I expect to see *elnb* expressed exclusively in the bulbus arteriosus. Mutants of *elna* should not show any expression.

6.1.3 Generation of an *elnb* Mutant Line

With the possibility of genetic compensation of *elna* and *elnb*, and to further the research of *elnb*'s function in zebrafish, a line of *elnb*^{sa/sa} fish is to be established and crossed with the *elna*^{sa/sa} fish.

Method: Traditional husbandry methods will be used to cross the necessary lines. dCAPs will be used for genotyping and observation of the embryos for phenotypic abnormalities will be conducted as was done with *elna*.

Expected Results: It is likely that a double knockout of both *elna* and *elnb* will not produce a viable line of zebrafish for use in adult experiments. Examination of the onset and time course of lethality and identifying the cause of death in double mutants will inform our understanding of elastin function in zebrafish. For creating a non-lethal model of SVAS a heterozygous loss of function of *elna* and a total loss of *elnb* may be of interest.

6.2 MECHANISTIC PATHWAYS ASSOCIATED WITH *ELN* LOSS

A better understanding of the connection between elastin mutations and impaired cardiovascular development in zebrafish is needed through probing of the molecular mechanisms. This work will also help test if these pathways are evolutionarily conserved among vertebrates. Prior studies have associated two pathways with elastin deficiency in vertebrates, integrin beta 3 (*Itgb3*) signaling and the Hippo pathways.

6.2.1 Integrin Beta 3 Signaling and Vessel Development

Elevated integrin beta 3 (*Itgb3*) signaling was found to be critical for the development of vessel wall thickening in a mouse model of SVAS (Ashish Misra et al., 2016). The integrin signaling studies will focus on *elna* mutants, as this gene appears to be the ortholog of mammalian elastin. However, *elnb* mutants may also be used for comparison, especially if double mutant studies suggest a functional overlap.

Method: Immunoblotting for phosphorylated and unphosphorylated focal adhesion kinase (FAK) and immunostaining for activated beta 3 integrin will be used to quantify integrin signaling. In addition, the expression of the *Itgb3* paralogs, *itgb3a* or *itgb3b* will be assessed by qPCR and/or *in situ* hybridization. For functional studies, *Itgb3* signaling will be inhibited using the small molecule inhibitor cilengitide (A. Misra et al., 2016).

Expected Results: If *elna* is the ortholog of mammalian *ELN*, I expect elevated *Itgb3* signaling upon *elna* deficiency, and a rescue of the mutant phenotype by *Itgb3* inhibition.

6.2.2 Hippo Signaling as a Mechanism of Disease

A study of *elnb* in zebrafish observed that knockdown of *yap*, a signal transducer of the Hippo pathway, resulted in a similar expansion of cardiomyocytes into the bulbus arteriosus as *elnb* knockdown did (Moriyama et al., 2016). As this is a correlative result, I am interested in obtaining more functional evidence for altered Hippo signaling as a possible mechanism of disease in *elnb* deficiency.

Method: Immunoblotting for phosphorylated and unphosphorylated Yap and immunostaining for Yap/Taz will be used to quantify Hippo signaling. For functional studies, constitutively active *yap* (5SA) mRNA (Asaoka, Hata, Namae, Furutani-Seiki, & Nishina, 2014) will be injected into *elnb* deficient embryos. Alternatively, Hippo signaling will be inhibited using the small molecule

inhibitors verteporfin, which inhibits YAP-TEAD interaction and transcriptional activation, or by 9E1, which inhibits MST1 kinase activity, or by MO knockdown of *yap*.

Expected Results: If *elnb*-up-regulates Hippo signaling to facilitate the differentiation of smooth muscle cells from heart field progenitors, I expect reduced Hippo signaling in the absence of *Elnb*, a rescue of *elnb*-related defects by constitutively active *yap*, and an exacerbated *elnb* phenotype by Hippo inhibition.

APPENDIX: TABLES

Table 29. Primers used in amplifying *elna* cDNA fragments

Amp #	Amp Name	Clone #	Amp Sizes (bp)	Forward Primer	Exon	Sequence	Reverse Primer	Exon	Sequence
1	21wb	6	845-860	<i>zf elna</i> I5'1.1s	5' UTR	aataaaaccagcacattcgg	<i>zf elna</i> E9.1a	13	tgggagattgagggggg
2	22.1	6	416-422	<i>zf elna</i> E5.1s	9	agcaaaggctggaaaagc	<i>zf elna</i> E16.1a*	16	atttagcagctttgcct
3	22.2	5	410-1391	<i>zf elna</i> E9.1s	13	agcaaggagtgtttcacgga	<i>zf elna</i> E32.1a*	32	tttgcttgagctgggtgta
4	22.3	4	601-712	<i>zf elna</i> E26.1s*	26	caggcaaaagctgctaaat	<i>zf elna</i> E36.3a	40	atttagtggttttgctcca
	22.3a	5	1009-1117	<i>zf elna</i> E23-24.1s*	23-24	tatcctgcgccaggaggt	<i>zf elna</i> E36.3a	40	atttagtggttttgctcca
5	23.1	6	319-448	<i>zf elna</i> E36.1s	40	tggagcaaaaccacctaataat	<i>zf elna</i> E41.1a	45	gccactgggaacagcaat
	23.1a	8	481-670	<i>zf elna</i> E36.1s*	36	tggaggaacaggtttggga	<i>zf elna</i> E41.1a	45	gccactgggaacagcaat
6	23.2	7	1003-1045	<i>zf elna</i> E41.1s*	41	aggagtacctggaggagtg	<i>zf elna</i> I56.1a*	3' UTR	aaacgaacaggactgggg

Amp: amplicon

Table 30. Primers used in amplifying *elnb* cDNA fragments

Amp #	Amp Name	Clone #	Amp Sizes (bp)	Forward Primer	Exon	Sequence	Reverse Primer	Exon	Sequence
1	4.1w	5	772	<i>zf elnb</i> I5'1.1s	5' UTR	cctaattacgtagttccttc	<i>zf elnb</i> E8.1a	8	gtcctattcctccagtgctaa
2	4.2b	4	1115	<i>zf elnb</i> E5.3s	5	tacctgggtggttttgggtgtgtgt	<i>zf elnb</i> E16.1a	16	atatccaccaaacacgccag
	4.2b2	1	893	<i>zf elnb</i> E6-7.1s	6--7	aataggtgtgggtggaag	<i>zf elnb</i> E14.1a	14	cacctggcagaactcctctt
3	4.4h	6	799-979	<i>zf elnb</i> E12.1s	12	taaagttggaagcctgggaa	<i>zf elnb</i> E22.2a	22	ccaagacctccaccaggaa
4	15.1b	4	796-1444	<i>zf elnb</i> E20.4s	20	ttctggttgggaggggtg	<i>zf elnb</i> E30.2a	30	aacactccctgggtccaaa
	15.1b2	4	692-1388	<i>zf elnb</i> E20-21.1s	20-21	gtcccgaagatatgctg	<i>zf elnb</i> E30.2a	30	aacactccctgggtccaaa
5	15.2g	5	1080-1293	<i>zf elnb</i> E29.1s	29	atgcagaggcaaaagctc	<i>zf elnb</i> E43.1a	43	tcccgcaactccataaa
6	18.1a	5	456-483	<i>zf elnb</i> E38.1s	38	agttggtggagtggaaagt	<i>zf elnb</i> E46.1a	46	ccaattccgctgcctatact
7	18.2a	7	572-761	<i>zf elnb</i> E45.1s	45	aacattaccaggagccaaacca	<i>zf elnb</i> E50.1a	50	tgctgctccataaactttt
8	18.3c	6	956-1013	<i>zf elnb</i> E48.1s	48	ttatggtggagctggaag	<i>zf elnb</i> E58.2a	3' UTR	gcgtgtgacaagttaaggga

Amp: amplicon

Table 31. Primers used to sequence *elna* cDNA fragments

Amp #, Name	1, 21wb	2, 22.1	3, 22.2	4, 22.3	4, 22.3a	5, 23.1	5, 23.1a	6, 23.2
Primer Name, Sequence	<i>zf elna</i> I5'1.1s aataaaaccagcacattcgg	<i>zf elna</i> 5.1s agcaaaggctggaaaagc	<i>zf elna</i> E9.1s agcaaggagtgtttcacgga	<i>zf elna</i> E26.1s* caggcaaaagctgctaataat	<i>zf elna</i> E23-24.1s* tatcctgcgccaggaggt	<i>zf elna</i> E36.1s tggagcaaaaccacctaataat	<i>zf elna</i> E36.1s* tggaggaacaggttttggga	<i>zf elna</i> E41.1s* aggagtagctggaggagtg
	<i>zf elna</i> 9.1a acccctcaaatctccca	<i>zf elna</i> E16.1a* atttagcagctttggcct	<i>zf elna</i> E32.1a* tttgcttgagctggtgta	<i>zf elna</i> E36.3a atttaggtggttttgcctca	<i>zf elna</i> E36.3a atttaggtggttttgcctca	<i>zf elna</i> E41.1a gccactgggaacagcaat	<i>zf elna</i> E41.1a gccactgggaacagcaat	<i>zf elna</i> I56.1a* aaacgaacaggactgggg
	M13F -20 (18mer) tgtaaaacgacggccagt	M13F -20 (18mer) tgtaaaacgacggccagt	M13F -20 (18mer) tgtaaaacgacggccagt	M13F -20 (18mer) tgtaaaacgacggccagt	M13F -20 (18mer) tgtaaaacgacggccagt	M13F -20 (18mer) tgtaaaacgacggccagt	M13F -20 (18mer) tgtaaaacgacggccagt	M13F -20 (18mer) tgtaaaacgacggccagt
	M13R (17mer) caggaacagctatgac	M13R (17mer) caggaacagctatgac	M13R (17mer) caggaacagctatgac	M13R (17mer) caggaacagctatgac	M13R (17mer) caggaacagctatgac	M13R (17mer) caggaacagctatgac	M13R (17mer) caggaacagctatgac	M13R (17mer) caggaacagctatgac
	<i>zf elna</i> KE4.1s aggaggatattggaggagctg	<i>zf elna</i> 9.1a acccctcaaatctccca	<i>zf elna</i> 13.2a caccagcaccaccagga	<i>zf elna</i> E29.1s ccgggtgttggaggactgta	<i>zf elna</i> E31.1a* aacaatcccagctcctactg	<i>zf elna</i> E36.1s* tggaggaacaggttttggga		<i>zf elna</i> E52.1a gatactcaaacaccgcc
	<i>zf elna</i> 1.1s gtggatatggtggtgctgga	<i>zf elna</i> 11.1a tccagcacctccacaaagc	<i>zf elna</i> E16.1a* atttagcagctttggcct	<i>zf elna</i> 34.1a ctggtgttgcctggact	<i>zf elna</i> 32-33.1s* taaatacggctcaggtgcgg			<i>zf elna</i> E50-51.1s* caggttggactgggaa
	<i>zf elna</i> 5.1s agcaaaggctggaaaagc	<i>zf elna</i> 5.1s agcaaaggctggaaaagc	<i>zf elna</i> E18-19.1s* taaatatggtgctgtccctgg	<i>zf elna</i> E36.3a atttaggtggttttgcctca	<i>zf elna</i> E33.1a* acagtcctccaacaccgga			<i>zf elna</i> E41.1a attgctgtcccagtgcc
				<i>zf elna</i> E25.2a attcttctggtggtgct	<i>zf elna</i> E27.1s* attcttctggtggtgccc			<i>zf elna</i> E51.1s aatcgggtggtgactgaca
				<i>zf elna</i> E36.1s* tggaggaacaggttttggga	<i>zf elna</i> E37-38.1s* aaatatggtttgggaagtgg			

Amp: amplicon

Table 32. Primers used to sequence *elnb* cDNA fragments

Amp #, Name	1, 4.1w	2, 4.2b	2, 4.2b2	3, 4.4h	4, 15.1b	4, 15.1b2	5, 15.2g	6, 18.1a	7, 18.2a	8, 18.3c	
Primer Name, Sequence	<i>zf elnb</i> I5'1.1s cctaattacgtagtgttccttc	<i>zf elnb</i> E5.3s tacctgggtgttttgggtgtggt	<i>zf elnb</i> E6-7.1s aataggtgtgggtggaaaag	<i>zf elnb</i> E12.1s taaagttggaaagcctgggaa	<i>zf elnb</i> E20.4s ttctggtttgggaggggtg	<i>zf elnb</i> E20-21.1s gtccccgaaggatgctg	<i>zf elnb</i> E29.1s atgcagaggcaaaagctc	<i>zf elnb</i> E38.1s agttgggtggagttggaagtg	<i>zf elnb</i> E45.1s aacattaccaggagccaaacca	<i>zf elnb</i> E48.1s ttatgggtggagctggaaag	
	<i>zf elnb</i> E8.1a gtcctattcctcagtgctaa	<i>zf elnb</i> E16.1a atatccaccaaacacgccag	<i>zf elnb</i> E14.1a cacctggcagaactcctctt	<i>zf elnb</i> E22.2a cccaagacctccaccaggaa	<i>zf elnb</i> E30.2a aacactcctgggtccaaa	<i>zf elnb</i> E30.2a aacactcctgggtccaaa	<i>zf elnb</i> E43.1a tccccgcaactccataaav	<i>zf elnb</i> E46.1a ccaattccgctgcctatact	<i>zf elnb</i> E50.1a tgctgctccataaactttt	<i>zf elnb</i> E58.2a gcgttgtgacaagttaaggga	
	M13F -20 (18mer) tgtaaaaacgacggccagt	M13F -20 (18mer) tgtaaaaacgacggccagt	M13F -20 (18mer) tgtaaaaacgacggccagt	M13F -20 (18mer) tgtaaaaacgacggccagt	M13F -20 (18mer) tgtaaaaacgacggccagt	M13F -20 (18mer) tgtaaaaacgacggccagt	M13F -20 (18mer) tgtaaaaacgacggccagt	M13F -20 (18mer) tgtaaaaacgacggccagt	M13F -20 (18mer) tgtaaaaacgacggccagt	M13F -20 (18mer) tgtaaaaacgacggccagt	M13F -20 (18mer) tgtaaaaacgacggccagt
	M13R (17mer) caggaaacagctatgac	M13R (17mer) caggaaacagctatgac	M13R (17mer) caggaaacagctatgac	M13R (17mer) caggaaacagctatgac	M13R (17mer) caggaaacagctatgac	M13R (17mer) caggaaacagctatgac	M13R (17mer) caggaaacagctatgac	M13R (17mer) caggaaacagctatgac	M13R (17mer) caggaaacagctatgac	M13R (17mer) caggaaacagctatgac	M13R (17mer) caggaaacagctatgac
	<i>zf elnb</i> E3.2s tggaggtcttgggggaattg		<i>zf elnb</i> E10.1s tgggcaggaggtatttattc	<i>zf elnb</i> E18.1s ttgggtaggaggagtacct	<i>zf elnb</i> E24.2a agttcctaaagtcccaccac	<i>zf elnb</i> E28.1a taatccaccaagtccaacacca	<i>zf elnb</i> E30.1a tccttgccaactccagatcct	<i>zf elnb</i> E42.1a ttcagttttaggtccttcg	<i>zf elnb</i> E46.1a ccaattccgctgcctatact	<i>zf elnb</i> E52.1s acaaggaggaattggtggag	
	<i>zf elnb</i> E5.2s aggaattggagcaggttgta			<i>zf elnb</i> E20.3s tcttgggaactggaggacttc	<i>zf elnb</i> E26.2s tggtggacttgggtggacta	<i>zf elnb</i> E24.2a agttcctaaagtcccaccac	<i>zf elnb</i> E38.1s agttgggtggagttggaagtg	<i>zf elnb</i> E43.1a tccccgcaactccataaaa	<i>zf elnb</i> E46.2a aactccaccaactcccaggga	<i>zf elnb</i> E52.1a acaaggaggaattggtggag	
					<i>zf elnb</i> E24.1s aacttggaggtggacttggga	<i>zf elnb</i> E20-21.1s gtccccgaaggatgctg	<i>zf elnb</i> E30.1s ttcctggaggtggatgga	<i>zf elnb</i> E45.1s aacattaccaggagccaaacca	<i>zf elnb</i> E46.1s agttgggtggagttcctggtg	<i>zf elnb</i> E53.1s tttgaggttatggggagtt	
					<i>zf elnb</i> E24.1a aaagtcccaccacgtccaag	<i>zf elnb</i> E22.2a cccaagacctcccaccaggaa			<i>zf elnb</i> E47.1s aaaagttagtggagctggaa	<i>zf elnb</i> E57.1a tatttggcggcttttgattg	
						<i>zf elnb</i> E25.1a			<i>zf elnb</i> e46.3s aaggaggacctggaagtata	<i>zf elnb</i> E50.2a ataaccacctggaccctct	
						<i>zf elnb</i> E26.2s tggtggacttgggtggacta				<i>zf elnb</i> E50.3s ttggagcccaggtggata	
										<i>zf elnb</i> E50-51.1s ttggtgccttggttatggt	
										<i>zf elnb</i> E56.1s ttttggcgtcctggtgct	

Amp: amplicon

Table 33. GenBank accession numbers of cDNA clones

Submission Name	Submission ID (Begins w/ BankIt)	GenBank Accession Number
<i>elna</i>		
<i>elna</i> 21wb - 1	2010963	KY986538
<i>elna</i> 21wb - 2	2013293	MF034388
<i>elna</i> 21wb - 6	2013294	MF034389
<i>elna</i> 21wb - 8	2013295	MF034390
<i>elna</i> 21wb - 10	2013287	MF034386
<i>elna</i> 21wb - 11	2013290	MF034387
<i>elna</i> 22.1 - 6	2013308	MF034394
<i>elna</i> 22.1 - 8	2013310	MF034395
<i>elna</i> 22.1 - 9	2013312	MF034396
<i>elna</i> 22.1 - 10	2013304	MF034392
<i>elna</i> 22.1 - 11	2013307	MF034393
<i>elna</i> 22.1 - 13	2013296	MF034391
<i>elna</i> 22.2 - 5	2013337	MF034401
<i>elna</i> 22.2 - 11	2013335	MF034399
<i>elna</i> 22.2 - 38	2013336	MF034400
<i>elna</i> 22.2 - 100	2013313	MF034397
<i>elna</i> 22.2 - 101	2013334	MF034398
<i>elna</i> 22.3 - 13	2013578	MF039678
<i>elna</i> 22.3 - 15	2013579	MF039677
<i>elna</i> 22.3 - 18	2015245	MF101833
<i>elna</i> 22.3 - 21	2013581	MF039676
<i>elna</i> 22.3a - 3	2013588	MF039675
<i>elna</i> 22.3a - 4	2013590	MF039674
<i>elna</i> 22.3a - 5	2013591	MF039673
<i>elna</i> 22.3a - 6	2013592	MF039672
<i>elna</i> 22.3a - 7	2013593	MF039671
<i>elna</i> 23.1 - 4	2013601	MF039668
<i>elna</i> 23.1 - 6	2013603	MF039667
<i>elna</i> 23.1 - 8	2013604	MF039666
<i>elna</i> 23.1 - 9	2013605	MF039665
<i>elna</i> 23.1 - 11	2013599	MF039670
<i>elna</i> 23.1 - 12	2013600	MF039669
<i>elna</i> 23.1a - 1	2013840	MF039664
<i>elna</i> 23.1a - 2	2013842	MF039663
<i>elna</i> 23.1a - 3	2013844	MF039662
<i>elna</i> 23.1a - 4	2013846	MF039661
<i>elna</i> 23.1a - 5	2013853	MF039660
<i>elna</i> 23.1a - 6	2013856	MF039659
<i>elna</i> 23.1a - 7	2013858	MF039658
<i>elna</i> 23.1a - 8	2013859	MF039657
<i>elna</i> 23.2 - 8	2014488	MF067537
<i>elna</i> 23.2 - 10	2013860	MF067532
<i>elna</i> 23.2 - 14	2014470	MF067533
<i>elna</i> 23.2 - 16	2014473	MF067534
<i>elna</i> 23.2 - 20	2014475	MF067535
<i>elna</i> 23.2 - 22	2014476	MF067536
<i>elna</i> 23.2 - 17	2014491	MF067538

<i>elnb</i>		
<i>elnb</i> 4.1w - 1	2016080	MF101834
<i>elnb</i> 4.1w - 3	2016080	MF101835
<i>elnb</i> 4.1w - 4	2016083	MF101836
<i>elnb</i> 4.1w - 5	2016083	MF101837
<i>elnb</i> 4.1w - 6	2016083	MF101838
<i>elnb</i> 4.2b - 7	2016894	MF118562
<i>elnb</i> 4.2b2 - 14	2016891	MF118563
<i>elnb</i> 4.2b2 - 23	2016891	MF118564
<i>elnb</i> 4.2b2 - 2	2016891	MF118565
<i>elnb</i> 4.2b2 - 13	2016891	MF118566
<i>elnb</i> 4.3h - 1	2016895	MF118567
<i>elnb</i> 4.3h - 2	2016895	MF118568
<i>elnb</i> 4.3h - 3	2016895	MF118569
<i>elnb</i> 4.3h - 4	2016895	MF118570
<i>elnb</i> 4.3h - 5	2016895	MF118571
<i>elnb</i> 4.3h - 6	2016895	MF118572
<i>elnb</i> 15.1b - 10	2016901	MF118573
<i>elnb</i> 15.1b - 13	2016902	MF118574
<i>elnb</i> 15.1b - 15	2016904	MF118575
<i>elnb</i> 15.1b - 16	2016905	MF118576
<i>elnb</i> 15.1b2 - 5	2016906	MF118577
<i>elnb</i> 15.1b2 - 2	2016906	MF118578
<i>elnb</i> 15.1b2 - 6	2016906	MF118579
<i>elnb</i> 15.1b2 - 4	2016906	MF118580
<i>elnb</i> 15.2g - 2	2016908	MF118581
<i>elnb</i> 15.2g - 4	2016908	MF118582
<i>elnb</i> 15.2g - 5	2016908	MF118583
<i>elnb</i> 15.2g - 6	2016908	MF118584
<i>elnb</i> 15.2g - 1	Failed Submission	*
<i>elnb</i> 18.1a - 3	2016910	MF118585
<i>elnb</i> 18.1a - 4	2016910	MF118586
<i>elnb</i> 18.1a - 5	2016910	MF118587
<i>elnb</i> 18.1a - 6	2016910	MF118588
<i>elnb</i> 18.1a - 1	2016910	MF118589
<i>elnb</i> 18.2a - 2	2016911	MF118590
<i>elnb</i> 18.2a - 3	2016911	MF118591
<i>elnb</i> 18.2a - 4	2016911	MF118592
<i>elnb</i> 18.2a - 5	2016911	MF118593
<i>elnb</i> 18.2a - 6	2016911	MF118594
<i>elnb</i> 18.2a - 7	2016911	MF118595
<i>elnb</i> 18.2a - 8	2016911	MF118596
<i>elnb</i> 18.3c - 3	2016913	MF118597
<i>elnb</i> 18.3c - 4	2016913	MF118598
<i>elnb</i> 18.3c - 5	2016913	MF118599
<i>elnb</i> 18.3c - 6	2016913	MF118600
<i>elnb</i> 18.3c - 8	2016913	MF118601
<i>elnb</i> 18.3c - 2	2016913	MF118602

* contains premature stop codon, so not allowed to submit to GenBank

BIBLIOGRAPHY

- Ackerman, B. A., Böer, A., Bennin, B., & Gottlieb, G. J. (2005). *Histologic Diagnosis of Inflammatory Skin Diseases: An Algorithmic Method Based on Pattern Analysis* (3rd ed.): Ardor Scribendi.
- Alberts, B., Johnson, A., Lewis, J., Raff, M., Roberts, K., & Walter, P. (2008). *Molecular Biology of the Cell* (5th ed.). New York, NY: Garland Science, Taylor & Francis Group, LLC.
- Almine, J. F., Bax, D. V., Mithieux, S. M., Nivison-Smith, L., Rnjak, J., Waterhouse, A., . . . Weiss, A. S. (2010). Elastin-based materials. *Chem Soc Rev*, *39*(9), 3371-3379. doi:10.1039/b919452p
- Arribas, S. M., Hinek, A., & Gonzalez, M. C. (2006). Elastic fibres and vascular structure in hypertension. *Pharmacol Ther*, *111*(3), 771-791. doi:10.1016/j.pharmthera.2005.12.003
- Asaoka, Y., Hata, S., Namae, M., Furutani-Seiki, M., & Nishina, H. (2014). The Hippo pathway controls a switch between retinal progenitor cell proliferation and photoreceptor cell differentiation in zebrafish. *PLoS One*, *9*(5), e97365. doi:10.1371/journal.pone.0097365
- Asnani, A., & Peterson, R. T. (2014). The zebrafish as a tool to identify novel therapies for human cardiovascular disease. *Dis Model Mech*, *7*(7), 763-767. doi:10.1242/dmm.016170
- Backstrom, N., Fagerberg, S., & Ellegren, H. (2008). Genomics of natural bird populations: a gene-based set of reference markers evenly spread across the avian genome. *Mol Ecol*, *17*(4), 964-980. doi:10.1111/j.1365-294X.2007.03551.x
- Badesch, D. B., Lee, P. D., Parks, W. C., & Stenmark, K. R. (1989). Insulin-like growth factor I stimulates elastin synthesis by bovine pulmonary arterial smooth muscle cells. *Biochem Biophys Res Commun*, *160*(1), 382-387.
- Bakkers, J. (2011). Zebrafish as a model to study cardiac development and human cardiac disease. *Cardiovasc Res*, *91*(2), 279-288. doi:10.1093/cvr/cvr098
- Baldock, C., Oberhauser, A. F., Ma, L., Lammie, D., Siegler, V., Mithieux, S. M., . . . Weiss, A. S. (2011). Shape of tropoelastin, the highly extensible protein that controls human tissue elasticity. *Proc Natl Acad Sci U S A*, *108*(11), 4322-4327. doi:10.1073/pnas.1014280108
- Baldwin, A. K., Simpson, A., Steer, R., Cain, S. A., & Kielty, C. M. (2013). Elastic fibres in health and disease. *Expert Rev Mol Med*, *15*, e8. doi:10.1017/erm.2013.9
- Barreiro, L. B., Laval, G., Quach, H., Patin, E., & Quintana-Murci, L. (2008). Natural selection has driven population differentiation in modern humans. *Nat Genet*, *40*(3), 340-345. doi:10.1038/ng.78
- Bartman, T., Walsh, E. C., Wen, K. K., McKane, M., Ren, J., Alexander, J., . . . Stainier, D. Y. (2004). Early myocardial function affects endocardial cushion development in zebrafish. *PLoS Biol*, *2*(5), E129. doi:10.1371/journal.pbio.0020129
- Bashey, R. I., Torii, S., & Angrist, A. (1967). Age-related collagen and elastin content of human heart valves. *J Gerontol*, *22*(2), 203-208.

- Bauer-Mehren, A., Bundschuh, M., Rautschka, M., Mayer, M. A., Sanz, F., & Furlong, L. I. (2011). Gene-disease network analysis reveals functional modules in mendelian, complex and environmental diseases. *PLoS One*, *6*(6), e20284. doi:10.1371/journal.pone.0020284
- Bax, D. V., Bernard, S. E., Lomas, A., Morgan, A., Humphries, J., Shuttleworth, C. A., . . . Kielty, C. M. (2003). Cell adhesion to fibrillin-1 molecules and microfibrils is mediated by alpha 5 beta 1 and alpha v beta 3 integrins. *J Biol Chem*, *278*(36), 34605-34616. doi:10.1074/jbc.M303159200
- Behm-Ansmant, I., & Izaurralde, E. (2006). Quality control of gene expression: a stepwise assembly pathway for the surveillance complex that triggers nonsense-mediated mRNA decay. *Genes Dev*, *20*(4), 391-398. doi:10.1101/gad.1407606
- Beis, D., Bartman, T., Jin, S. W., Scott, I. C., D'Amico, L. A., Ober, E. A., . . . Jungblut, B. (2005). Genetic and cellular analyses of zebrafish atrioventricular cushion and valve development. *Development*, *132*(18), 4193-4204. doi:10.1242/dev.01970
- Berk, D. R., Bentley, D. D., Bayliss, S. J., Lind, A., & Urban, Z. (2012). Cutis laxa: a review. *J Am Acad Dermatol*, *66*(5), 842 e841-817. doi:10.1016/j.jaad.2011.01.004
- Bosman, F. T., & Stamenkovic, I. (2003). Functional structure and composition of the extracellular matrix. *J Pathol*, *200*(4), 423-428. doi:10.1002/path.1437
- Bournele, D., & Beis, D. (2016). Zebrafish models of cardiovascular disease. *Heart Fail Rev*, *21*(6), 803-813. doi:10.1007/s10741-016-9579-y
- Bressan, G. M., Pasquali-Ronchetti, I., Fornieri, C., Mattioli, F., Castellani, I., & Volpin, D. (1986). Relevance of aggregation properties of tropoelastin to the assembly and structure of elastic fibers. *J Ultrastruct Mol Struct Res*, *94*(3), 209-216.
- Callewaert, B., Renard, M., Huchtagowder, V., Albrecht, B., Hausser, I., Blair, E., . . . Urban, Z. (2011). New insights into the pathogenesis of autosomal-dominant cutis laxa with report of five ELN mutations. *Hum Mutat*, *32*(4), 445-455. doi:10.1002/humu.21462
- Cardiovascular diseases (CVDs). (2017, May 17, 2017). *Fact Sheets: World Health Organization*. Retrieved from [http://www.who.int/en/news-room/fact-sheets/detail/cardiovascular-diseases-\(cvds\)](http://www.who.int/en/news-room/fact-sheets/detail/cardiovascular-diseases-(cvds))
- Chen, J. N., Haffter, P., Odenthal, J., Vogelsang, E., Brand, M., van Eeden, F. J., . . . Nusslein-Volhard, C. (1996). Mutations affecting the cardiovascular system and other internal organs in zebrafish. *Development*, *123*, 293-302.
- Chung, M., Miao, M., Stahl, R. J., Chan, E., Parkinson, J., & Keeley, F. W. (2006). Sequences and domain structures of mammalian, avian, amphibian and teleost tropoelastins: Clues to the evolutionary history of elastins. *Matrix Biology*, *25*(8), 492-504. doi:10.1016/j.matbio.2006.08.258
- Comper, W. D. (1996). *Extracellular Matrix* (Vol. Volume 2). Amsterdam, The Netherlands: CRC Press.
- Cox, B. A., Starcher, B. C., & Urry, D. W. (1973). Coacervation of alpha-elastin results in fiber formation. *Biochim Biophys Acta*, *317*(1), 209-213.
- Czirok, A., Zach, J., Kozel, B. A., Mecham, R. P., Davis, E. C., & Rongish, B. J. (2006). Elastic fiber macro-assembly is a hierarchical, cell motion-mediated process. *J Cell Physiol*, *207*(1), 97-106. doi:10.1002/jcp.20573
- Data & Statistics. (2018, January 8, 2018). *Congenital Heart Defects. Centers for Disease Control and Prevention*. Retrieved from <https://www.cdc.gov/ncbddd/heartdefects/data.html>

- Dietz, H. C., & Mecham, R. P. (2000). Mouse models of genetic diseases resulting from mutations in elastic fiber proteins. *Matrix Biol*, 19(6), 481-488.
- Fazio, M. J., Mattei, M. G., Passage, E., Chu, M. L., Black, D., Solomon, E., . . . Uitto, J. (1991). Human elastin gene: new evidence for localization to the long arm of chromosome 7. *Am J Hum Genet*, 48(4), 696-703.
- Friedman, W. F., & Roberts, W. C. (1966). Vitamin D and the supravalvar aortic stenosis syndrome. The transplacental effects of vitamin D on the aorta of the rabbit. *Circulation*, 34(1), 77-86.
- Gosline, J. M. (1980). The elastic properties of rubber-like proteins and highly extensible tissues. *Symp Soc Exp Biol*, 34, 332-357.
- Gray, W. R., Sandberg, L. B., & Foster, J. A. (1973). Molecular model for elastin structure and function. *Nature*, 246(5434), 461-466.
- Greutmann, M., Tobler, D., Sharma, N. C., Vonder Muhll, I., Mebus, S., Kaemmerer, H., . . . Silversides, C. K. (2012). Cardiac outcomes in adults with supravalvar aortic stenosis. *Eur Heart J*, 33(19), 2442-2450. doi:10.1093/eurheartj/ehs206
- Grimes, A. C., Stadt, H. A., Shepherd, I. T., & Kirby, M. L. (2006). Solving an enigma: arterial pole development in the zebrafish heart. *Dev Biol*, 290(2), 265-276. doi:10.1016/j.ydbio.2005.11.042
- Gupta, T., & Mullins, M. C. (2010). Dissection of organs from the adult zebrafish. *J Vis Exp*(37). doi:10.3791/1717
- Hahn, S., Garvin, A. M., Di Naro, E., & Holzgreve, W. (1998). Allele drop-out can occur in alleles differing by a single nucleotide and is not alleviated by preamplification or minor template increments. *Genet Test*, 2(4), 351-355. doi:10.1089/gte.1998.2.351
- Halloran, B. G., & Baxter, B. T. (1995). Pathogenesis of aneurysms. *Semin Vasc Surg*, 8(2), 85-92.
- He, D., Chung, M., Chan, E., Alleyne, T., Ha, K. C., Miao, M., . . . Parkinson, J. (2007). Comparative genomics of elastin: Sequence analysis of a highly repetitive protein. *Matrix Biol*, 26(7), 524-540. doi:10.1016/j.matbio.2007.05.005
- High Blood Pressure Facts. (2018). *Centers for Disease Control and Prevention*. Retrieved from https://www.cdc.gov/dhdsdp/data_statistics/fact_sheets/fs_bloodpressure.htm
- Hinton, R. B., Adelman-Brown, J., Witt, S., Krishnamurthy, V. K., Osinska, H., Sakthivel, B., . . . Benson, D. W. (2010). Elastin haploinsufficiency results in progressive aortic valve malformation and latent valve disease in a mouse model. *Circ Res*, 107(4), 549-557. doi:10.1161/CIRCRESAHA.110.221358
- Hu, N., Sedmera, D., Yost, H. J., & Clark, E. B. (2000). Structure and function of the developing zebrafish heart. *Anat Rec*, 260(2), 148-157.
- Hu, Q., Shifren, A., Sens, C., Choi, J., Szabo, Z., Starcher, B. C., . . . Urban, Z. (2010). Mechanisms of emphysema in autosomal dominant cutis laxa. *Matrix Biol*, 29(7), 621-628. doi:10.1016/j.matbio.2010.06.005
- Hurlstone, A. F., Haramis, A. P., Wienholds, E., Begthel, H., Korving, J., Van Eeden, F., . . . Clevers, H. (2003). The Wnt/beta-catenin pathway regulates cardiac valve formation. *Nature*, 425(6958), 633-637. doi:10.1038/nature02028
- Hwang, J., & Maquat, L. E. (2011). Nonsense-mediated mRNA decay (NMD) in animal embryogenesis: to die or not to die, that is the question. *Curr Opin Genet Dev*, 21(4), 422-430. doi:10.1016/j.gde.2011.03.008

- Hynes, R. O., & Naba, A. (2012). Overview of the matrisome--an inventory of extracellular matrix constituents and functions. *Cold Spring Harb Perspect Biol*, 4(1), a004903. doi:10.1101/cshperspect.a004903
- Icardo, J. M. (2017). 1 - Heart Morphology and Anatomy. In A. K. Gamperl, T. E. Gillis, A. P. Farrell, & C. J. Brauner (Eds.), *Fish Physiology* (Vol. Volume 36, Part A, pp. 1-54): Academic Press.
- Icardo, J. M., & Colvee, E. (2011). The atrioventricular region of the teleost heart. A distinct heart segment. *Anat Rec (Hoboken)*, 294(2), 236-242. doi:10.1002/ar.21320
- Indik, Z., Yeh, H., Ornstein-Goldstein, N., Sheppard, P., Anderson, N., Rosenbloom, J. C., . . . Rosenbloom, J. (1987). Alternative splicing of human elastin mRNA indicated by sequence analysis of cloned genomic and complementary DNA. *Proc Natl Acad Sci U S A*, 84(16), 5680-5684.
- Jensen, S. A., Vrhovski, B., & Weiss, A. S. (2000). Domain 26 of tropoelastin plays a dominant role in association by coacervation. *J Biol Chem*, 275(37), 28449-28454. doi:10.1074/jbc.M004265200
- Jopling, C., Sleep, E., Raya, M., Marti, M., Raya, A., & Izpisua Belmonte, J. C. (2010). Zebrafish heart regeneration occurs by cardiomyocyte dedifferentiation and proliferation. *Nature*, 464(7288), 606-609. doi:10.1038/nature08899
- Just, S., Hirth, S., Berger, I. M., Fishman, M. C., & Rottbauer, W. (2016). The mediator complex subunit Med10 regulates heart valve formation in zebrafish by controlling Tbx2b-mediated Has2 expression and cardiac jelly formation. *Biochem Biophys Res Commun*, 477(4), 581-588. doi:10.1016/j.bbrc.2016.06.088
- Kagan, H. M., & Li, W. (2003). Lysyl oxidase: properties, specificity, and biological roles inside and outside of the cell. *J Cell Biochem*, 88(4), 660-672. doi:10.1002/jcb.10413
- Kahari, V. M., Chen, Y. Q., Bashir, M. M., Rosenbloom, J., & Uitto, J. (1992). Tumor necrosis factor-alpha down-regulates human elastin gene expression. Evidence for the role of AP-1 in the suppression of promoter activity. *J Biol Chem*, 267(36), 26134-26141.
- Kahari, V. M., Olsen, D. R., Rhudy, R. W., Carrillo, P., Chen, Y. Q., & Uitto, J. (1992). Transforming growth factor-beta up-regulates elastin gene expression in human skin fibroblasts. Evidence for post-transcriptional modulation. *Lab Invest*, 66(5), 580-588.
- Krebs, J. M., & Zador, A. M. (2015). Sources of PCR-induced distortions in high-throughput sequencing data sets. *Nucleic Acids Res*, 43(21), e143. doi:10.1093/nar/gkv717
- Keeley, F. W. (2013). The Evolution of Elastin. 73-119. doi:10.1007/978-3-642-36002-2_4
- Kelleher, C. M., McLean, S. E., & Mecham, R. P. (2004). Vascular extracellular matrix and aortic development. *Curr Top Dev Biol*, 62, 153-188. doi:10.1016/S0070-2153(04)62006-0
- Kielty, C. M., Sherratt, M. J., & Shuttleworth, C. A. (2002). Elastic fibres. *J Cell Sci*, 115(Pt 14), 2817-2828.
- Kikuchi, K. (2014). Advances in understanding the mechanism of zebrafish heart regeneration. *Stem Cell Res*, 13(3 Pt B), 542-555. doi:10.1016/j.scr.2014.07.003
- Kikuchi, K., Holdway, J. E., Werdich, A. A., Anderson, R. M., Fang, Y., Egnaczyk, G. F., . . . Poss, K. D. (2010). Primary contribution to zebrafish heart regeneration by gata4(+) cardiomyocytes. *Nature*, 464(7288), 601-605. doi:10.1038/nature08804
- Kimmel, C. B., Ballard, W. W., Kimmel, S. R., Ullmann, B., & Schilling, T. F. (1995). Stages of Embryonic Development of the Zebrafish. *Developmental Dynamics*(203), 253-310.

- Kozel, B. A., Rongish, B. J., Czirok, A., Zach, J., Little, C. D., Davis, E. C., . . . Mecham, R. P. (2006). Elastic fiber formation: a dynamic view of extracellular matrix assembly using timer reporters. *J Cell Physiol*, 207(1), 87-96. doi:10.1002/jcp.20546
- Kuang, P. P., Zhang, X. H., Rich, C. B., Foster, J. A., Subramanian, M., & Goldstein, R. H. (2007). Activation of elastin transcription by transforming growth factor-beta in human lung fibroblasts. *Am J Physiol Lung Cell Mol Physiol*, 292(4), L944-952. doi:10.1152/ajplung.00184.2006
- Lacro, R. V., & Smooth, L. B. (2006). Cardiovascular Disease in Williams-Beuren Syndrome In *Williams-Beuren Syndrome: Research, Evaluation, and Treatment* (1st ed., pp. 107-124). Baltimore, Maryland: Johns Hopkins University Press.
- Langheinrich, U., Vacun, G., & Wagner, T. (2003). Zebrafish embryos express an orthologue of HERG and are sensitive toward a range of QT-prolonging drugs inducing severe arrhythmia. *Toxicol Appl Pharmacol*, 193(3), 370-382.
- Li, D. Y., Brooke, B., Davis, E. C., Mecham, R. P., Sorensen, L. K., Boak, B. B., . . . Keating, M. T. (1998). Elastin is an essential determinant of arterial morphogenesis. *Nature*, 393(6682), 276-280. doi:10.1038/30522
- Li, D. Y., Faury, G., Taylor, D. G., Davis, E. C., Boyle, W. A., Mecham, R. P., . . . Keating, M. T. (1998). Novel arterial pathology in mice and humans hemizygous for elastin. *J Clin Invest*, 102(10), 1783-1787. doi:10.1172/JCI4487
- Lieschke, G. J., & Currie, P. D. (2007). Animal models of human disease: zebrafish swim into view. *Nat Rev Genet*, 8(5), 353-367. doi:10.1038/nrg2091
- Martin, R. T., & Bartman, T. (2009). Analysis of heart valve development in larval zebrafish. *Dev Dyn*, 238(7), 1796-1802. doi:10.1002/dvdy.21976
- Mauviel, A., Chen, Y. Q., Kahari, V. M., Ledo, I., Wu, M., Rudnicka, L., & Uitto, J. (1993). Human recombinant interleukin-1 beta up-regulates elastin gene expression in dermal fibroblasts. Evidence for transcriptional regulation in vitro and in vivo. *J Biol Chem*, 268(9), 6520-6524.
- McElhinney, D. B., Petrossian, E., Tworetzky, W., Silverman, N. H., & Hanley, F. L. (2000). Issues and outcomes in the management of supra-avalvular aortic stenosis. *Ann Thorac Surg*, 69(2), 562-567.
- Mecham, R. (2018). Hart's Elastin Stain: Paraffin Sections. *Tissue Fixation and Staining Techniques*. Retrieved from <http://www.mechamlab.wustl.edu/Lab%20Web%20Page.data/Library/MethodsPDFs/HartsElastinParaffin.pdf>
- Mecham, R. P. (2018). Elastin in lung development and disease pathogenesis. *Matrix Biol*. doi:10.1016/j.matbio.2018.01.005
- Medicine, I. o. (2010). *Rare Diseases and Orphan Products: Accelerating Research and Development*. Washington, DC: The National Academies Press.
- Merla, G., Brunetti-Pierri, N., Piccolo, P., Micale, L., & Loviglio, M. (2012). Supravalvular Aortic Stenosis Elastin Arteriopathy. *Circulation: Cardiovascular Genetics*, 5(6), 692-696. doi:10.1161/CIRCGENETICS.112.962860
- Metcalfe, K., Rucka, A. K., Smoot, L., Hofstadler, G., Tuzler, G., McKeown, P., . . . Tassabehji, M. (2000). Elastin: mutational spectrum in supra-avalvular aortic stenosis. *Eur J Hum Genet*, 8(12), 955-963. doi:10.1038/sj.ejhg.5200564

- Miao, M., Bruce, A. E., Bhanji, T., Davis, E. C., & Keeley, F. W. (2007). Differential expression of two tropoelastin genes in zebrafish. *Matrix Biol*, *26*(2), 115-124. doi:10.1016/j.matbio.2006.09.011
- Micale, L., Turturo, M. G., Fusco, C., Augello, B., Jurado, L. A., Izzi, C., . . . Merla, G. (2010). Identification and characterization of seven novel mutations of elastin gene in a cohort of patients affected by supravalvular aortic stenosis. *Eur J Hum Genet*, *18*(3), 317-323. doi:10.1038/ejhg.2009.181
- Midwood, K. S., & Schwarzbauer, J. E. (2002). Elastic fibers: building bridges between cells and their matrix. *Curr Biol*, *12*(8), R279-281.
- Milewicz, D. M., Urban, Z., & Boyd, C. (2000). Genetic disorders of the elastic fiber system. *Matrix Biol*, *19*(6), 471-480.
- Misra, A., Sheikh, A. Q., Kumar, A., Luo, J., Zhang, J., Hinton, R. B., . . . Greif, D. M. (2016). Integrin beta3 inhibition is a therapeutic strategy for supravalvular aortic stenosis. *J Exp Med*, *213*(3), 451-463. doi:10.1084/jem.20150688
- Misra, A., Sheikh, A. Q., Kumar, A., Luo, J., Zhang, J., Hinton, R. B., . . . Greif, D. M. (2016). Integrin β 3 inhibition is a therapeutic strategy for supravalvular aortic stenosis. *The Journal of Experimental Medicine*, *213*(3), 451-463. doi:10.1084/jem.20150688
- Mitchell, M. B., & Goldberg, S. P. (2011). Supravalvar aortic stenosis in infancy. *Semin Thorac Cardiovasc Surg Pediatr Card Surg Annu*, *14*(1), 85-91. doi:10.1053/j.pcsu.2011.01.013
- Moorman, A., Webb, S., Brown, N. A., Lamers, W., & Anderson, R. H. (2003). Development of the heart: (1) formation of the cardiac chambers and arterial trunks. *Heart*, *89*(7), 806-814.
- Moriyama, Y., Ito, F., Takeda, H., Yano, T., Okabe, M., Kuraku, S., . . . Koshiba-Takeuchi, K. (2016). Evolution of the fish heart by sub/neofunctionalization of an elastin gene. *Nature communications*, *7*, 10397. doi:10.1038/ncomms10397
- Murphey, R. D., & Zon, L. I. (2006). Small molecule screening in the zebrafish. *Methods*, *39*(3), 255-261. doi:10.1016/j.ymeth.2005.09.019
- Nagy, E., & Maquat, L. E. (1998). A rule for termination-codon position within intron-containing genes: when nonsense affects RNA abundance. *Trends Biochem Sci*, *23*(6), 198-199.
- The NCBI Eukaryotic Genome Annotation Pipeline. (2018, March 26, 2018). *NCBI: Genome*. Retrieved from https://www.ncbi.nlm.nih.gov/genome/annotation_euk/process/#gnomon
- Neff, M. M., Neff, J. D., Chory, J., & Pepper, A. E. (1998). dCAPS, a simple technique for the genetic analysis of single nucleotide polymorphisms: experimental applications in *Arabidopsis thaliana* genetics. *Plant J*, *14*(3), 387-392.
- Neff, M. M., Turk, E., & Kalishman, M. (2002). dCAPS Finder 2.0. Retrieved from <http://helix.wustl.edu/dcaps/dcaps.html>
- Nguyen, C. T., Lu, Q., Wang, Y., & Chen, J. N. (2008). Zebrafish as a model for cardiovascular development and disease. *Drug Discov Today Dis Models*, *5*(3), 135-140. doi:10.1016/j.ddmod.2009.02.003
- Norrgard, K., & Schultz, J. (2008). Using SNP data to examine human phenotypic differences. . Retrieved 05/21/2018 <https://www.nature.com/scitable/topicpage/using-snp-data-to-examine-human-phenotypic-706>

- Nwankwo, T., Yoon, S. S., Burt, V., & Gu, Q. (2013). Hypertension among adults in the United States: National Health and Nutrition Examination Survey, 2011-2012. *NCHS Data Brief*(133), 1-8.
- Ostuni, A., Bochicchio, B., Armentano, M. F., Bisaccia, F., & Tamburro, A. M. (2007). Molecular and supramolecular structural studies on human tropoelastin sequences. *Biophys J*, *93*(10), 3640-3651. doi:10.1529/biophysj.107.110809
- Park, S., Seo, E. J., Yoo, H. W., & Kim, Y. (2006). Novel mutations in the human elastin gene (ELN) causing isolated supra-aortic stenosis. *Int J Mol Med*, *18*(2), 329-332.
- Partridge, S. M., Davis, H. F., & Adair, G. S. (1955). The chemistry of connective tissues. 2. Soluble proteins derived from partial hydrolysis of elastin. *Biochem J*, *61*(1), 11-21.
- Pawlaczyk, M., Lelonkiewicz, M., & Wieczorowski, M. (2013). Age-dependent biomechanical properties of the skin. *Postepy Dermatol Alergol*, *30*(5), 302-306. doi:10.5114/pdia.2013.38359
- Pelster, B., & Burggren, W. W. (1996). Disruption of hemoglobin oxygen transport does not impact oxygen-dependent physiological processes in developing embryos of zebra fish (*Danio rerio*). *Circ Res*, *79*(2), 358-362.
- Pepe, A., Guerra, D., Bochicchio, B., Quaglino, D., Gheduzzi, D., Pasquali Ronchetti, I., & Tamburro, A. M. (2005). Dissection of human tropoelastin: supramolecular organization of polypeptide sequences coded by particular exons. *Matrix Biol*, *24*(2), 96-109. doi:10.1016/j.matbio.2005.01.004
- Pierce, R. A., Kolodziej, M. E., & Parks, W. C. (1992). 1,25-Dihydroxyvitamin D3 represses tropoelastin expression by a posttranscriptional mechanism. *J Biol Chem*, *267*(16), 11593-11599.
- Pober, B. R., Johnson, M., & Urban, Z. (2008). Mechanisms and treatment of cardiovascular disease in Williams-Beuren syndrome. *J Clin Invest*, *118*(5), 1606-1615. doi:10.1172/JCI35309
- Potapov, V., & Ong, J. L. (2017). Examining Sources of Error in PCR by Single-Molecule Sequencing. *PLoS One*, *12*(1), e0169774. doi:10.1371/journal.pone.0169774
- Raya, A., Koth, C. M., Buscher, D., Kawakami, Y., Itoh, T., Raya, R. M., . . . Izpisua-Belmonte, J. C. (2003). Activation of Notch signaling pathway precedes heart regeneration in zebrafish. *Proc Natl Acad Sci U S A*, *100* Suppl 1, 11889-11895. doi:10.1073/pnas.1834204100
- Reese, M. G. (2018). BDGP: Splice Site Prediction by Neural Network Retrieved from http://www.fruitfly.org/seq_tools/splice.html
- Richter, T., Nestler-Parr, S., Babela, R., Khan, Z. M., Tesoro, T., Molsen, E., . . . Outcomes Research Rare Disease Special Interest, G. (2015). Rare Disease Terminology and Definitions-A Systematic Global Review: Report of the ISPOR Rare Disease Special Interest Group. *Value Health*, *18*(6), 906-914. doi:10.1016/j.jval.2015.05.008
- Rosenbloom, J., Bashir, M., Yeh, H., Rosenbloom, J., Ornstein-Goldstein, N., Fazio, M., . . . Uitto, J. (1991). Regulation of elastin gene expression. *Ann N Y Acad Sci*, *624*, 116-136.
- Rossi, A., Kontarakis, Z., Gerri, C., Nolte, H., Hölper, S., Krüger, M., & Stainier, D. Y. R. (2015). Genetic compensation induced by deleterious mutations but not gene knockdowns. *Nature*, *524*(7564), 230-233. doi:10.1038/nature14580

- Rutenberg, J. B., Fischer, A., Jia, H., Gessler, M., Zhong, T. P., & Mercola, M. (2006). Developmental patterning of the cardiac atrioventricular canal by Notch and Hairy-related transcription factors. *Development*, *133*(21), 4381-4390. doi:10.1242/dev.02607
- Sadler, L. S., Pober, B. R., Grandinetti, A., Scheiber, D., Fekete, G., Sharma, A. N., & Urban, Z. (2001). Differences by sex in cardiovascular disease in Williams syndrome. *J Pediatr*, *139*(6), 849-853. doi:10.1067/mpd.2001.118889
- Sato, F., Wachi, H., Ishida, M., Nonaka, R., Onoue, S., Urban, Z., . . . Seyama, Y. (2007). Distinct steps of cross-linking, self-association, and maturation of tropoelastin are necessary for elastic fiber formation. *J Mol Biol*, *369*(3), 841-851. doi:10.1016/j.jmb.2007.03.060
- Scherz, P. J., Huisken, J., Sahai-Hernandez, P., & Stainier, D. Y. (2008). High-speed imaging of developing heart valves reveals interplay of morphogenesis and function. *Development*, *135*(6), 1179-1187. doi:10.1242/dev.010694
- Schroeder, J. A., Jackson, L. F., Lee, D. C., & Camenisch, T. D. (2003). Form and function of developing heart valves: coordination by extracellular matrix and growth factor signaling. *J Mol Med (Berl)*, *81*(7), 392-403. doi:10.1007/s00109-003-0456-5
- Scott, D. J., Campbell, D. N., Clarke, D. R., Goldberg, S. P., Karlin, D. R., & Mitchell, M. B. (2009). Twenty-year surgical experience with congenital supraaortic stenosis. *Ann Thorac Surg*, *87*(5), 1501-1507; discussion 1507-1508. doi:10.1016/j.athoracsur.2009.01.070
- Shapiro, S. D., Endicott, S. K., Province, M. A., Pierce, J. A., & Campbell, E. J. (1991). Marked longevity of human lung parenchymal elastic fibers deduced from prevalence of D-aspartate and nuclear weapons-related radiocarbon. *J Clin Invest*, *87*(5), 1828-1834. doi:10.1172/JCI115204
- Shifren, A., & Mecham, R. P. (2006). The stumbling block in lung repair of emphysema: elastic fiber assembly. *Proc Am Thorac Soc*, *3*(5), 428-433. doi:10.1513/pats.200601-009AW
- Simmons, D. (2008). The use of animal models in studying genetic disease: transgenesis and induced mutation. *Nature Education* *1*(1):70. Retrieved from <https://www.nature.com/scitable/topicpage/the-use-of-animal-models-in-studying-855>
- Singh, A. R., Sivadas, A., Sabharwal, A., Vellarikal, S. K., Jayarajan, R., Verma, A., . . . Sivasubbu, S. (2016). Chamber Specific Gene Expression Landscape of the Zebrafish Heart. *PLoS One*, *11*(1), e0147823. doi:10.1371/journal.pone.0147823
- Song, Y. L., Ford, J. W., Gordon, D., & Shanley, C. J. (2000). Regulation of lysyl oxidase by interferon-gamma in rat aortic smooth muscle cells. *Arterioscler Thromb Vasc Biol*, *20*(4), 982-988.
- Staff, Z. (2016). Genotype: AB/Tuebingen. *Mutation Details Curation of Older Features*. Retrieved from <https://zfin.org/ZDB-GENO-010924-10>
- Stainier, D. Y., Fouquet, B., Chen, J. N., Warren, K. S., Weinstein, B. M., Meiler, S. E., . . . Fishman, M. C. (1996). Mutations affecting the formation and function of the cardiovascular system in the zebrafish embryo. *Development*, *123*, 285-292.
- Starcher, B., Aycok, R. L., & Hill, C. H. (2005). Multiple roles for elastic fibers in the skin. *J Histochem Cytochem*, *53*(4), 431-443. doi:10.1369/jhc.4A6484.2005
- Starcher, B. C., & Urry, D. W. (1973). Elastin coacervate as a matrix for calcification. *Biochem Biophys Res Commun*, *53*(1), 210-216.
- Stevens, E. D., & Randall, D. J. (1967). Changes in blood pressure, heart rate and breathing rate during moderate swimming activity in rainbow trout. *J Exp Biol*, *46*(2), 307-315.

- Strand, T. M., Segelbacher, G., Quintela, M., Xiao, L., Axelsson, T., & Hoglund, J. (2012). Can balancing selection on MHC loci counteract genetic drift in small fragmented populations of black grouse? *Ecol Evol*, *2*(2), 341-353. doi:10.1002/ece3.86
- Szabo, Z., Crepeau, M. W., Mitchell, A. L., Stephan, M. J., Puntel, R. A., Yin Loke, K., . . . Urban, Z. (2006). Aortic aneurysmal disease and cutis laxa caused by defects in the elastin gene. *J Med Genet*, *43*(3), 255-258. doi:10.1136/jmg.2005.034157
- Timmerman, L. A., Grego-Bessa, J., Raya, A., Bertran, E., Perez-Pomares, J. M., Diez, J., . . . de la Pompa, J. L. (2004). Notch promotes epithelial-mesenchymal transition during cardiac development and oncogenic transformation. *Genes Dev*, *18*(1), 99-115. doi:10.1101/gad.276304
- Tofolean, D. E., Mazilu, L., Staniceanu, F., Mocanu, L., Suceveanu, A. I., Baz, R. O., . . . Voinea, F. (2015). Clinical presentation of a patient with cutis laxa with systemic involvement: a case report. *Rom J Morphol Embryol*, *56*(3), 1205-1210.
- Tu, S., & Chi, N. C. (2012). Zebrafish models in cardiac development and congenital heart birth defects. *Differentiation*, *84*(1), 4-16. doi:10.1016/j.diff.2012.05.005
- Tu, Y., & Weiss, A. S. (2008). Glycosaminoglycan-mediated coacervation of tropoelastin abolishes the critical concentration, accelerates coacervate formation, and facilitates spherule fusion: implications for tropoelastin microassembly. *Biomacromolecules*, *9*(7), 1739-1744. doi:10.1021/bm7013153
- Tu, Y., & Weiss, A. S. (2010). Transient tropoelastin nanoparticles are early-stage intermediates in the coacervation of human tropoelastin whose aggregation is facilitated by heparan sulfate and heparin decasaccharides. *Matrix Biol*, *29*(2), 152-159. doi:10.1016/j.matbio.2009.10.003
- Uitto, J., Christiano, A. M., Kahari, V. M., Bashir, M. M., & Rosenbloom, J. (1991). Molecular biology and pathology of human elastin. *Biochem Soc Trans*, *19*(4), 824-829.
- Uitto, J., Ryhanen, L., Abraham, P. A., & Perejda, A. J. (1982). Elastin in diseases. *J Invest Dermatol*, *79 Suppl 1*, 160s-168s.
- Urban, Z., Gao, J., Pope, F. M., & Davis, E. C. (2005). Autosomal dominant cutis laxa with severe lung disease: synthesis and matrix deposition of mutant tropoelastin. *J Invest Dermatol*, *124*(6), 1193-1199. doi:10.1111/j.0022-202X.2005.23758.x
- Urban, Z., Michels, V. V., Thibodeau, S. N., Davis, E. C., Bonnefont, J. P., Munnich, A., . . . Boyd, C. D. (2000). Isolated supravalvular aortic stenosis: functional haploinsufficiency of the elastin gene as a result of nonsense-mediated decay. *Hum Genet*, *106*(6), 577-588.
- Urban, Z., Michels, V. V., Thibodeau, S. N., Donis-Keller, H., Csiszar, K., & Boyd, C. D. (1999). Supravalvular aortic stenosis: a splice site mutation within the elastin gene results in reduced expression of two aberrantly spliced transcripts. *Hum Genet*, *104*(2), 135-142.
- Urban, Z., Riazi, S., Seidl, T. L., Katahira, J., Smoot, L. B., Chitayat, D., . . . Hinek, A. (2002). Connection between elastin haploinsufficiency and increased cell proliferation in patients with supravalvular aortic stenosis and Williams-Beuren syndrome. *Am J Hum Genet*, *71*(1), 30-44. doi:10.1086/341035
- Van Doren, S. R. (2015). Matrix metalloproteinase interactions with collagen and elastin. *Matrix Biol*, *44-46*, 224-231. doi:10.1016/j.matbio.2015.01.005
- Vesely, I. (1998). The role of elastin in aortic valve mechanics. *J Biomech*, *31*(2), 115-123.

- Vrhovski, B., Jensen, S., & Weiss, A. S. (1997). Coacervation characteristics of recombinant human tropoelastin. *Eur J Biochem*, 250(1), 92-98.
- Vrhovski, B., & Weiss, A. S. (1998). Biochemistry of tropoelastin. *Eur J Biochem*, 258(1), 1-18.
- Wachi, H., Sato, F., Nakazawa, J., Nonaka, R., Szabo, Z., Urban, Z., . . . Seyama, Y. (2007). Domains 16 and 17 of tropoelastin in elastic fibre formation. *Biochem J*, 402(1), 63-70. doi:10.1042/BJ20061145
- Wagenseil, J. E., & Mecham, R. P. (2012). Elastin in large artery stiffness and hypertension. *J Cardiovasc Transl Res*, 5(3), 264-273. doi:10.1007/s12265-012-9349-8
- Walsh, E. C., & Stainier, D. Y. (2001). UDP-glucose dehydrogenase required for cardiac valve formation in zebrafish. *Science*, 293(5535), 1670-1673. doi:10.1126/science.293.5535.1670
- Wang, Y., Cong, Y., Li, J., Li, X., Li, B., & Qi, S. (2013). Comparison of invasive blood pressure measurements from the caudal ventral artery and the femoral artery in male adult SD and Wistar rats. *PLoS One*, 8(4), e60625. doi:10.1371/journal.pone.0060625
- Weinstein, B. M., Stemple, D. L., Driever, W., & Fishman, M. C. (1995). Gridlock, a localized heritable vascular patterning defect in the zebrafish. *Nat Med*, 1(11), 1143-1147.
- Weir, E. K., Joffe, H. S., Blaufuss, A. H., & Beighton, P. (1977). Cardiovascular abnormalities in cutis laxa. *Eur J Cardiol*, 5(3), 255-261.
- Westerfield, M. (2007). *THE ZEBRAFISH BOOK: A guide for the laboratory use of zebrafish (Danio rerio)* (4th Edition ed.). Eugene: University of Oregon Press.
- Whitesell, T. R., Kennedy, R. M., Carter, A. D., Rollins, E. L., Georgijevic, S., Santoro, M. M., & Childs, S. J. (2014). An alpha-smooth muscle actin (acta2/alphasma) zebrafish transgenic line marking vascular mural cells and visceral smooth muscle cells. *PLoS One*, 9(3), e90590. doi:10.1371/journal.pone.0090590
- Wise, S. G., & Weiss, A. S. (2009). Tropoelastin. *Int J Biochem Cell Biol*, 41(3), 494-497. doi:10.1016/j.biocel.2008.03.017
- Wise, S. G., Yeo, G. C., Hiob, M. A., Rnjak-Kovacina, J., Kaplan, D. L., Ng, M. K., & Weiss, A. S. (2014). Tropoelastin: a versatile, bioactive assembly module. *Acta Biomater*, 10(4), 1532-1541. doi:10.1016/j.actbio.2013.08.003
- Wittkopp, N., Huntzinger, E., Weiler, C., Sauliere, J., Schmidt, S., Sonawane, M., & Izaurralde, E. (2009). Nonsense-mediated mRNA decay effectors are essential for zebrafish embryonic development and survival. *Mol Cell Biol*, 29(13), 3517-3528. doi:10.1128/MCB.00177-09
- Wu, W. J., & Weiss, A. S. (1999). Deficient coacervation of two forms of human tropoelastin associated with supravalvular aortic stenosis. *Eur J Biochem*, 266(1), 308-314.
- Yelon, D. (2001). Cardiac patterning and morphogenesis in zebrafish. *Dev Dyn*, 222(4), 552-563. doi:10.1002/dvdy.1243
- Yeo, G. C., Keeley, F. W., & Weiss, A. S. (2011). Coacervation of tropoelastin. *Adv Colloid Interface Sci*, 167(1-2), 94-103. doi:10.1016/j.cis.2010.10.003
- Yeo, G. C., Tarakanova, A., Baldock, C., Wise, S. G., Buehler, M. J., & Weiss, A. S. (2016). Subtle balance of tropoelastin molecular shape and flexibility regulates dynamics and hierarchical assembly. *Sci Adv*, 2(2), e1501145. doi:10.1126/sciadv.1501145
- Zhan, X., Dixon, A., Batbayar, N., Bragin, E., Ayas, Z., Deuschova, L., . . . Bruford, M. W. (2015). Exonic versus intronic SNPs: contrasting roles in revealing the population genetic

- differentiation of a widespread bird species. *Heredity (Edinb)*, 114(1), 1-9.
doi:10.1038/hdy.2014.59
- Zhao, Z., Fu, Y. X., Hewett-Emmett, D., & Boerwinkle, E. (2003). Investigating single nucleotide polymorphism (SNP) density in the human genome and its implications for molecular evolution. *Gene*, 312, 207-213.
- Zhong, T. P., Rosenberg, M., Mohideen, M. A., Weinstein, B., & Fishman, M. C. (2000). gridlock, an HLH gene required for assembly of the aorta in zebrafish. *Science*, 287(5459), 1820-1824.
- Zhou, Y., Cashman, T. J., Nevis, K. R., Obregon, P., Carney, S. A., Liu, Y., . . . Burns, C. G. (2011). Latent TGF-beta binding protein 3 identifies a second heart field in zebrafish. *Nature*, 474(7353), 645-648. doi:10.1038/nature10094